

Chiral symmetry in nuclear medium observed in spectroscopy of pionic atoms + η' -mesic nuclei for $U_A(1)$ anomaly

RIKEN Nishina Center
Kenta Itahashi

- Nature Physics **19**, 788 (2023)
Article DOI: 10.1038/s41567-023-02001-x
- Nature Physics **19**, 764 (2023)
News and Views "Modified in Medium"



Chiral symmetry in nuclear medium observed in spectroscopy of pionic atoms

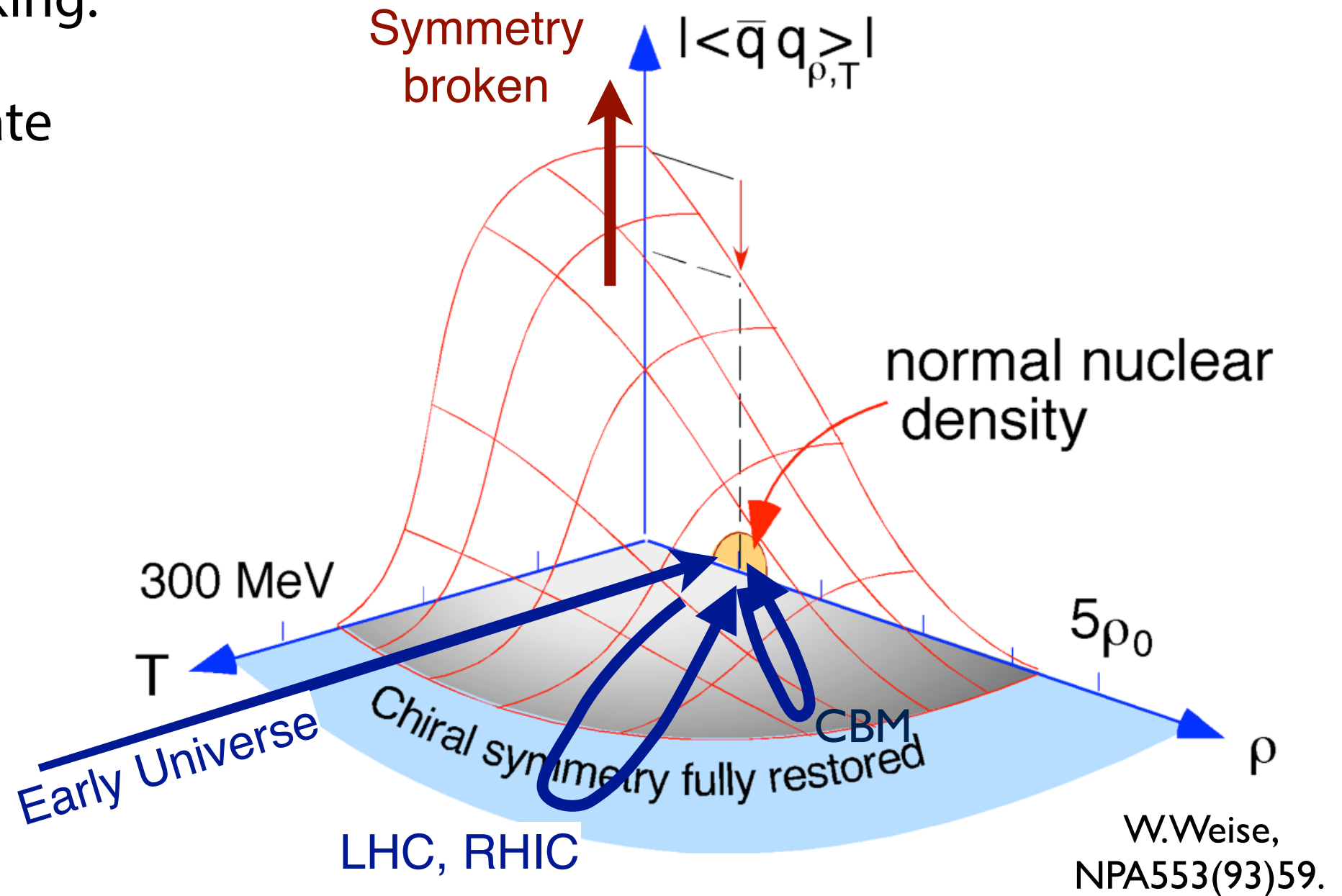
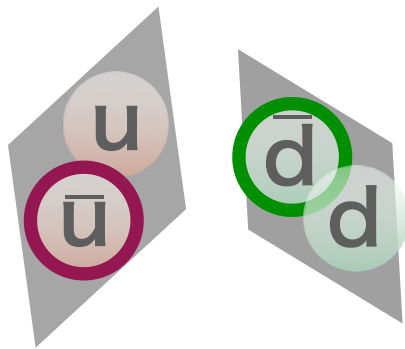
- **Dominant symmetry of the vacuum in low-energy region.**
- **Spontaneous breakdown due to non-perturbative strong interaction.**
- **Non-trivial structure of the QCD vacuum.**

- Nature Physics **19**, 788 (2023)
Article DOI: 10.1038/s41567-023-02001-x
- Nature Physics **19**, 764 (2023)
News and Views "Modified in Medium"

Chiral condensate, order parameter of chiral symmetry

One of order parameters of χ -symmetry breaking:

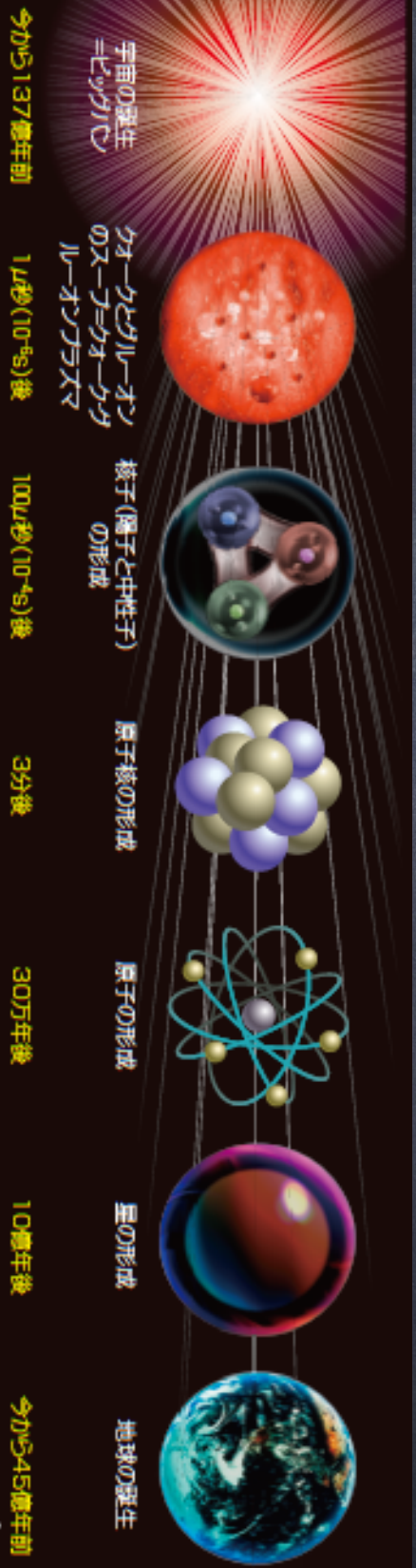
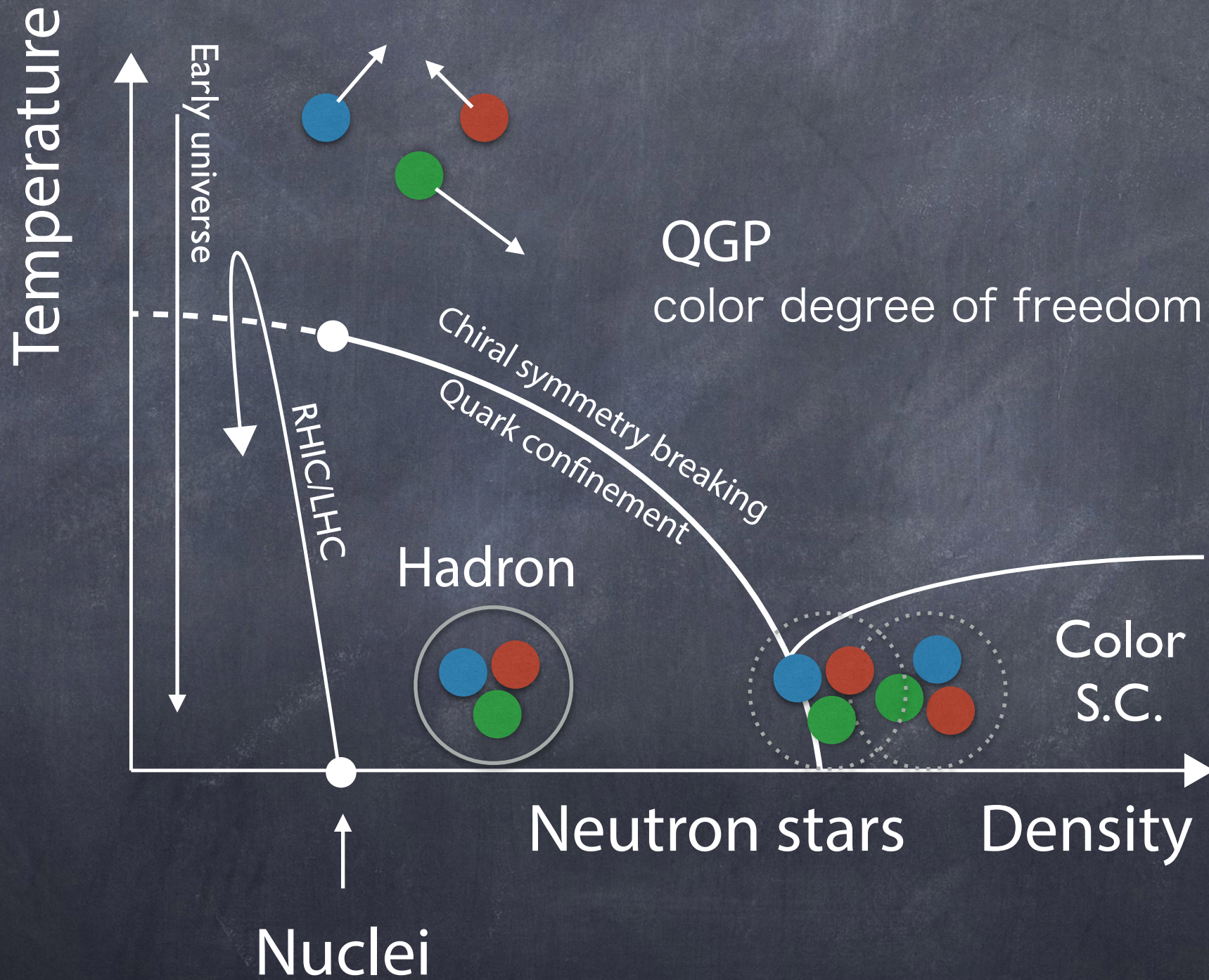
Chiral condensate



Analysis of material properties
of QCD vacuum

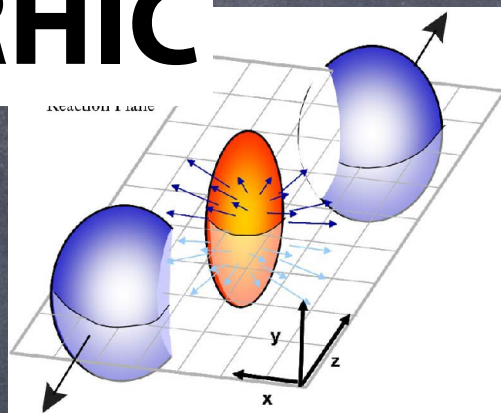
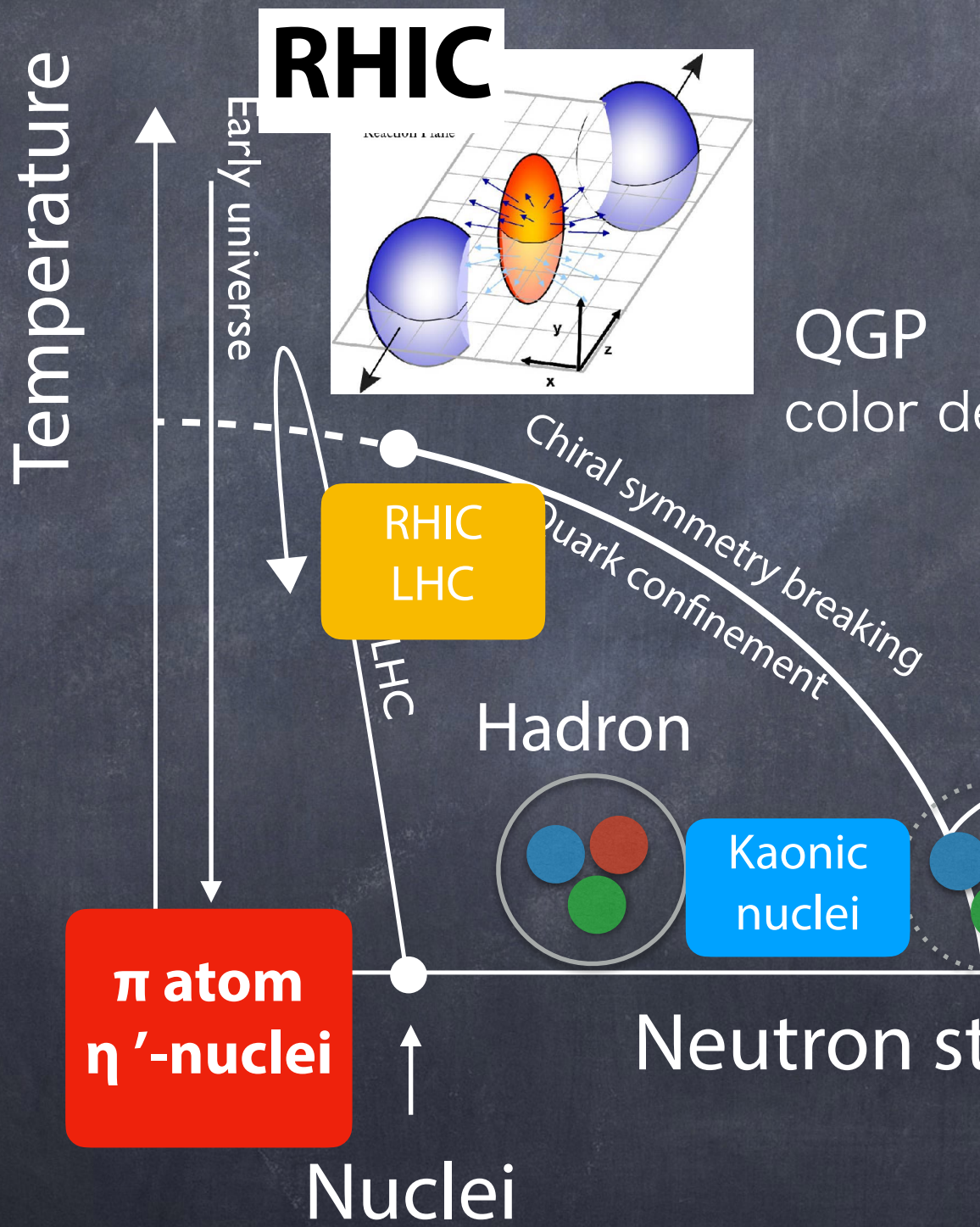
Material properties of vacuum

Properties of QCD vacuum
depend on temperature and matter-density



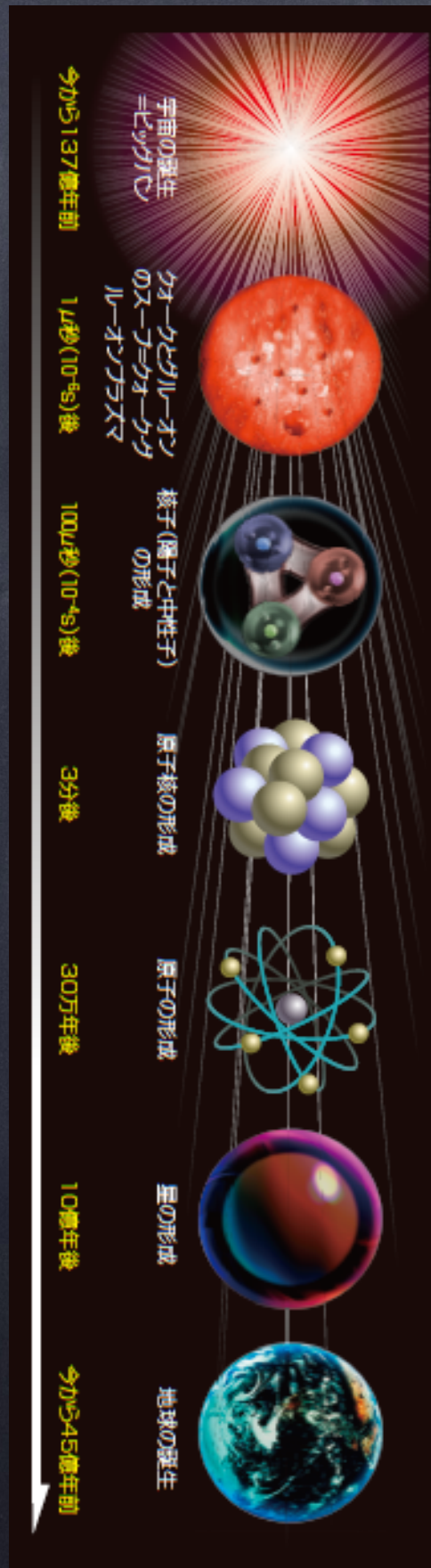
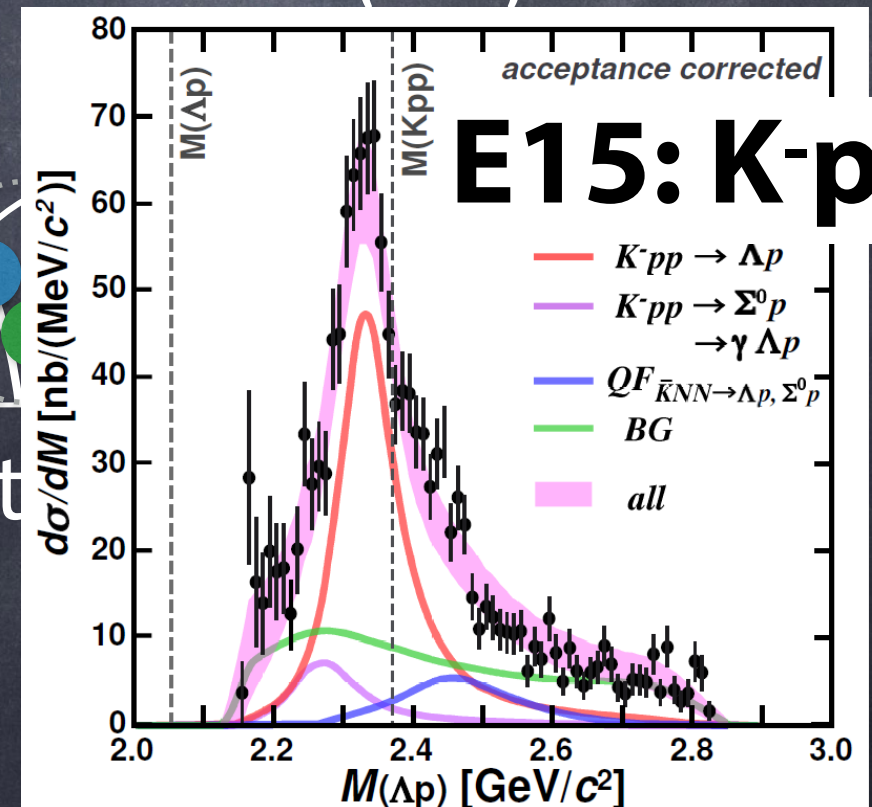
Material properties of vacuum

Properties of QCD vacuum depend on temperature and matter-density

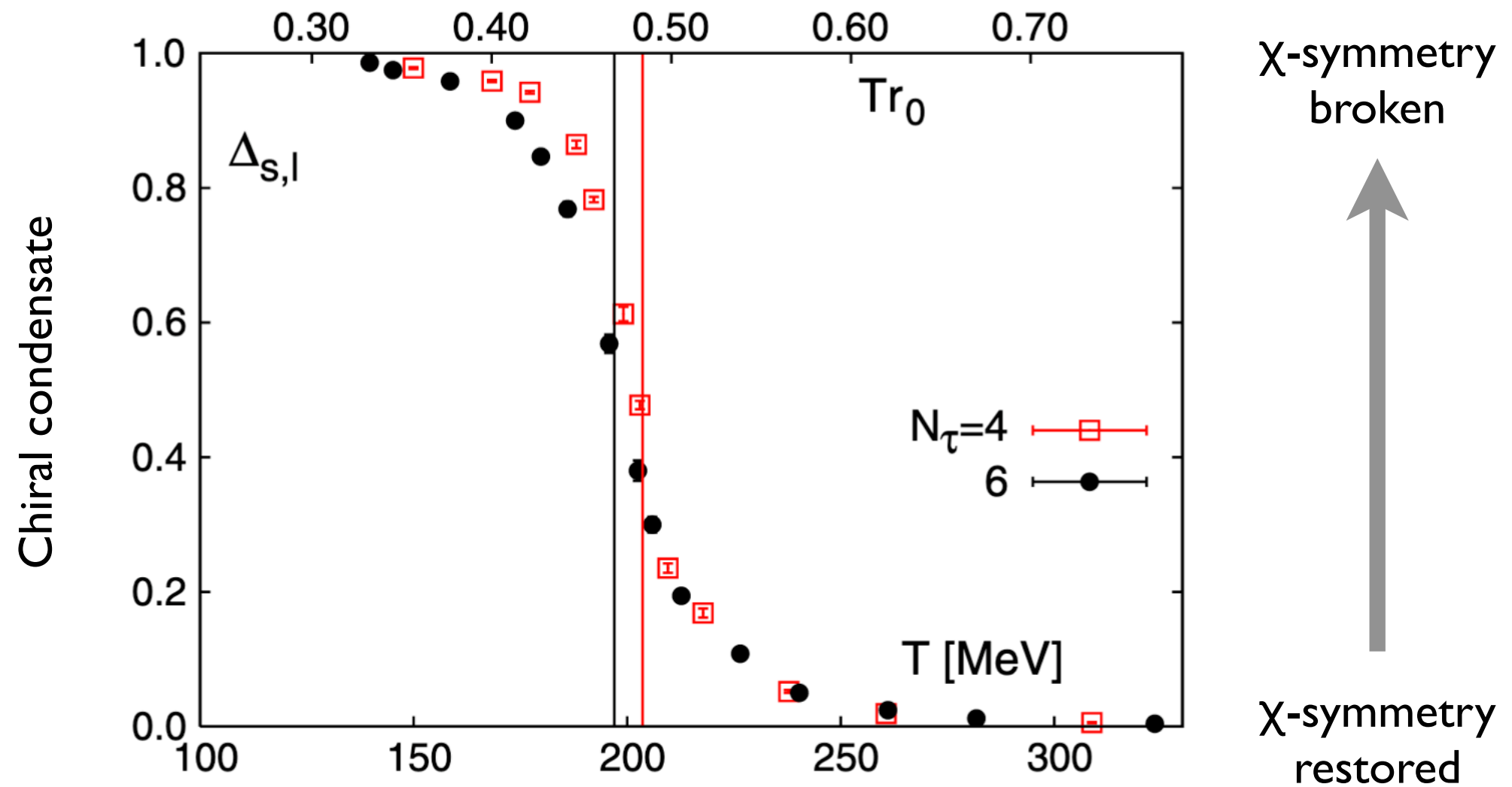


QGP
color degree of freedom

PLB789(2019)620.
PRC102(2020)044002.

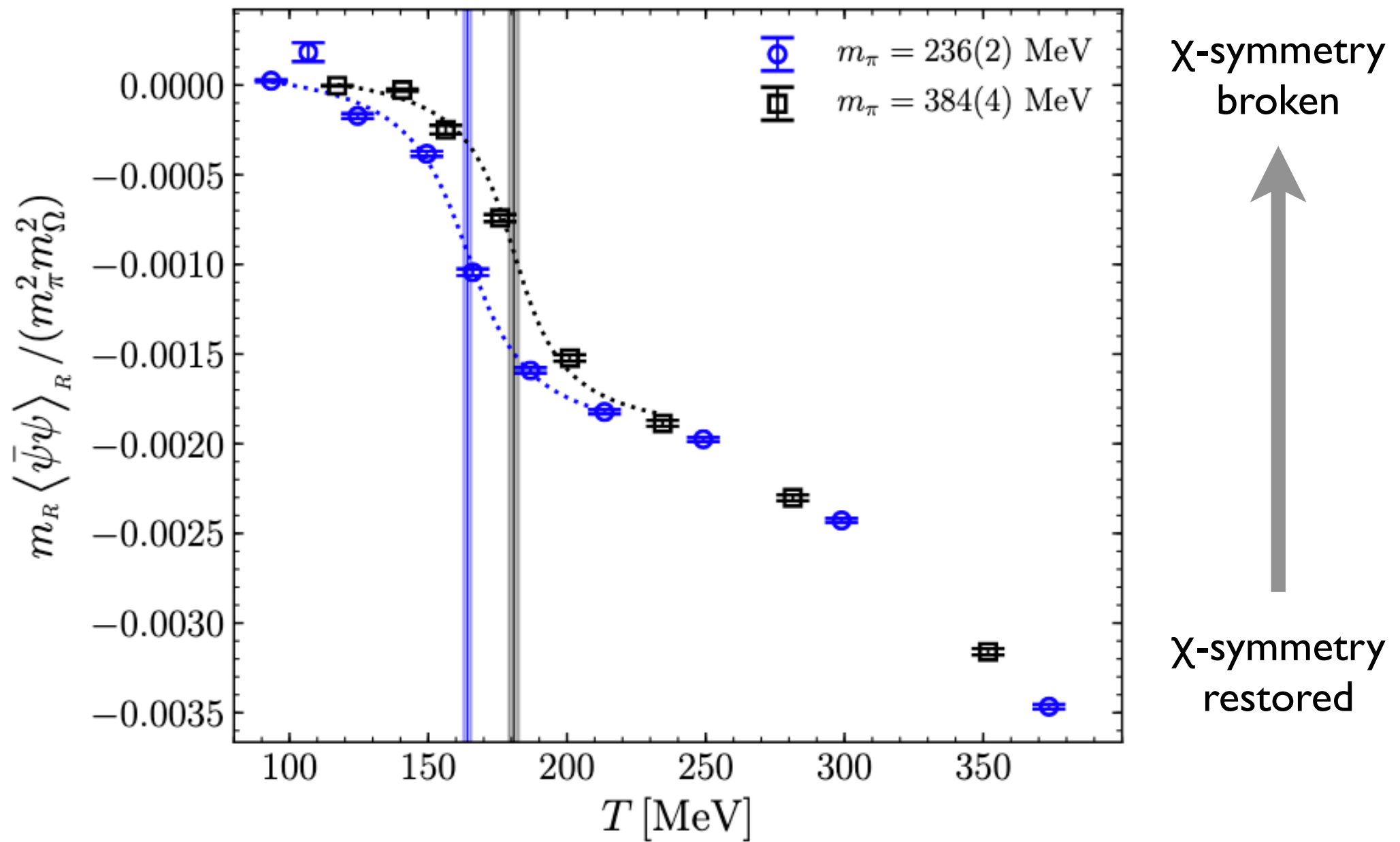


Lattice QCD calculated T dependence of chiral condensate



Temperature dependence of the chiral condensate from lattice QCD with 2 + 1 quark flavours and almost physical quark masses

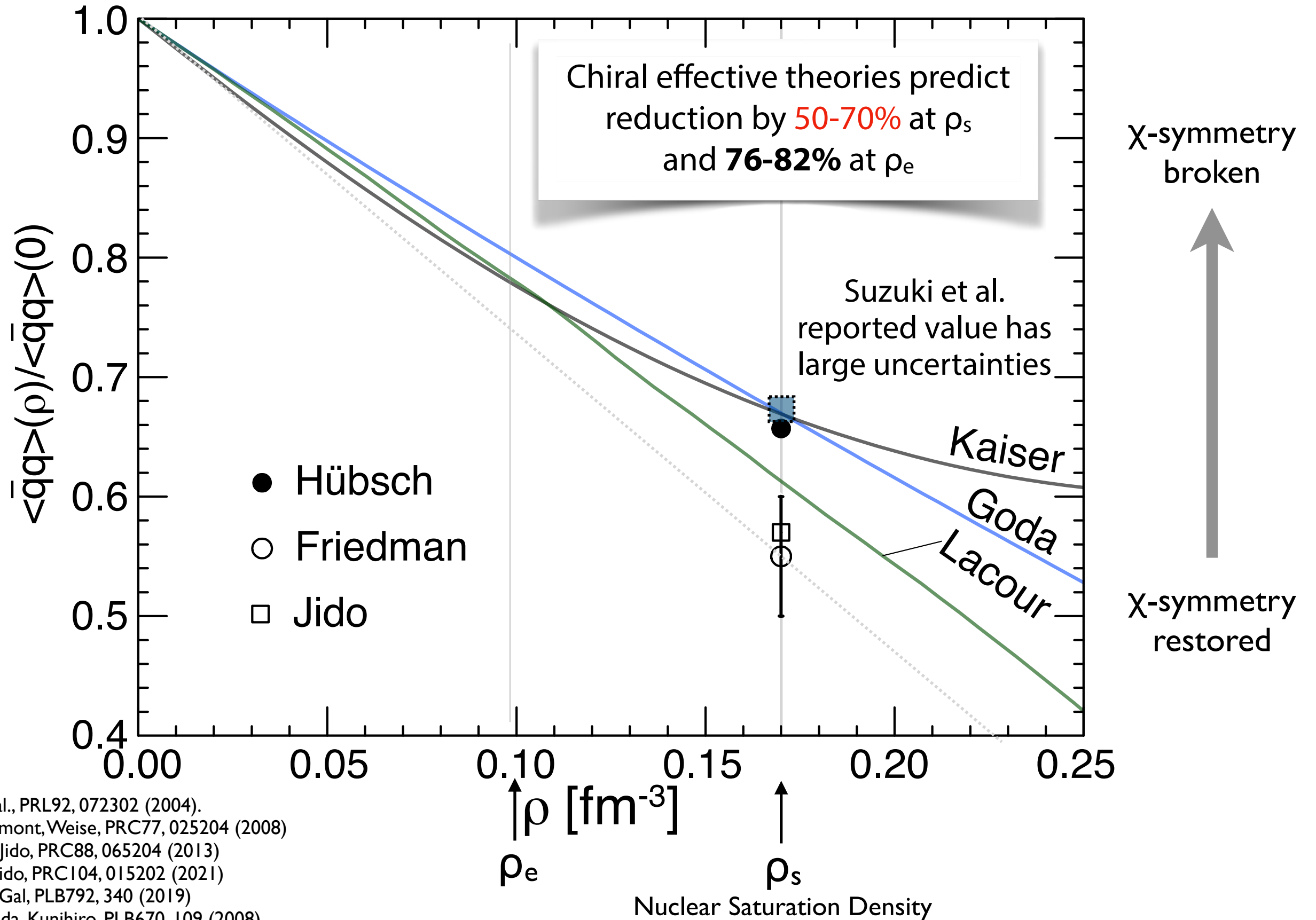
Lattice QCD calculated T dependence of chiral condensate



Remark: sign problem makes it difficult for lattice to approach non-zero ρ region

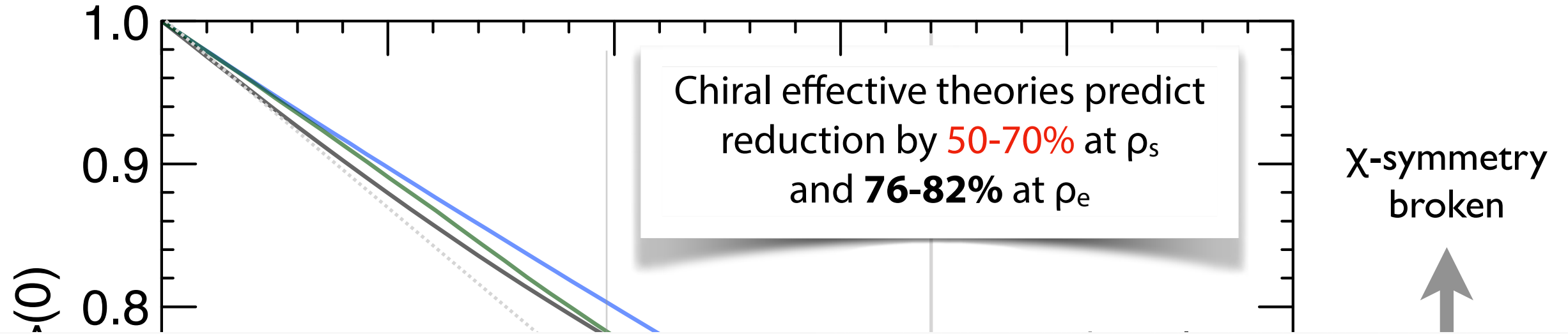
Jon-Ivar Skullerud
PRD105(2022)034504

ρ dependence of $\langle \bar{q}q \rangle$ known so far

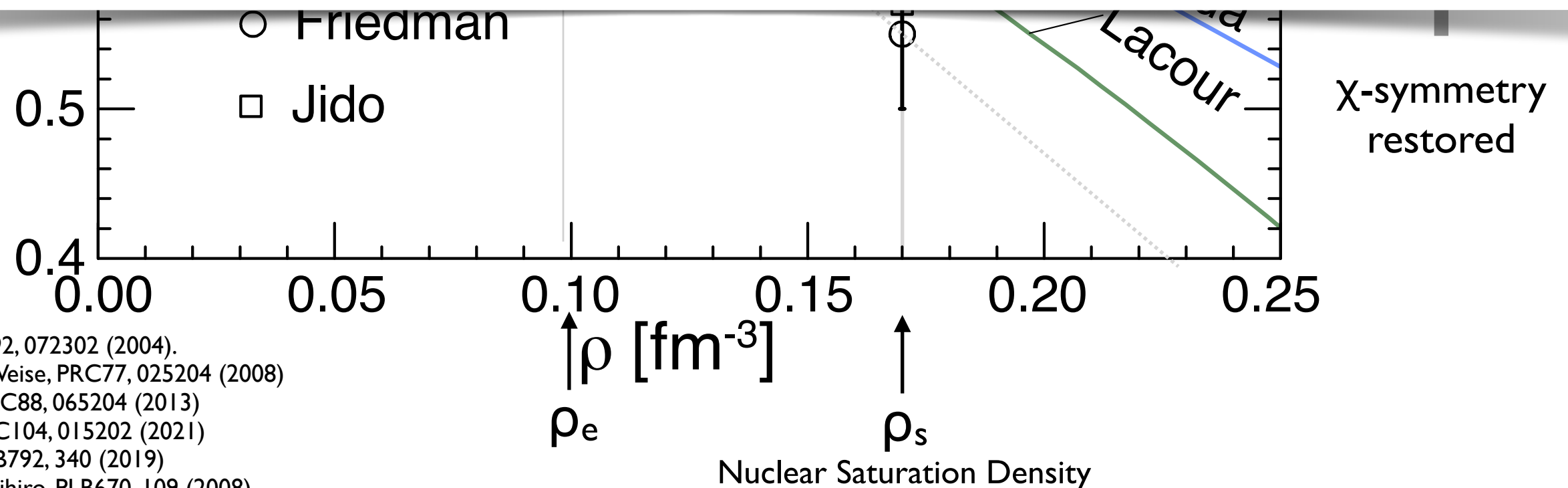


Suzuki et al., PRL92, 072302 (2004).
 Kaiser, Homont, Weise, PRC77, 025204 (2008)
 Goda and Jido, PRC88, 065204 (2013)
 Huebsch, Jido, PRC104, 015202 (2021)
 Friedman, Gal, PLB792, 340 (2019)
 Jido, Hatsuda, Kunihiro, PLB670, 109 (2008)
 Lacour, Oller, Meissner, J. Phys. G. 37, 125002 (2010)

ρ dependence of $\langle \bar{q}q \rangle$ known so far



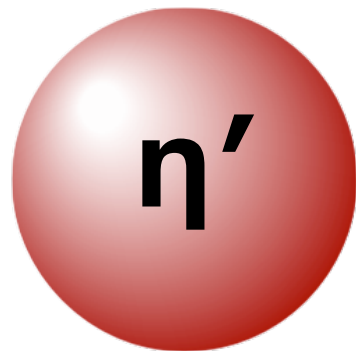
Need high-quality experimental information to quantify $\langle \bar{q}q \rangle$ reduction and confirm theoretical scenario of vacuum evolution

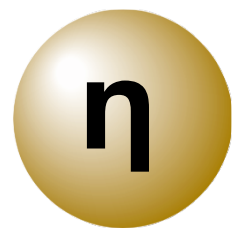


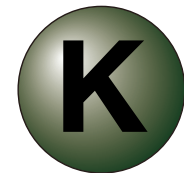
Suzuki et al., PRL92, 072302 (2004).
 Kaiser, Homont, Weise, PRC77, 025204 (2008)
 Goda and Jido, PRC88, 065204 (2013)
 Huebsch, Jido, PRC104, 015202 (2021)
 Friedman, Gal, PLB792, 340 (2019)
 Jido, Hatsuda, Kunihiro, PLB670, 109 (2008)
 Lacour, Oller, Meissner, J. Phys. G. 37, 125002 (2010)

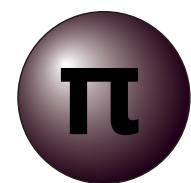
Pseudo-scalar mesons

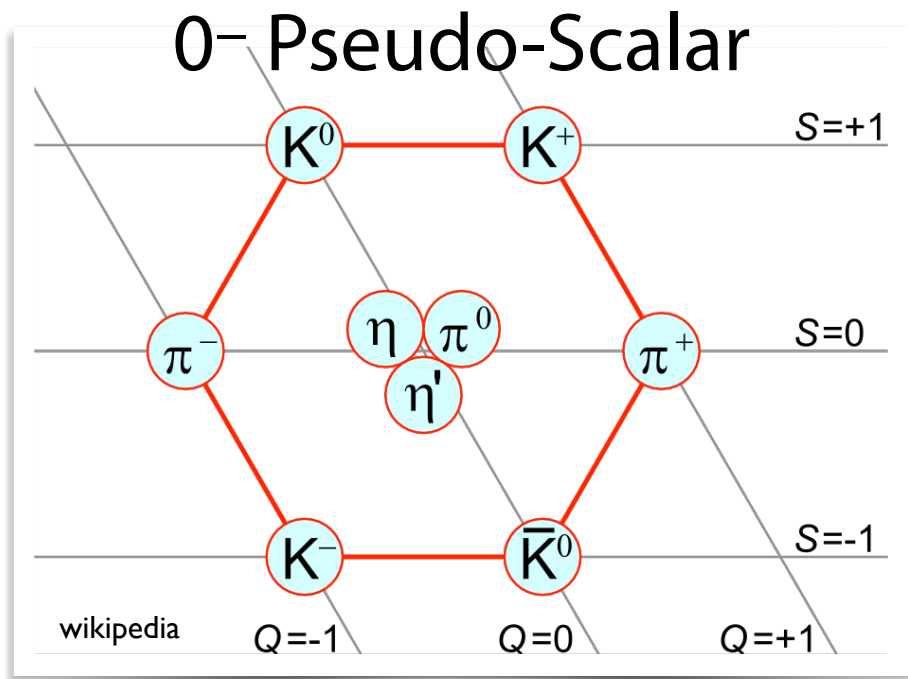
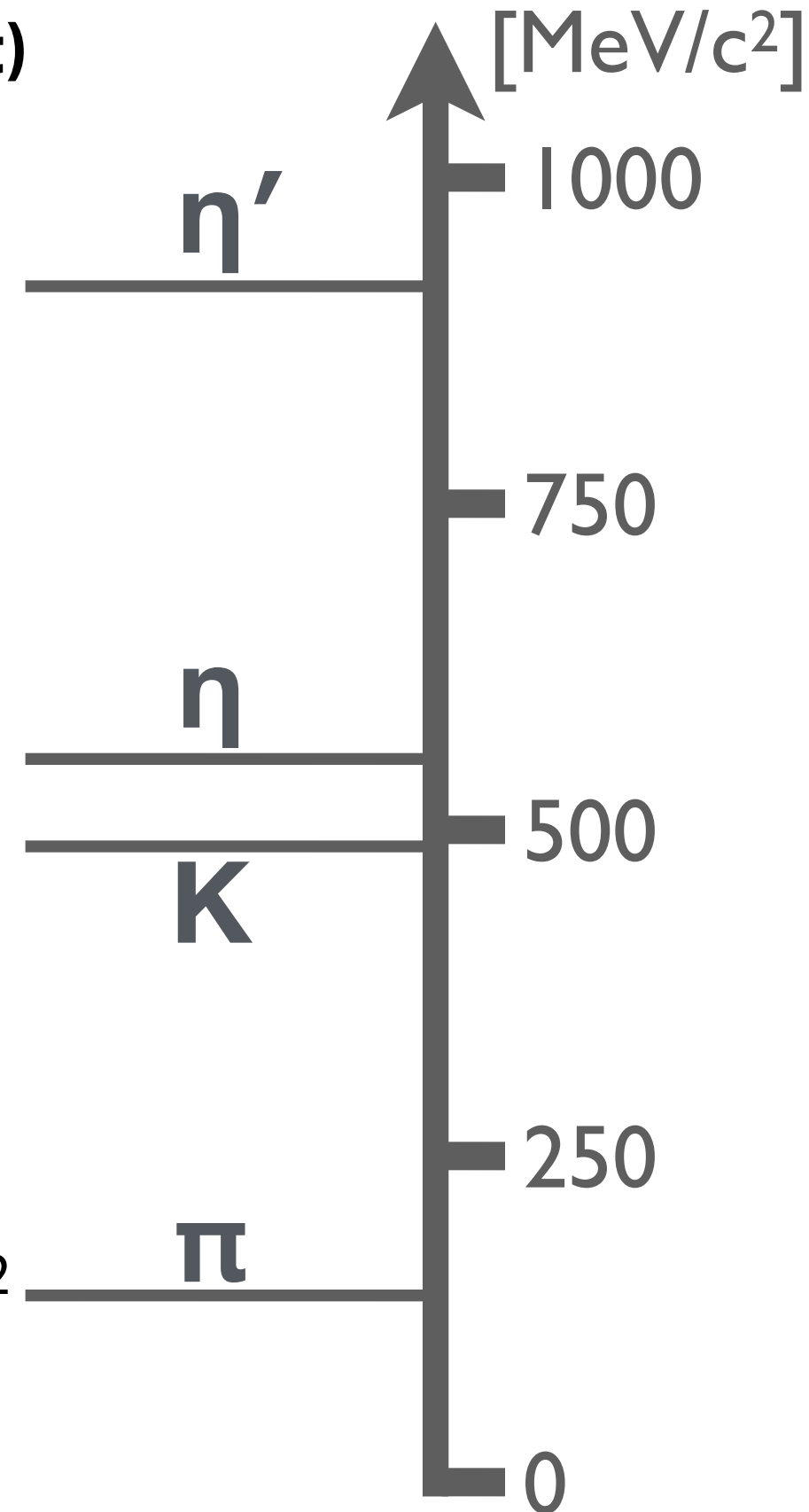
(in the lowest-mass nonet)

 η' $M=958 \text{ MeV}/c^2$

 η $M=548 \text{ MeV}/c^2$

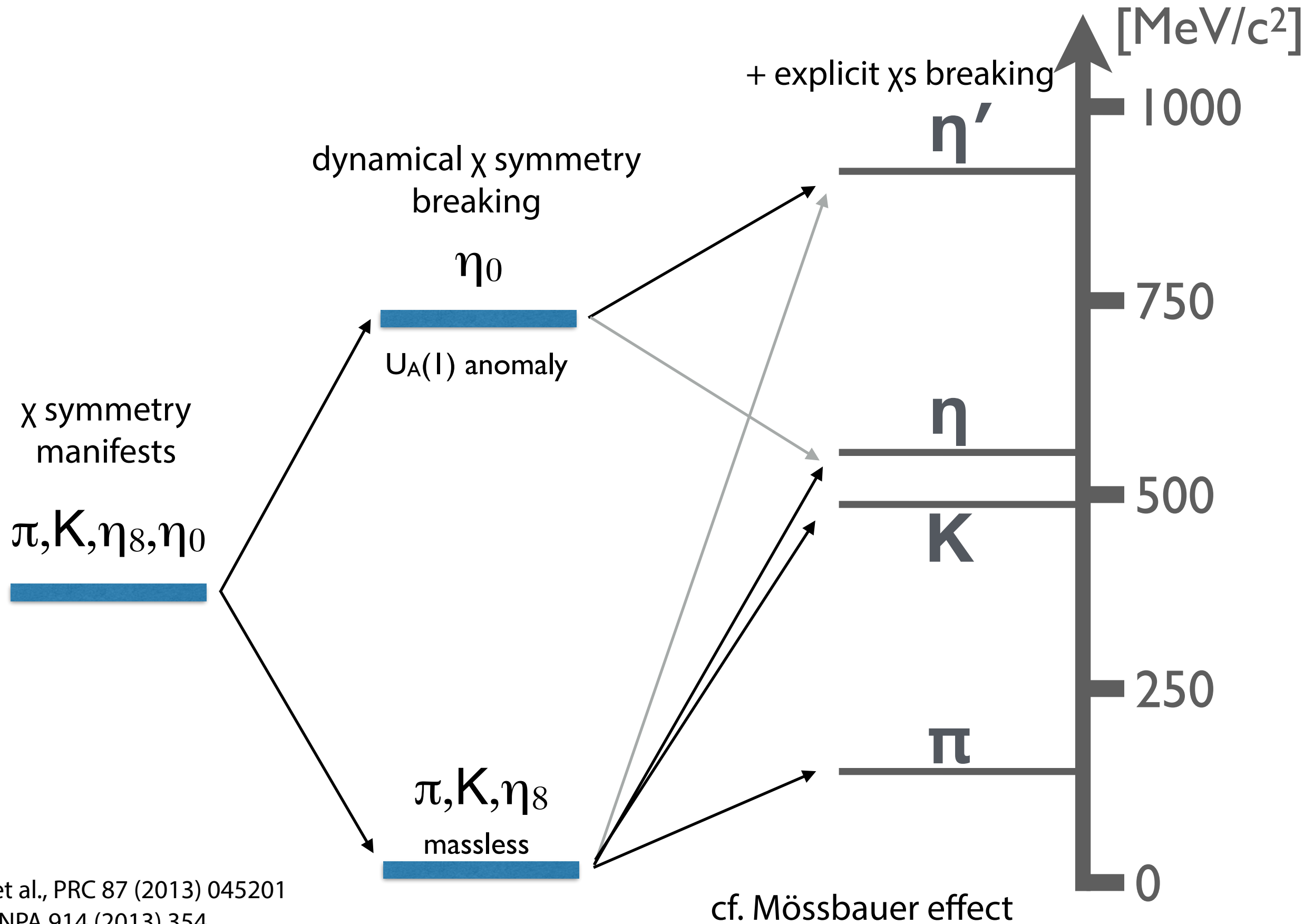
 K $M=498 \text{ MeV}/c^2$

 π $M=140 \text{ MeV}/c^2$

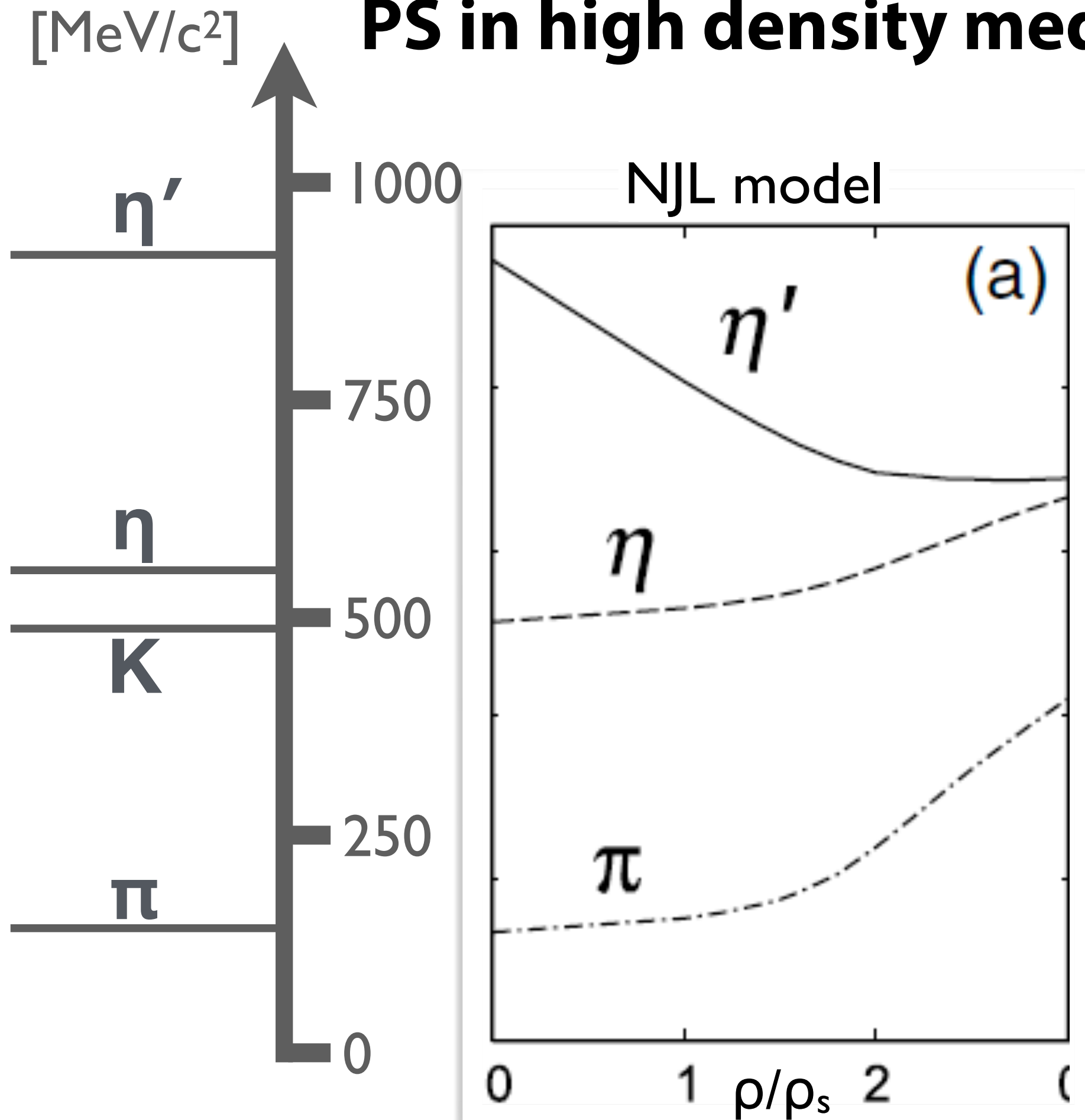


Masses of Pseudo-Scalar Mesons

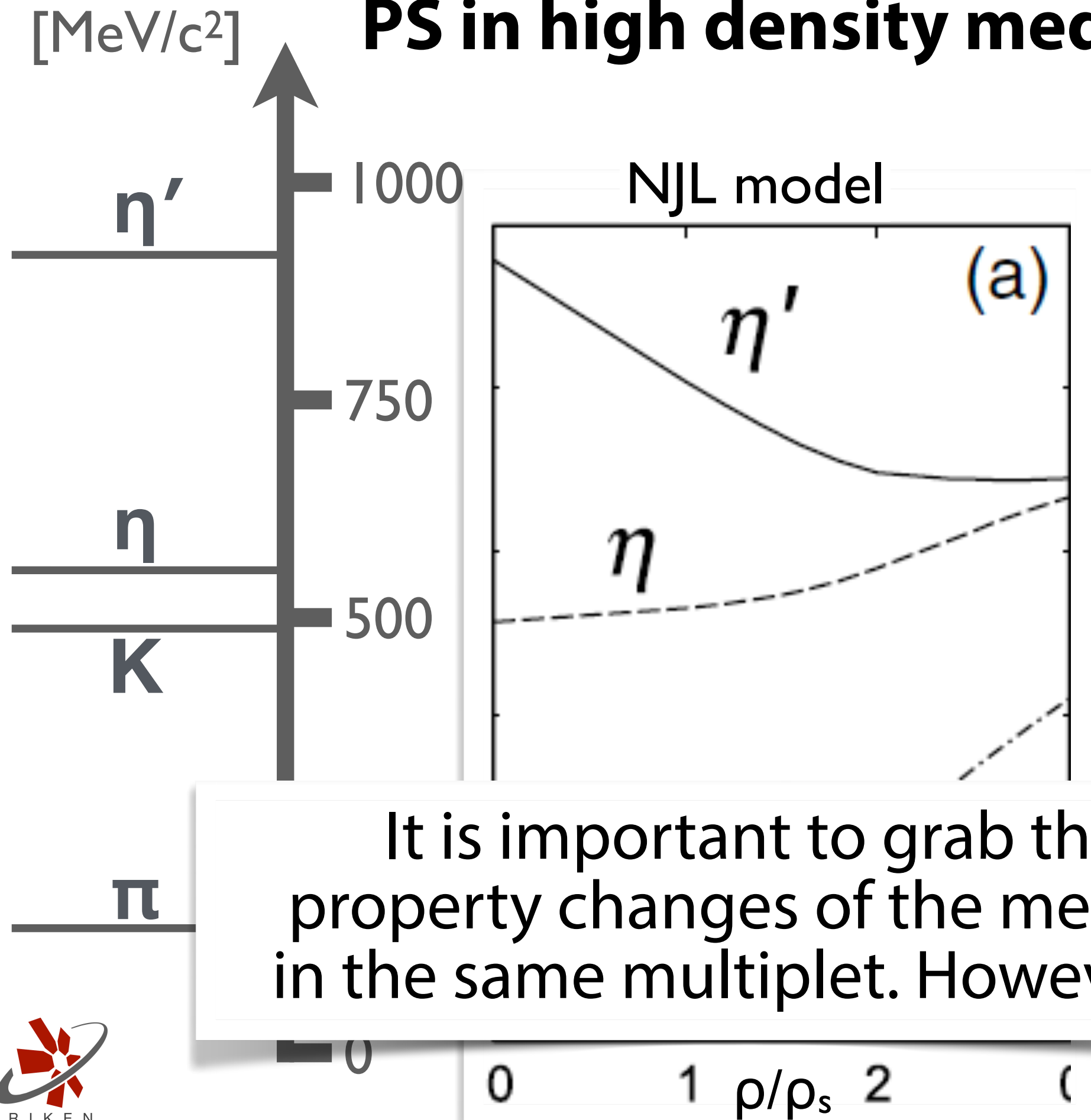
with various symmetry breaking patterns



PS in high density medium



PS in high density medium

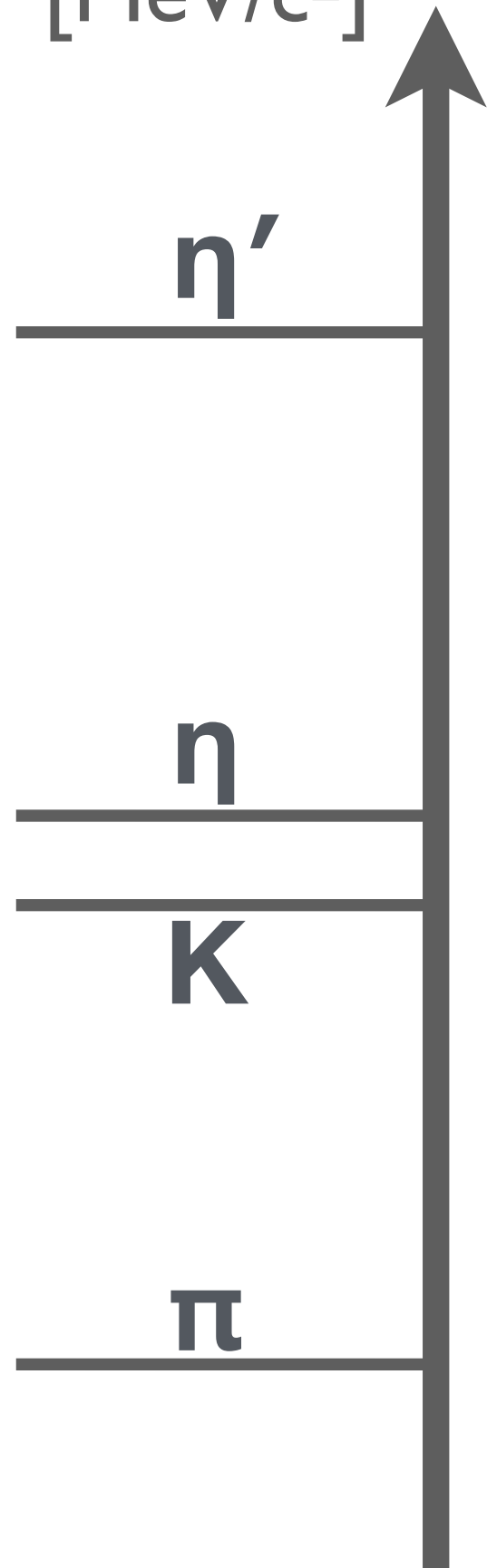


REMARK
 Δm between
 η - η' , (σ, π)
 (ρ, a_1) are important

It is important to grab the property changes of the mesons in the same multiplet. However...

Topics in mesic atoms/nuclei

[MeV/c²]



→ **$U_A(1)$ anomaly**
gluon dynamics
instanton-induced interaction

Strong coupling to $N^*(1535)$
→ χ -symmetry in baryon sector

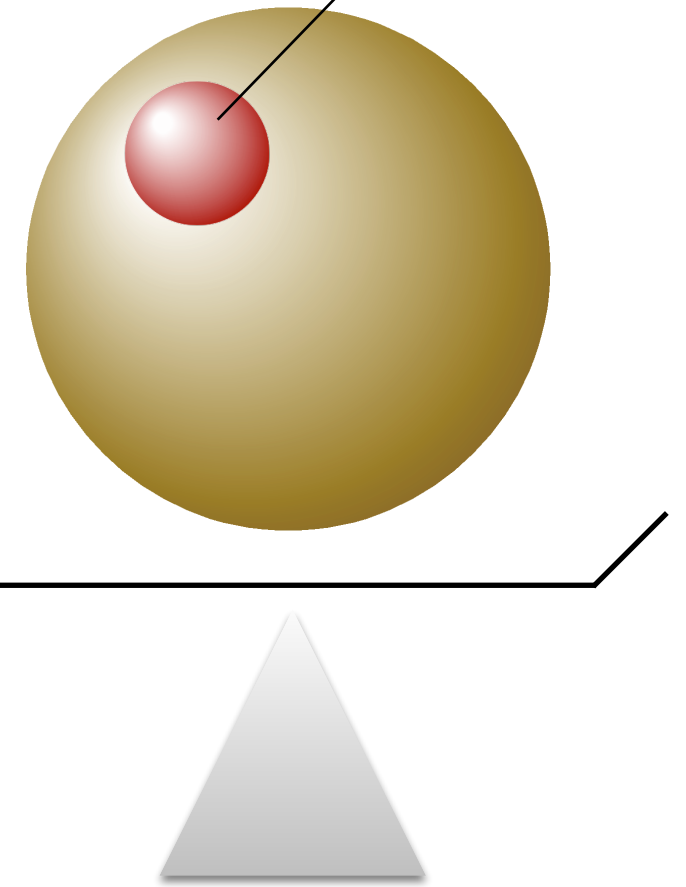
→ Kaonic nuclei $\rho > \rho_0$
 $\Lambda(1405)$

Relation to neutron stars

→ quantitative est. of **chiral condensate**
sensitivity to nuclear structure (neutron skins)

Hadrons as probes

$\pi, K^-, \eta, \eta' \dots$

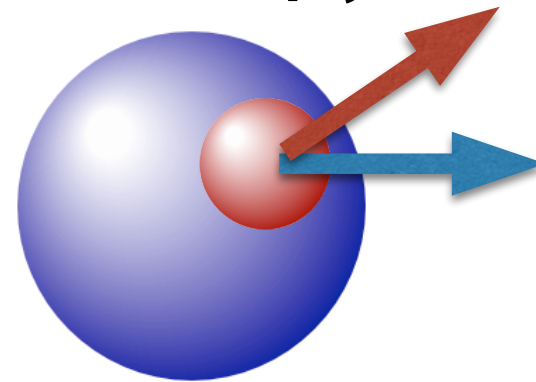


Experimental spectroscopy of meson in nuclear matter

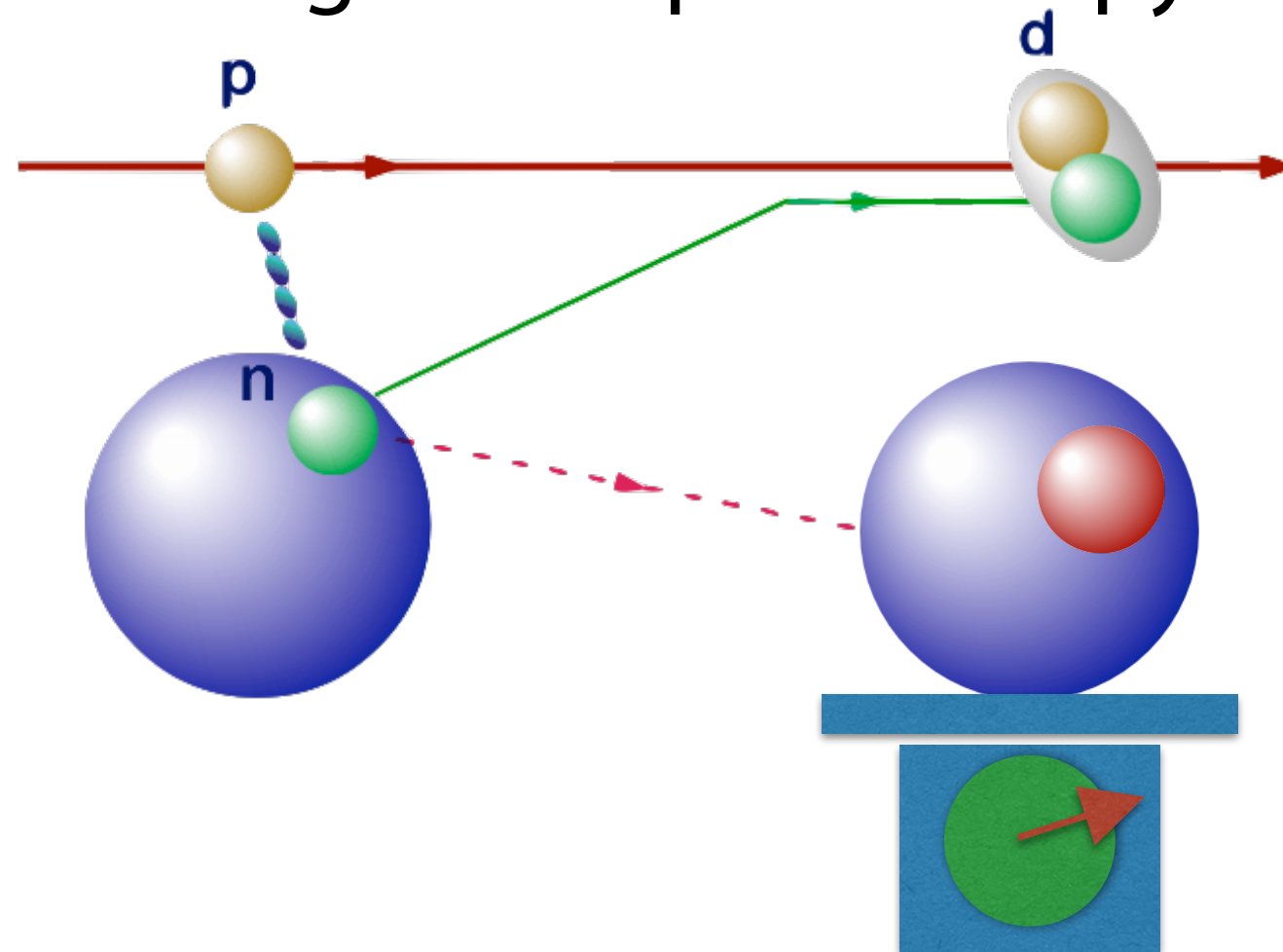
Experimental spectroscopy of meson in nuclear matter

Invariant mass spectroscopy

ex. $\phi \rightarrow e^+e^-$

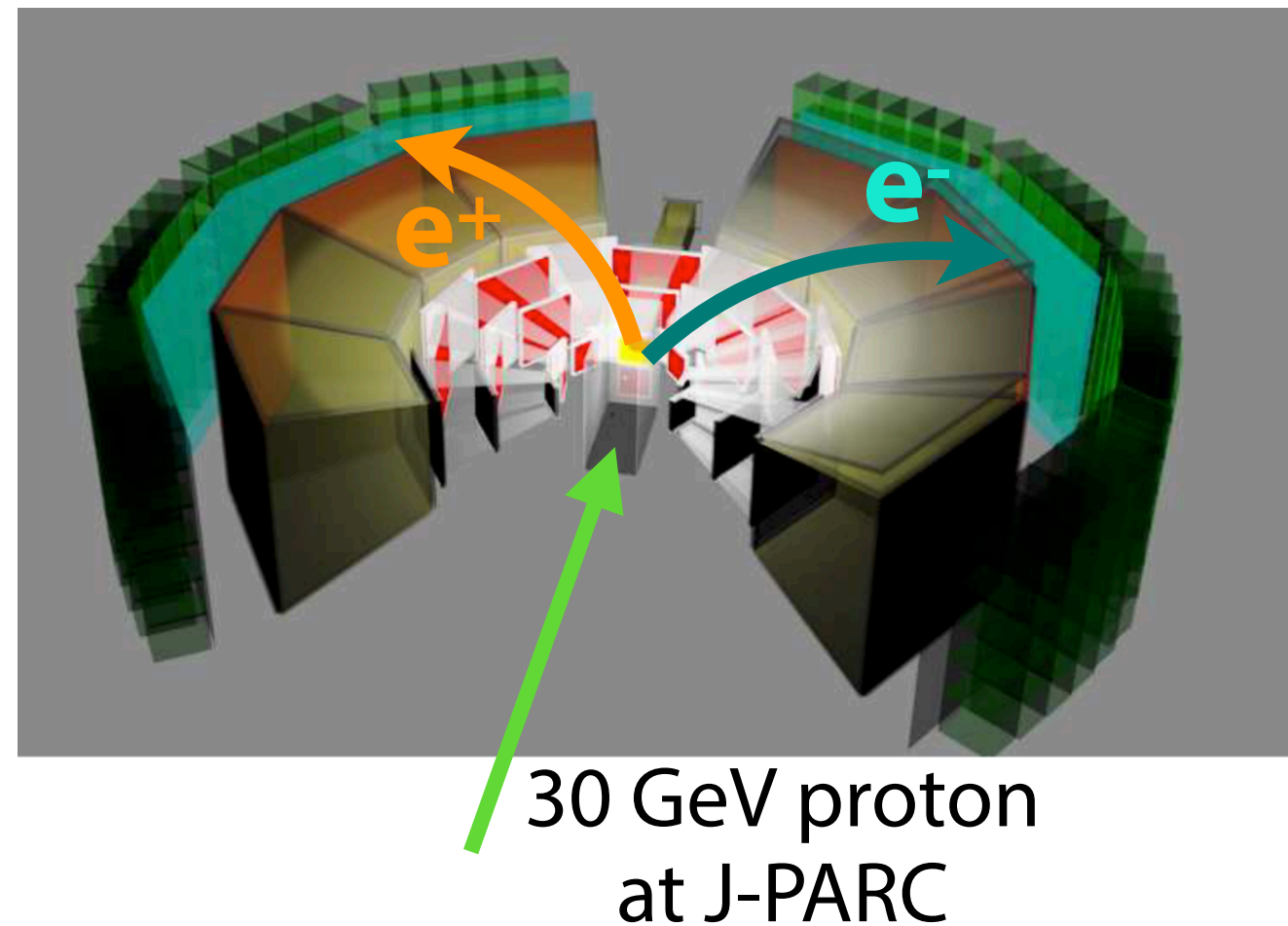
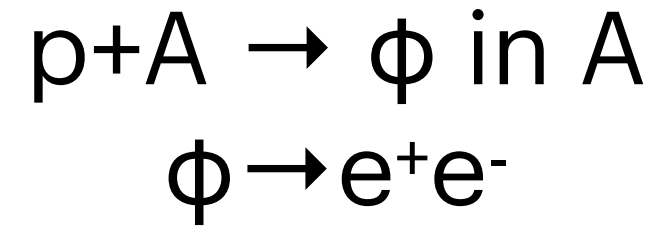
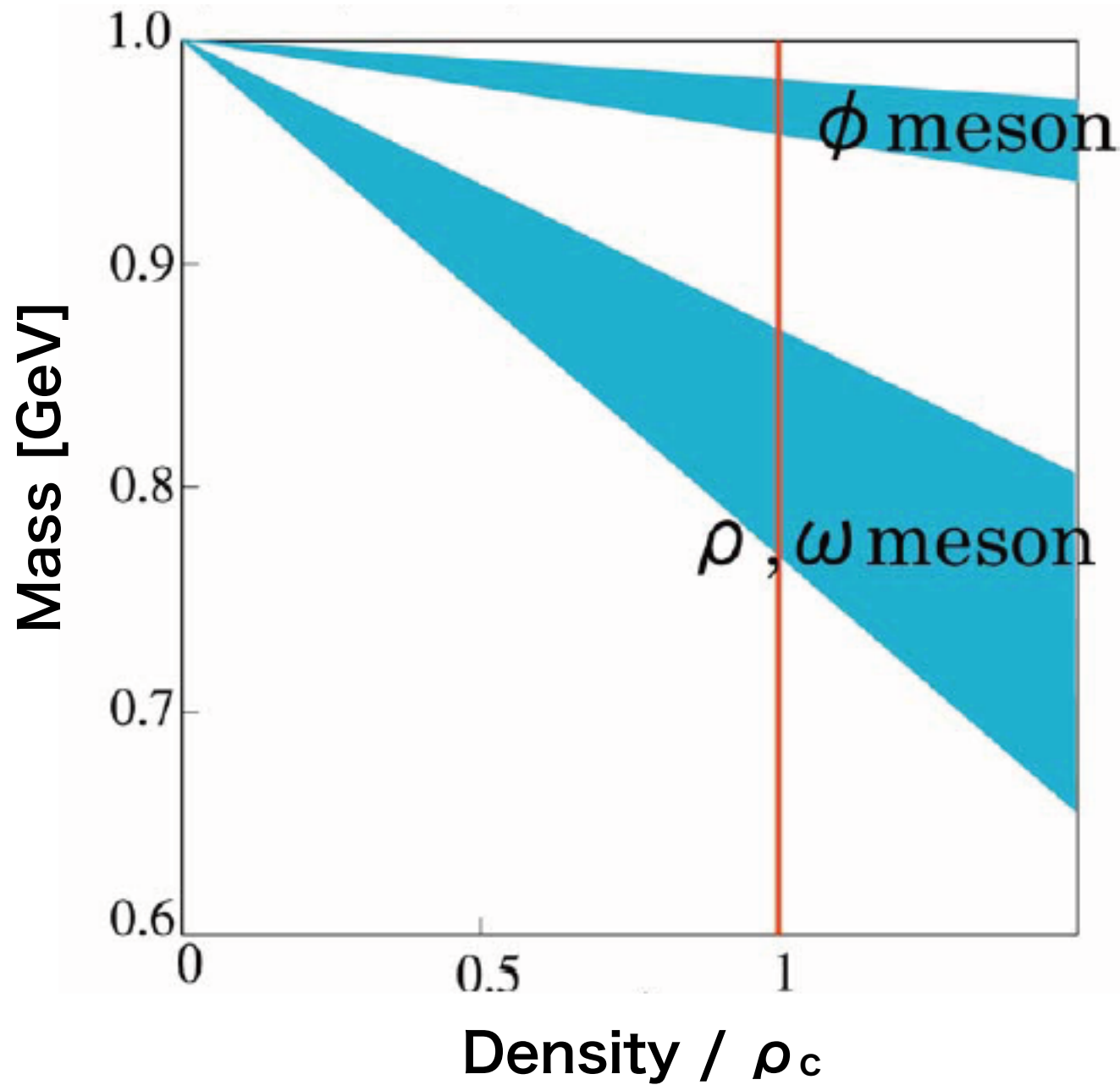


Missing mass spectroscopy



Meson masses and QCD medium effect

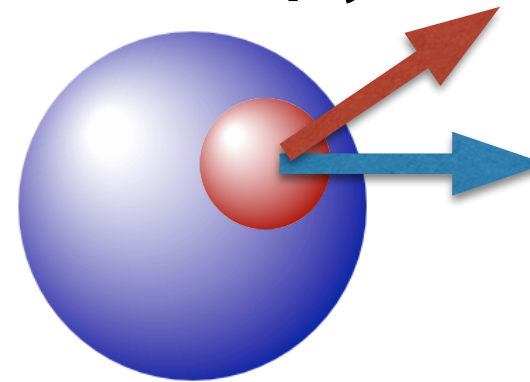
Vector meson mass modification (c.f. J-PARC E16)



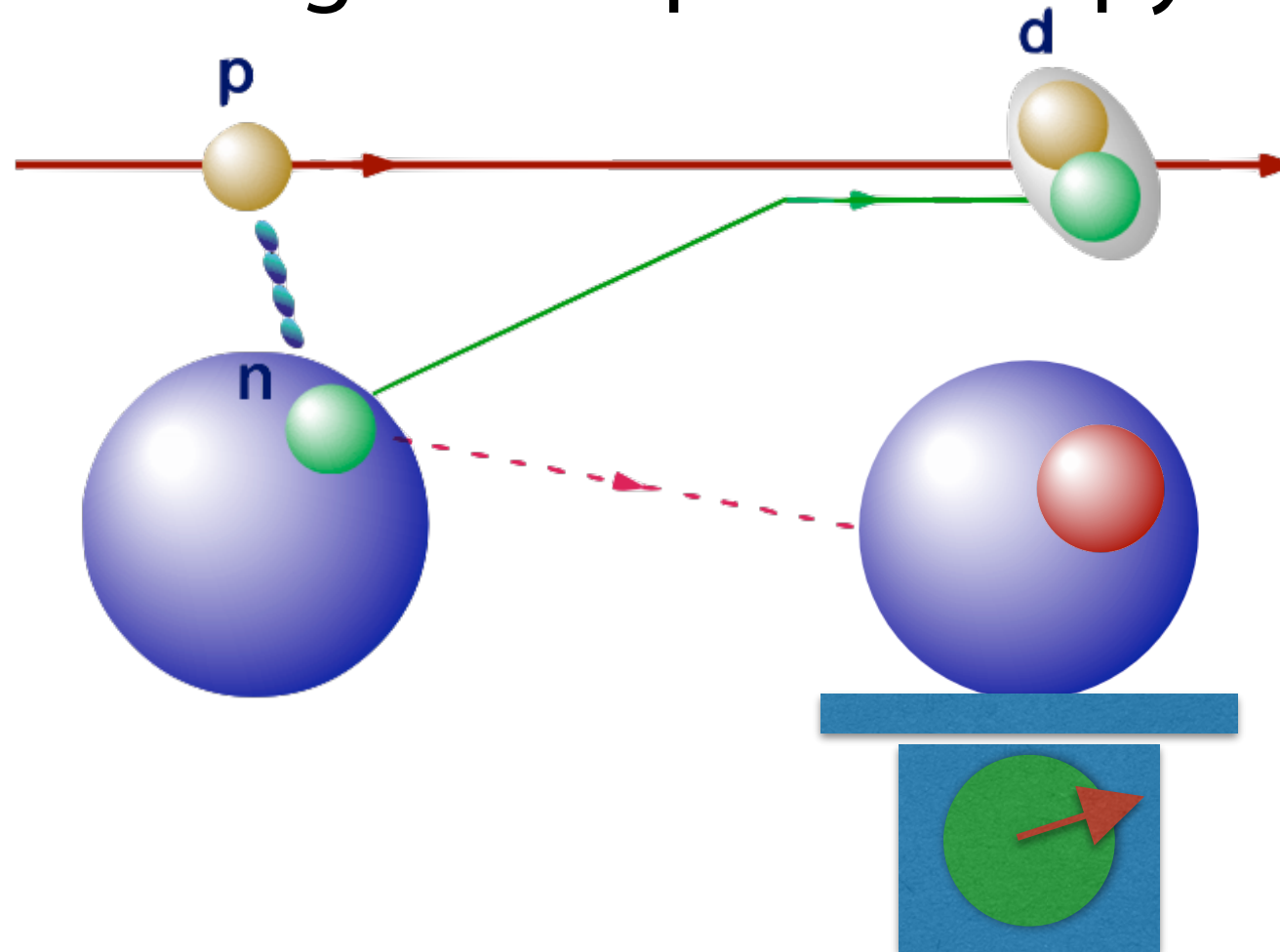
Experimental spectroscopy of meson in nuclear matter

Invariant mass spectroscopy

ex. $\phi \rightarrow e^+e^-$



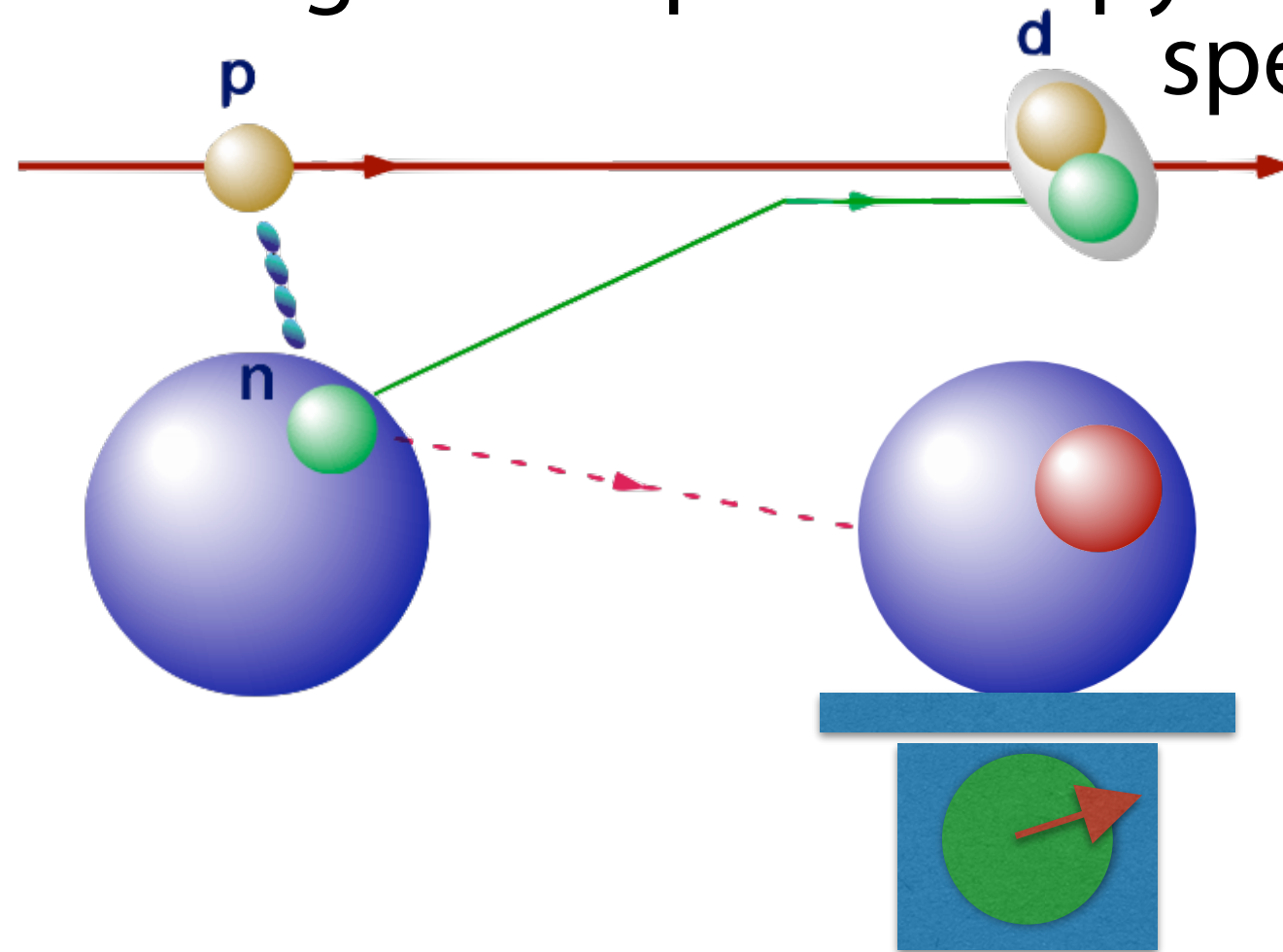
Missing mass spectroscopy



Experimental spectroscopy of meson in nuclear matter

- **Quantum object**
including meson + nuclei
- **Lorentz invariant**
isolated object in vacuum

Missing mass spectroscopy in reaction spectroscopy

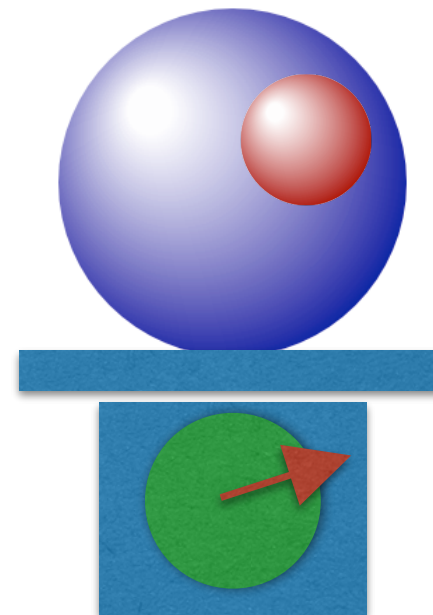


Experimental spectroscopy of meson in nuclear matter

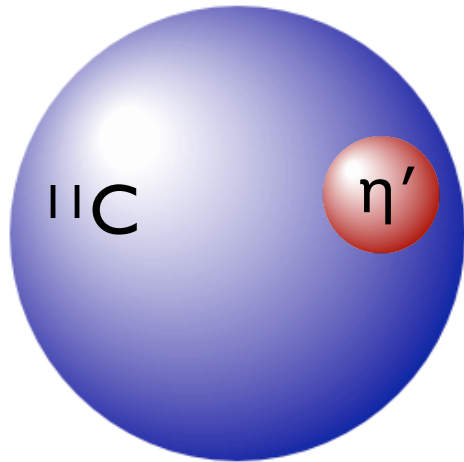
- **Quantum object**
including meson + nuclei
- **Lorentz invariant**
isolated object in vacuum

Missing mass spectroscopy in reaction spectroscopy

- **η' -mesic nuclei**
- **Pionic atoms**



Search for η' -mesic nuclei



System of an η' meson and a nucleus bound by the strong interaction

Spectroscopy η' -mesic nuclei provides information of the strong interaction leading to understanding of the origin of the very large mass of η' due to $\mathbf{U_A(1)}$ anomaly

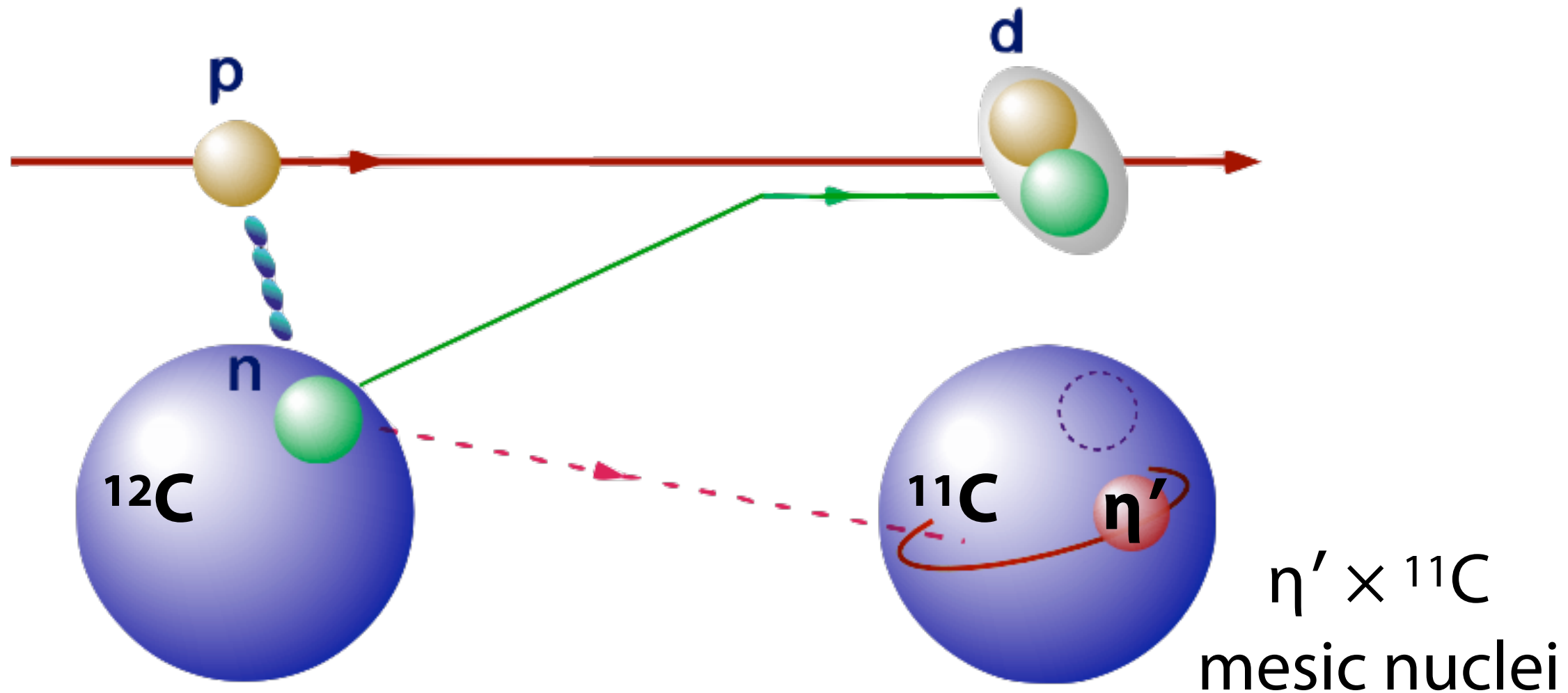
η problem

Mass of η' is much larger than quark model expectations

η' Mesic Nuclei in (p,d) Reaction

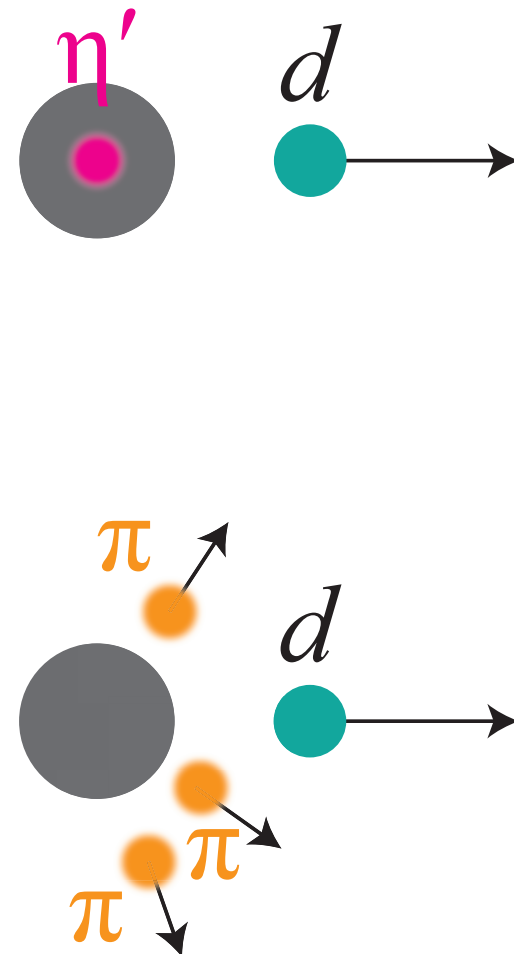
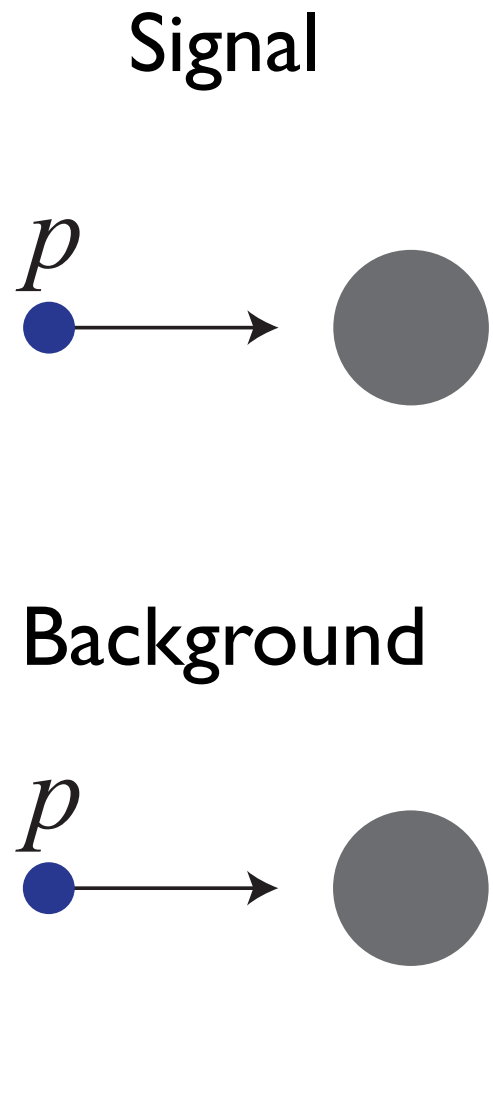
Missing mass measurement of

$(p,d) = \eta'$ transfer + neutron pickup reaction

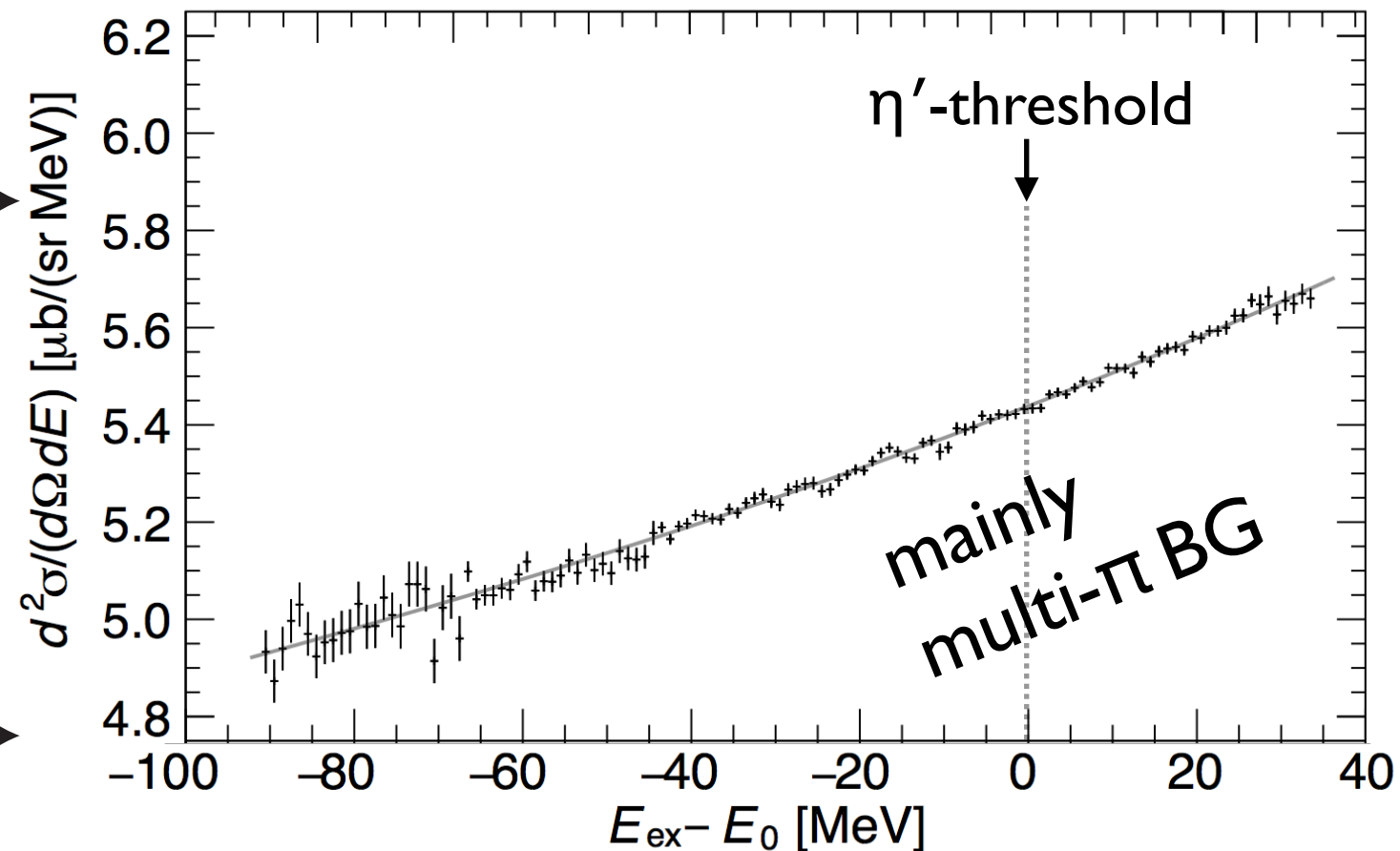


$$\underline{T_p = 2.50 \text{ GeV} \rightarrow q \sim 400 \text{ MeV}/c}$$

Step1: Missing-mass of (p,d) **inclusive** measurement



S437 $^{12}\text{C}(p,d)$ in 2014 at FRS/GSI

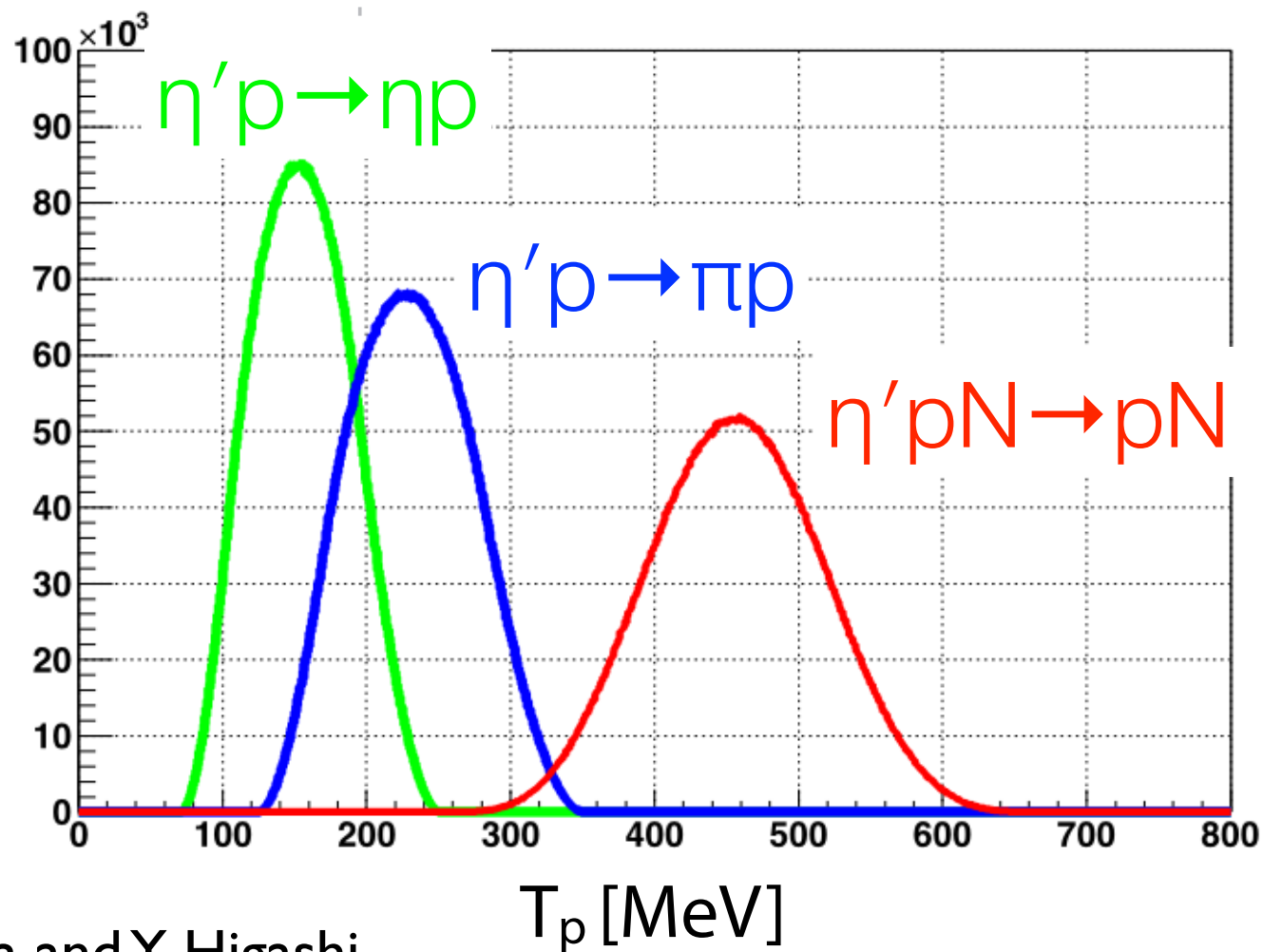
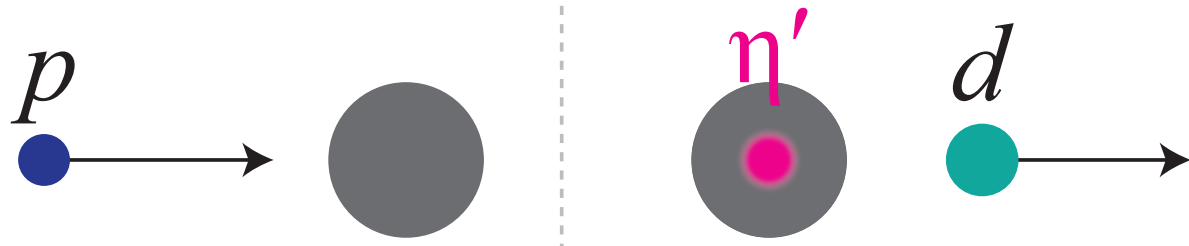


Y.K.Tanaka et al., Phys. Rev. Lett. **117**, 202501 (2016)

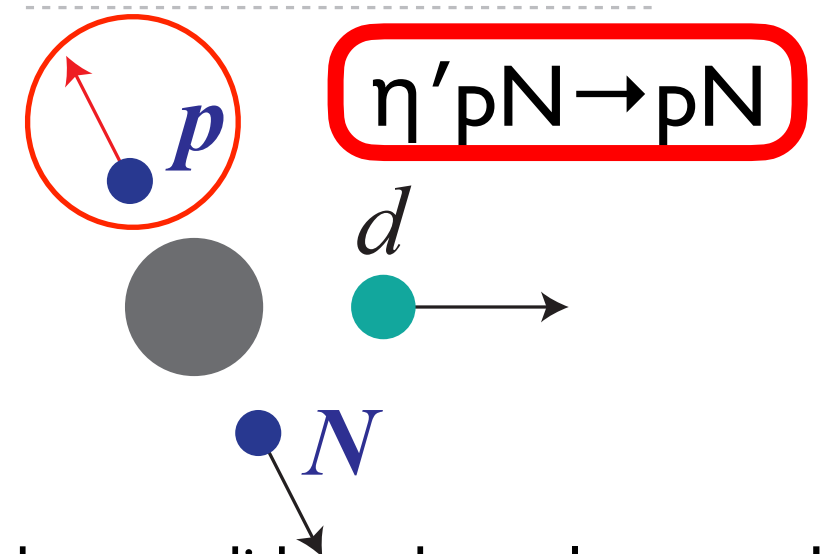
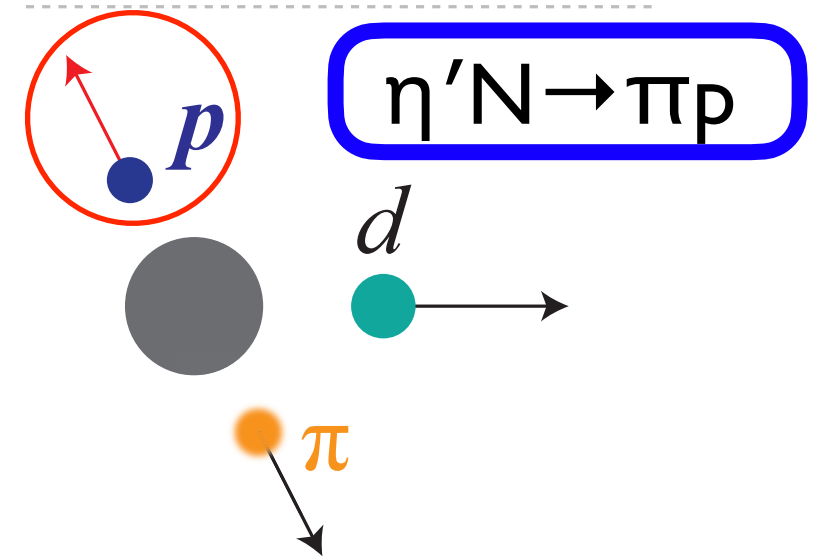
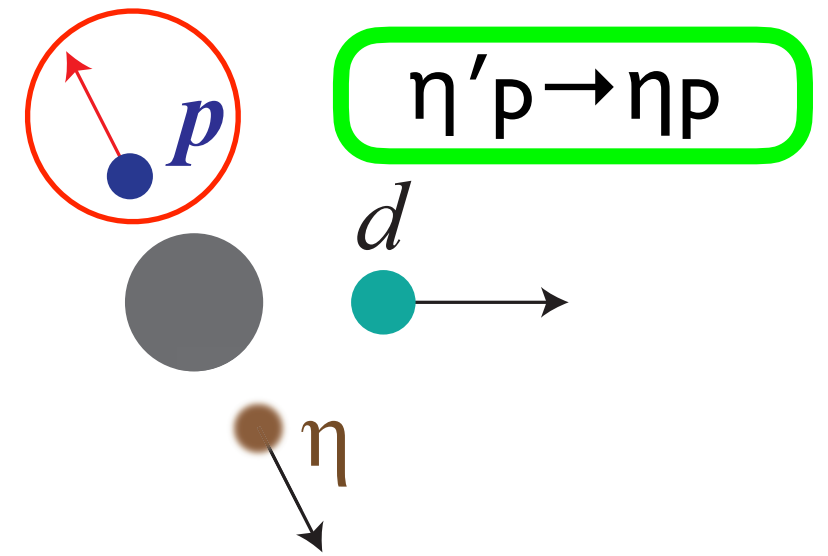
We achieved extremely high statistical sensitivity demonstrating very good performance of FRS. But, no peak was observed. Major BG=multi π . S/BG cross sections must be $\sim 1/100$

Step 2: **Semi-exclusive** measurement of $^{12}\text{C}(p,dp)$ reaction (GSI-S490, 2022)

Signal



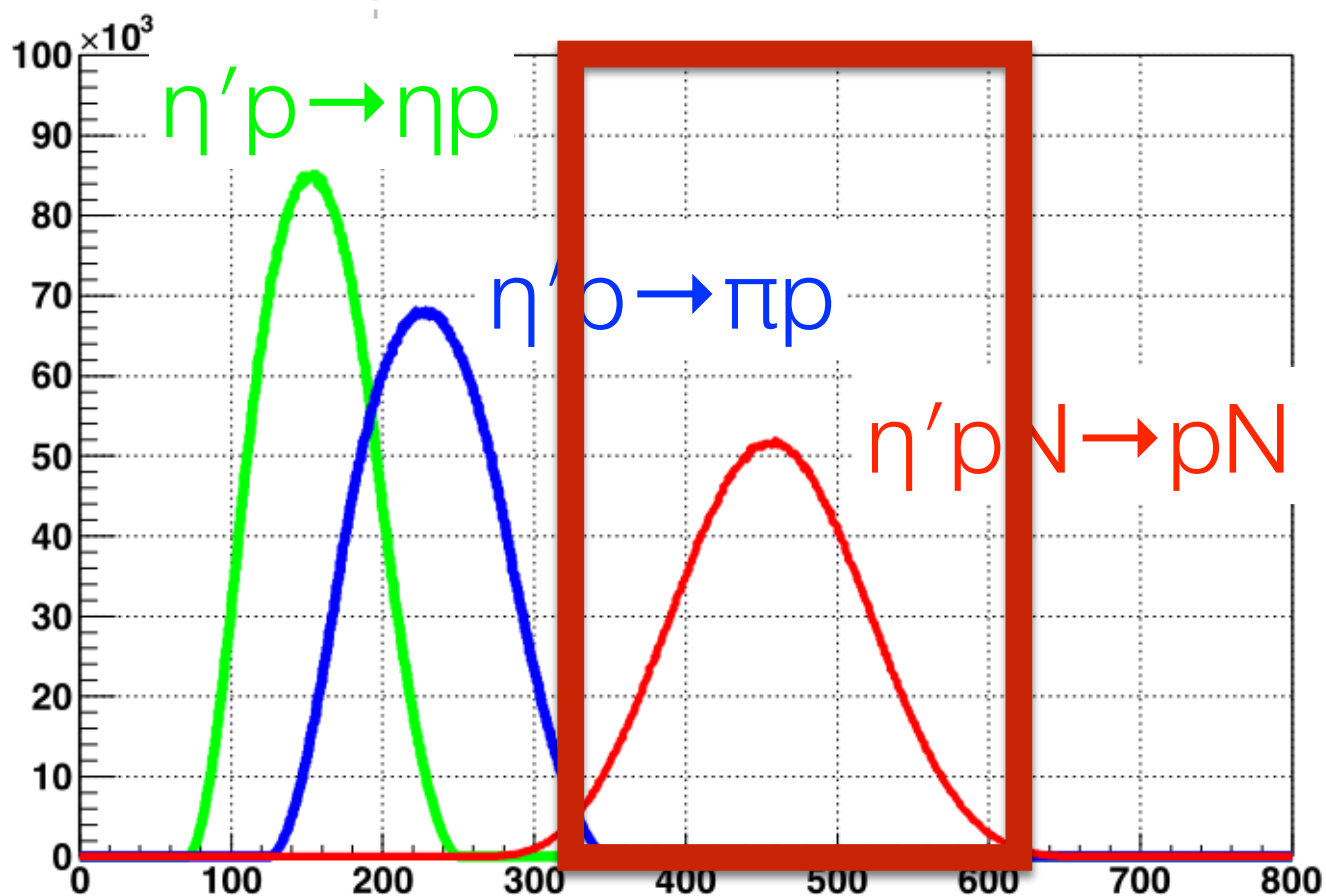
3 major decay modes of η' -mesic nuclei



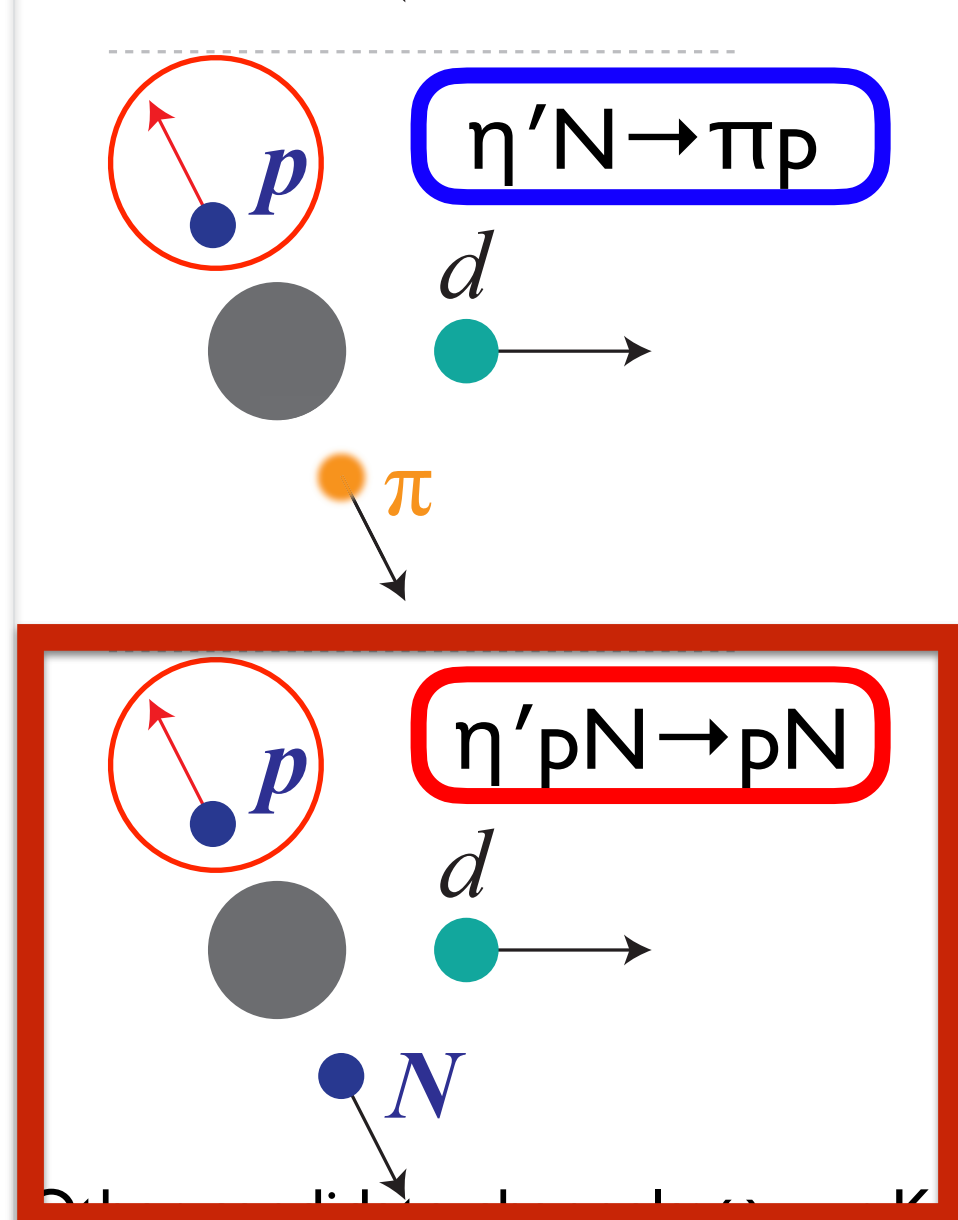
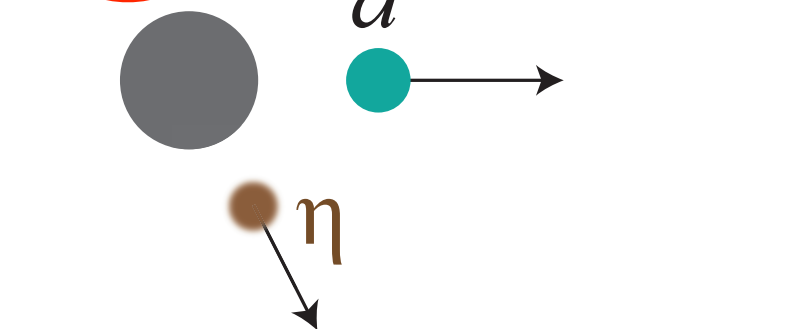
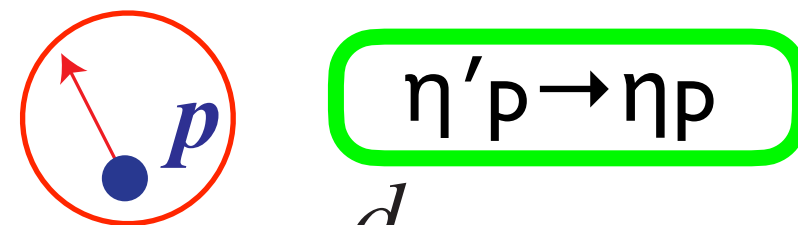
Step 2: Semi-exclusive measurement of $^{12}\text{C}(p,dp)$ reaction (GSI-S490, 2022)

p

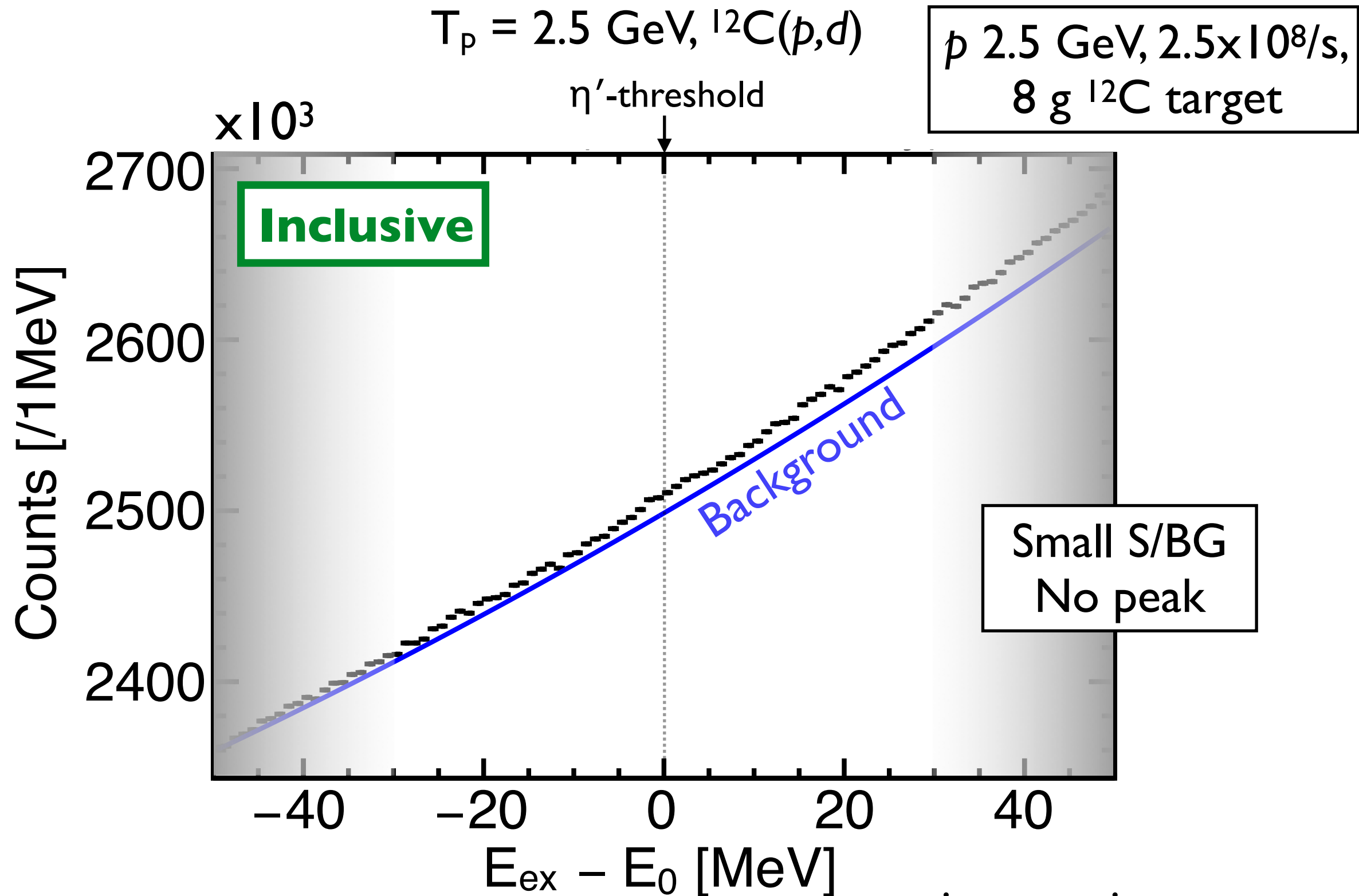
Detect p (300-600 MeV) emitted in the decay of η' -nuclei for semi-exclusive measurement.
 $f \sim 100$ improvement in S/BG



3 major decay modes of η' -mesic nuclei



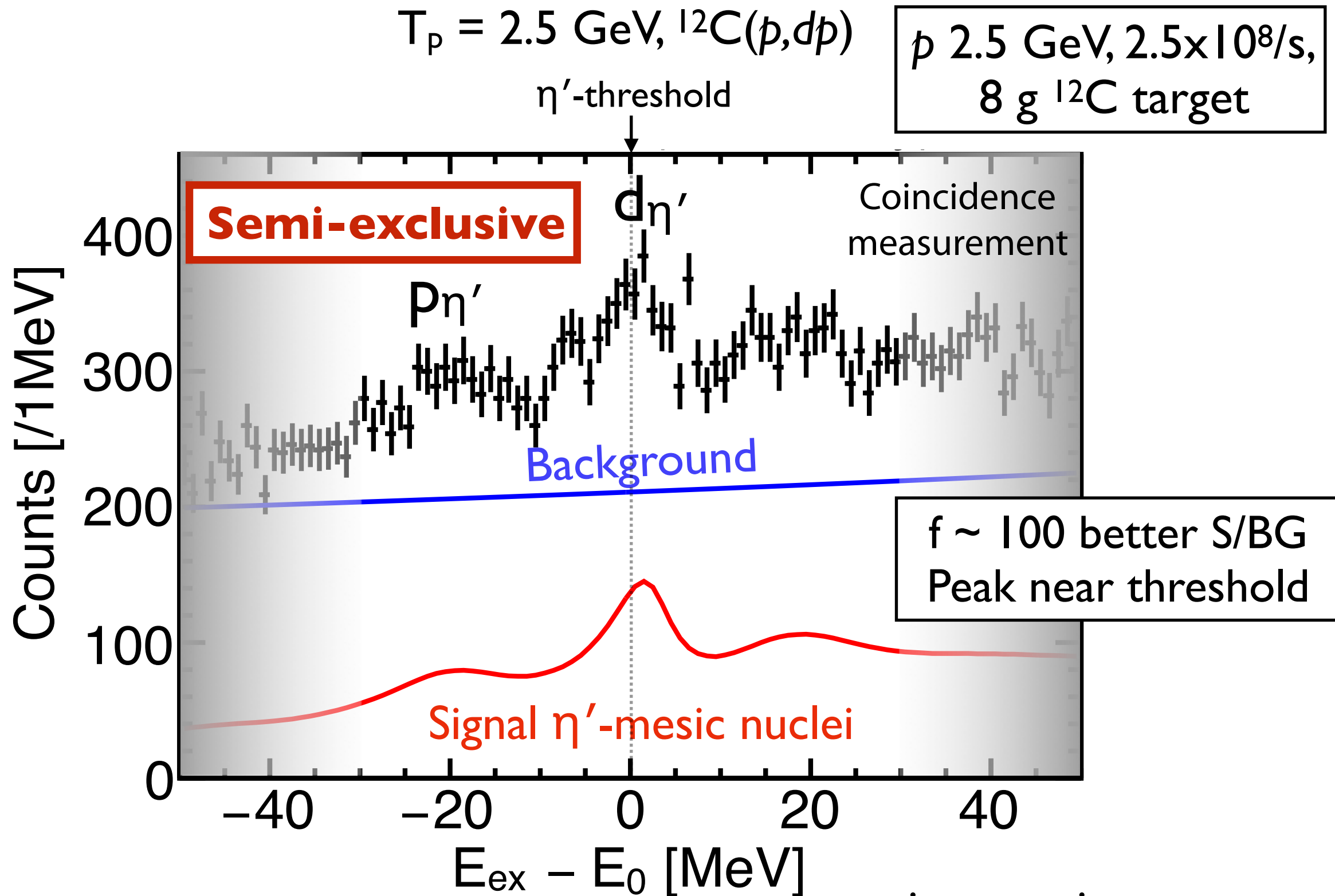
Expected spectrum in 4 days of DAQ at FRS



A: $U(r=0) = -90 - 17i \text{ MeV}$
a parameter set of chiral unitary model

microscopic transport
simulation

Expected spectrum in 4 days of DAQ at FRS

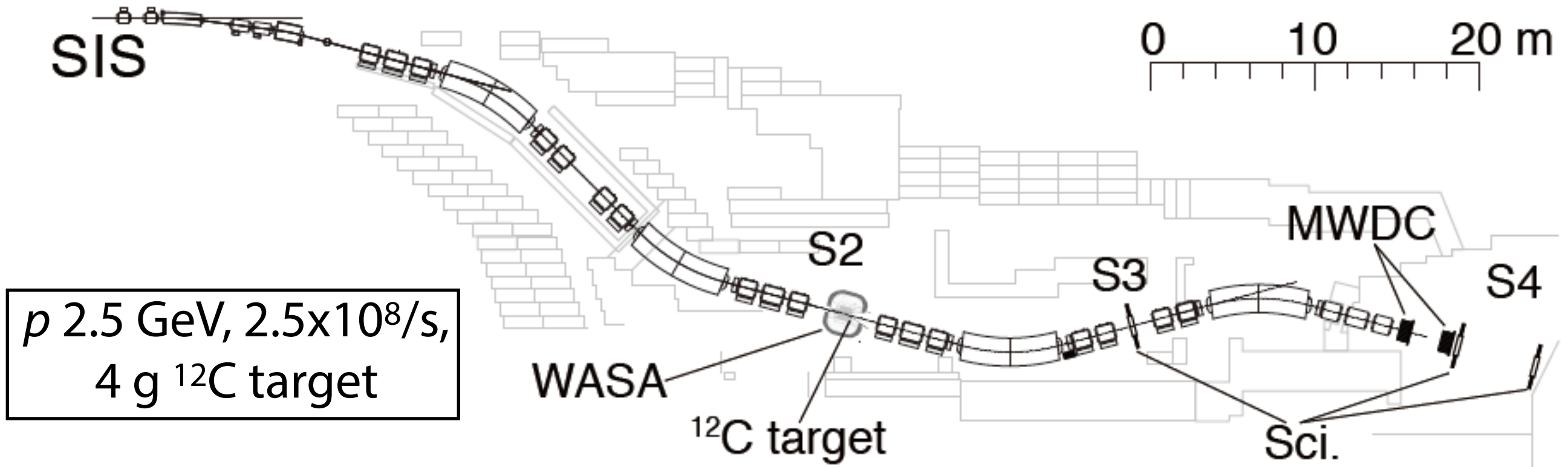


A: $U(r=0) = -90 - 17i \text{ MeV}$
 a parameter set of chiral unitary model

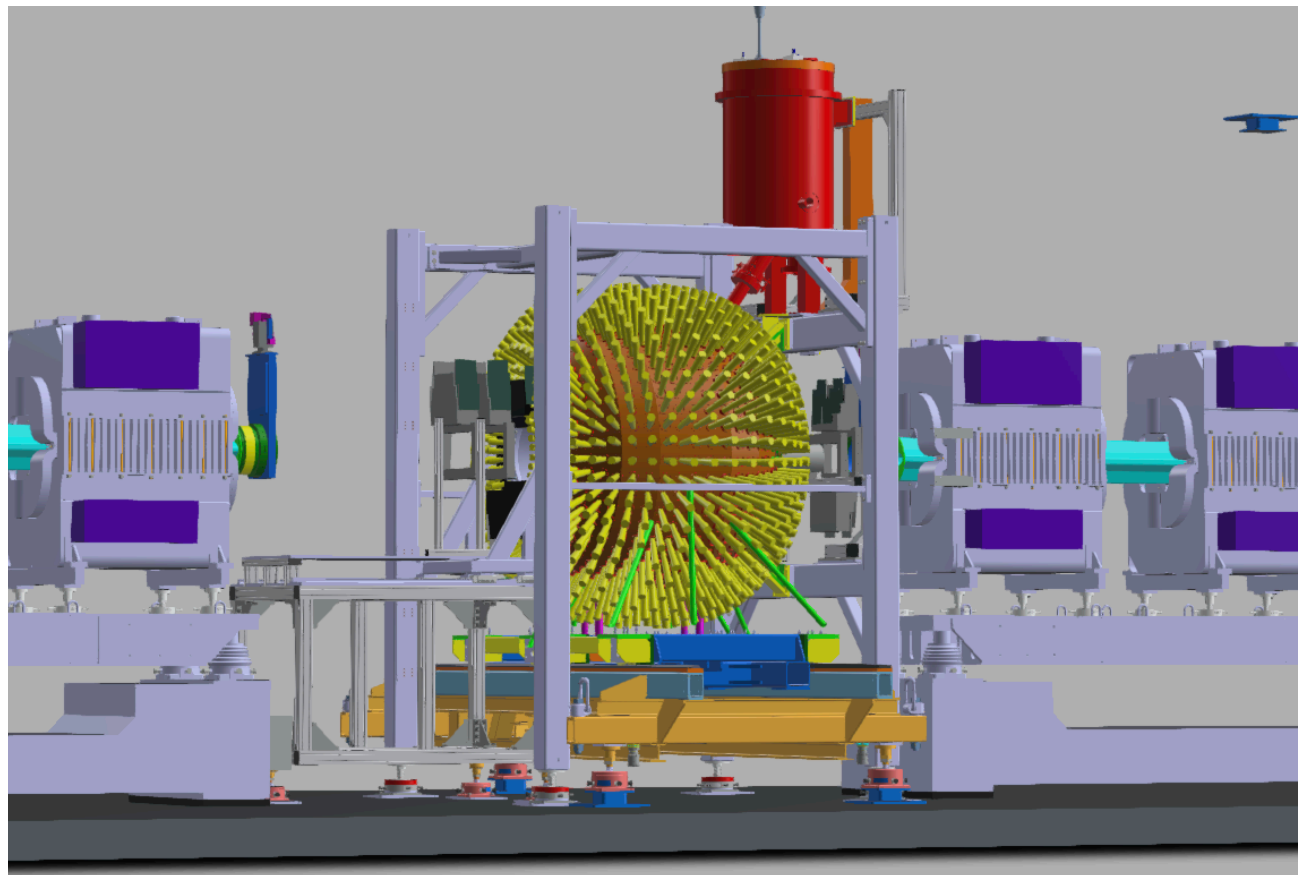
microscopic transport
simulation

Experimental setup

S457- η'



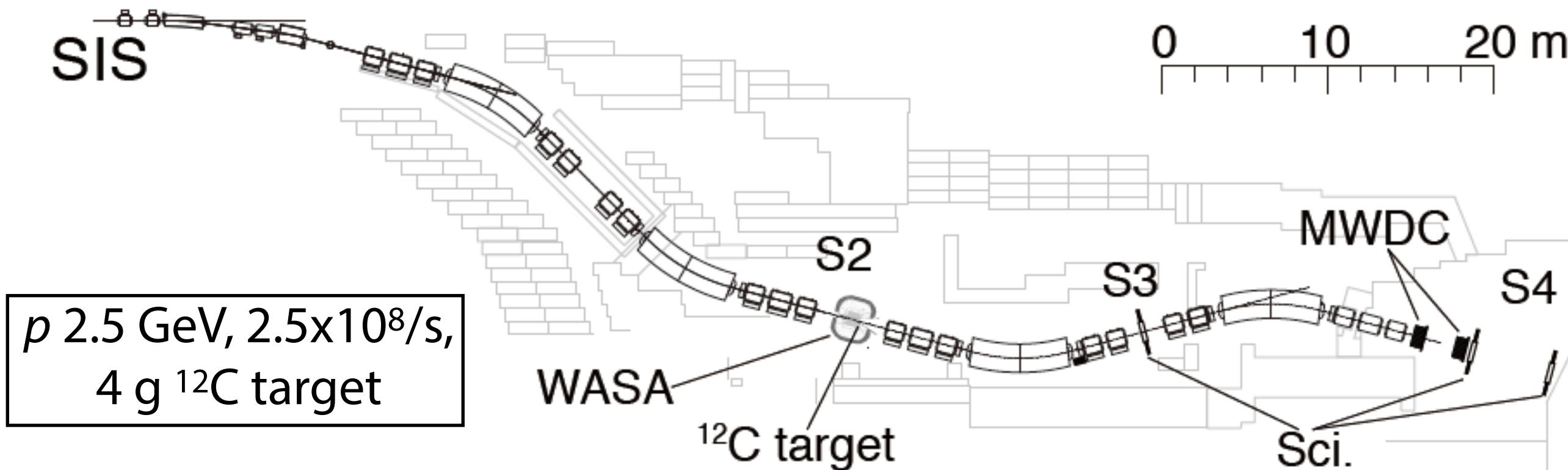
WASA in S2



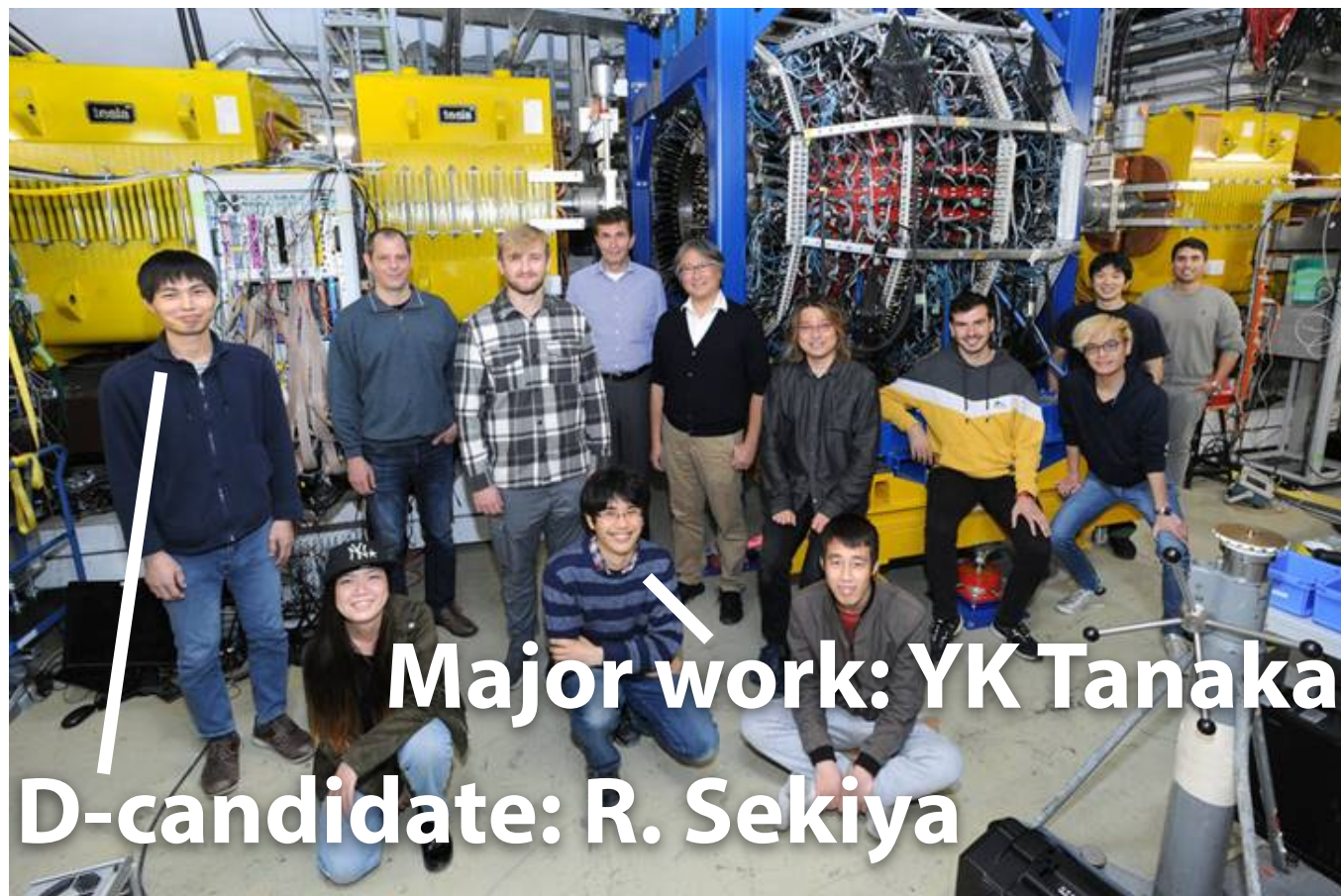
FRS S2-S2: forward spectrometer with ~ 2.5 MeV energy resolution
WASA: $\eta' NN \rightarrow NN$ tagging

Experimental setup

S457- η'



Together with HypHI exp.



Expected rates

@S4

40 kHz (proton)

150 Hz (deuteron)

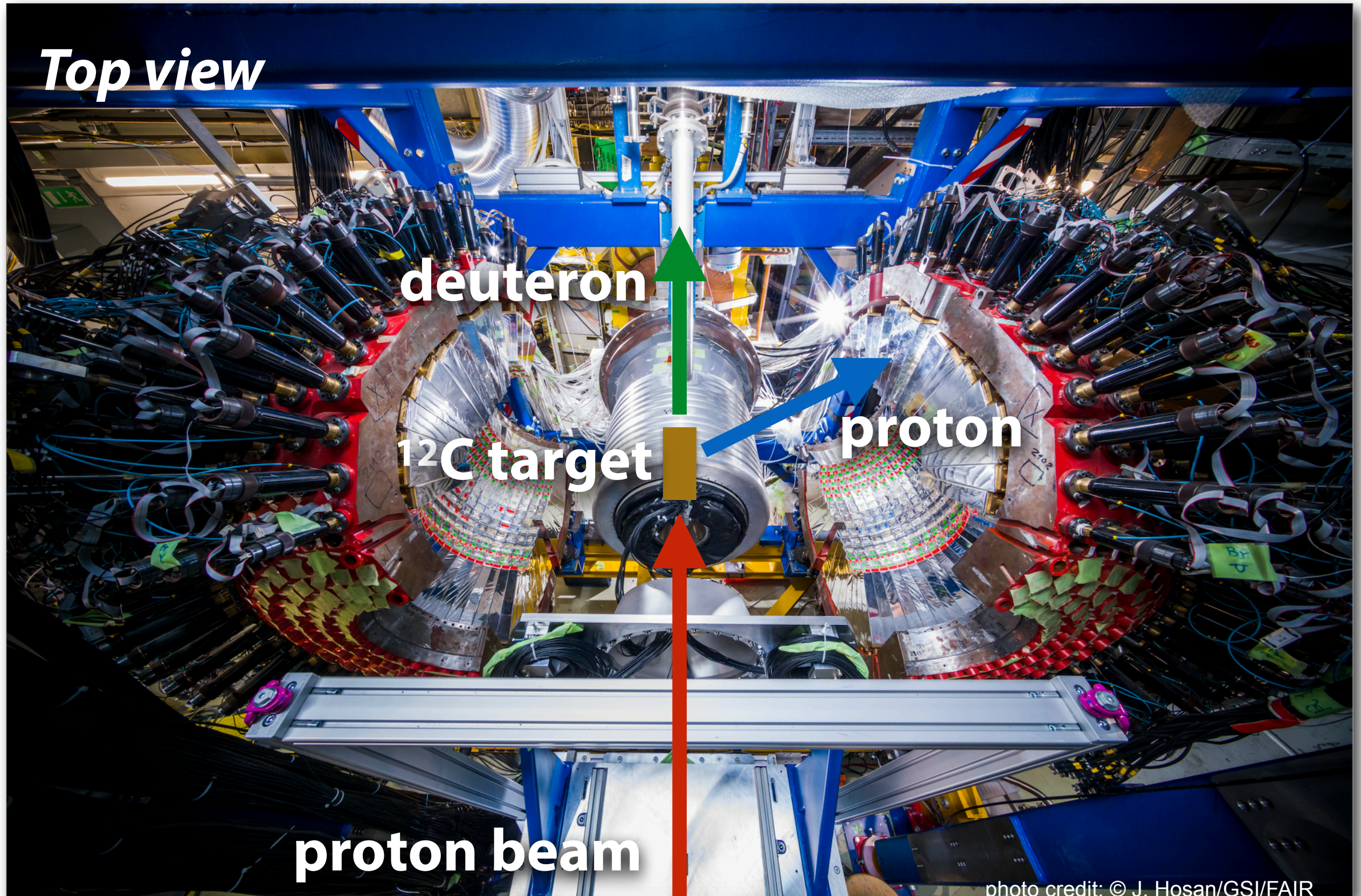
@WASA

10 MHz (π)

25 MHz (proton)

Support from WASA-at-COSY
Esp. Prof. P. Moskal (Krakow)

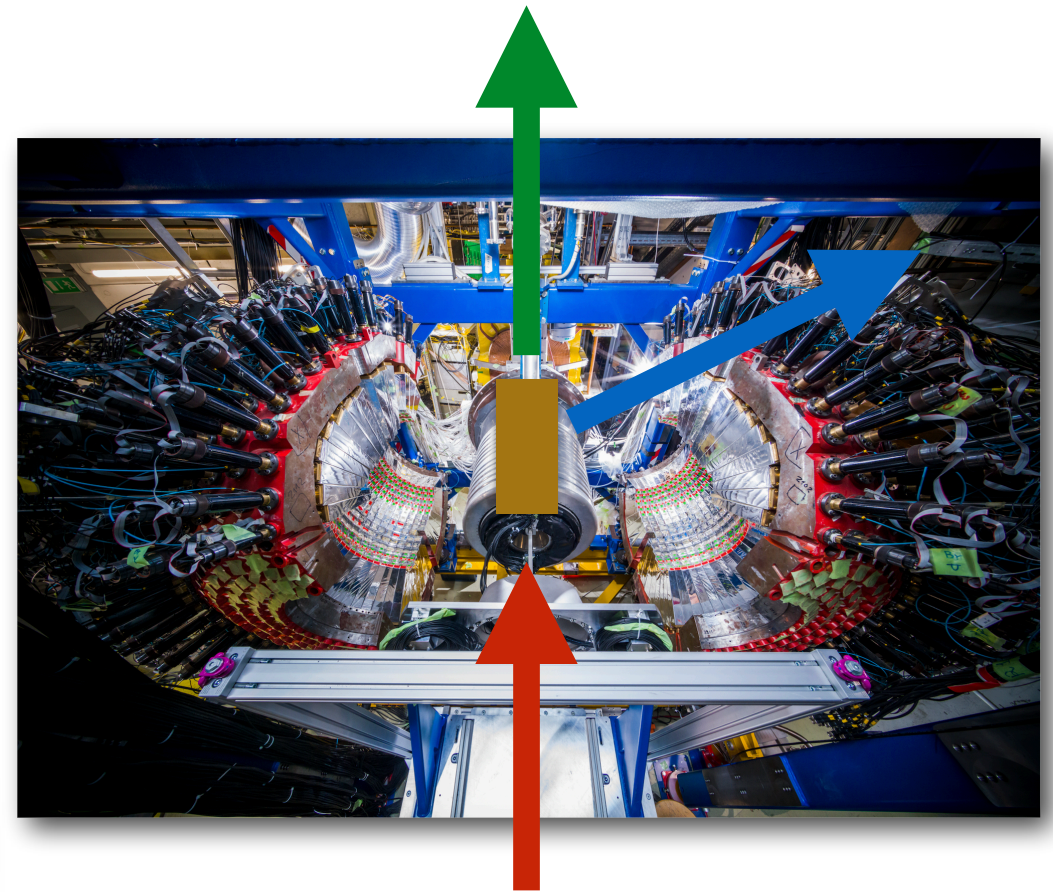
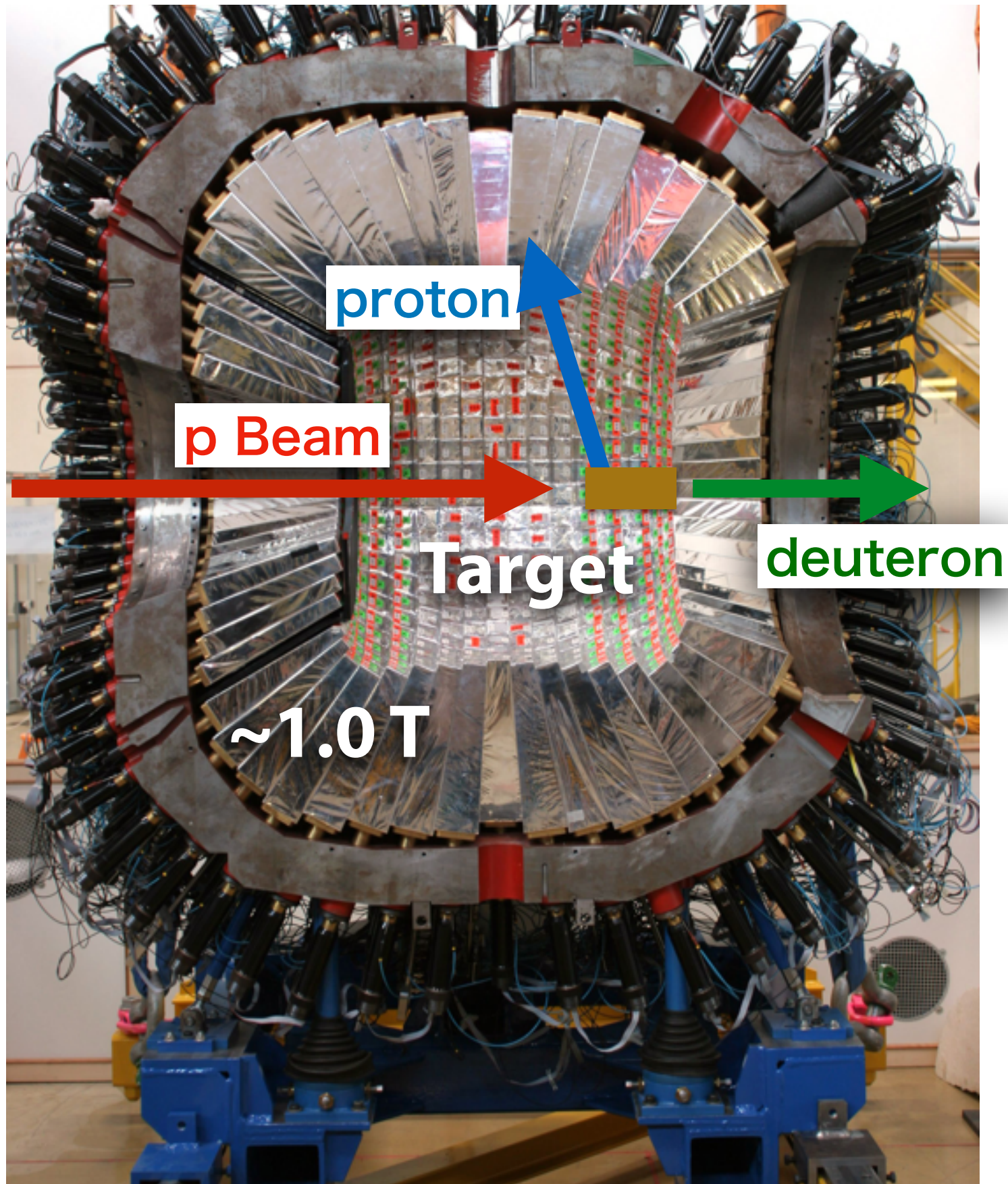
GSI-S490 WASA at FRS for η' mesic nuclei(2022)



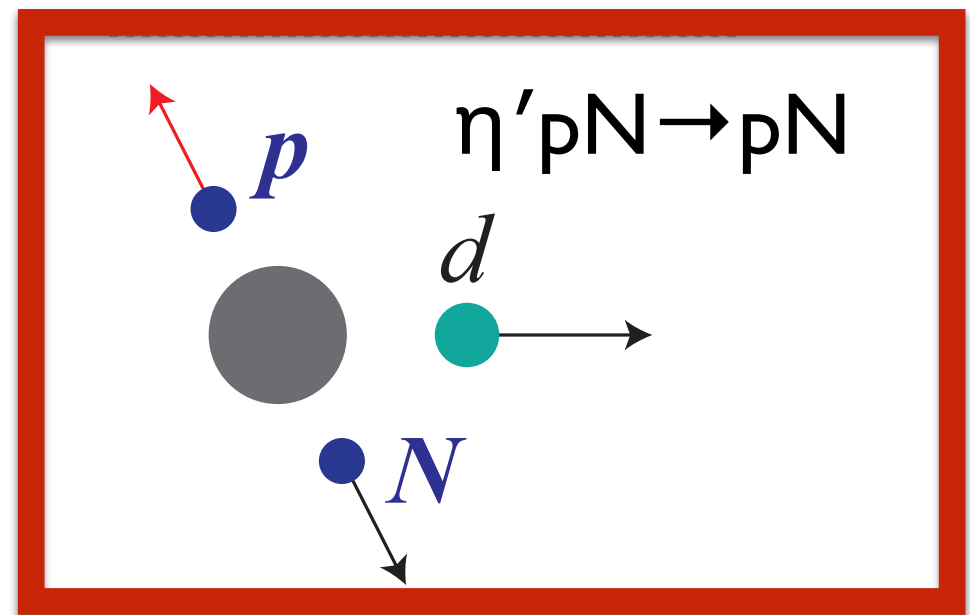
S490 Spokesperson: KI
co-Spokesperson: Y.K. Tanaka

D-candidate: R. Sekiya

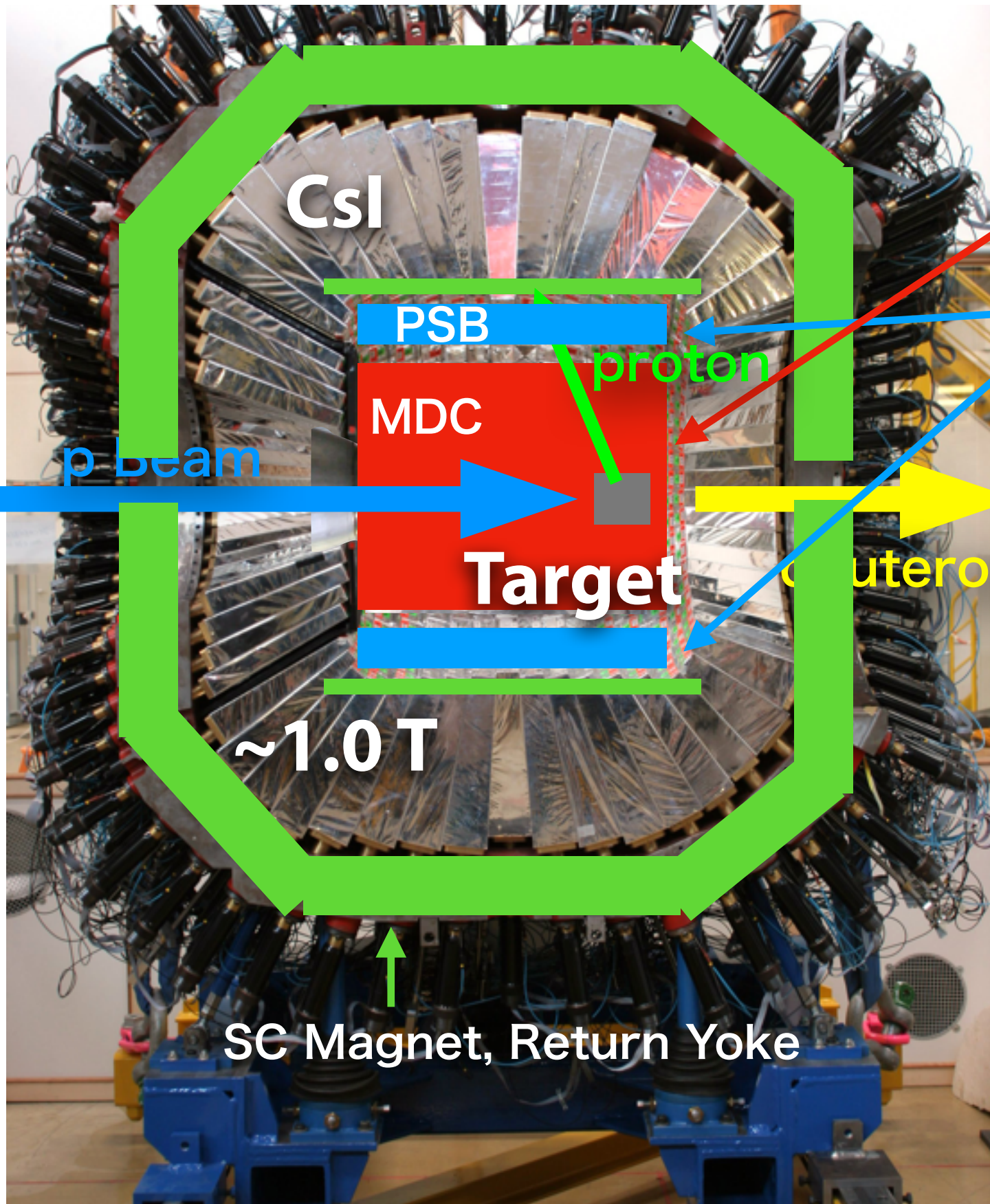
Detectors in WASA



High energy proton tagging
in coincidence with *forward d*

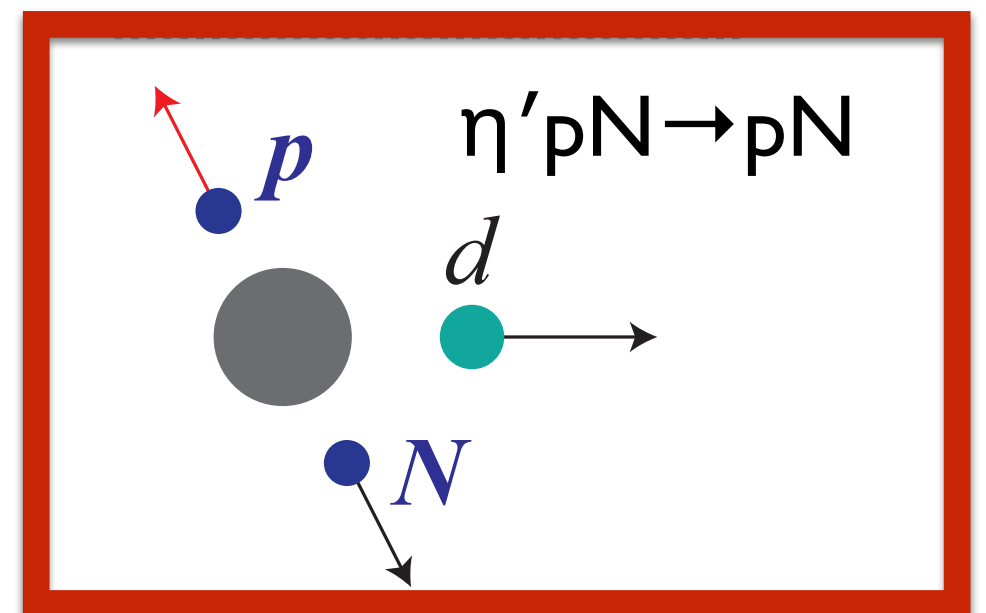


Detectors in WASA

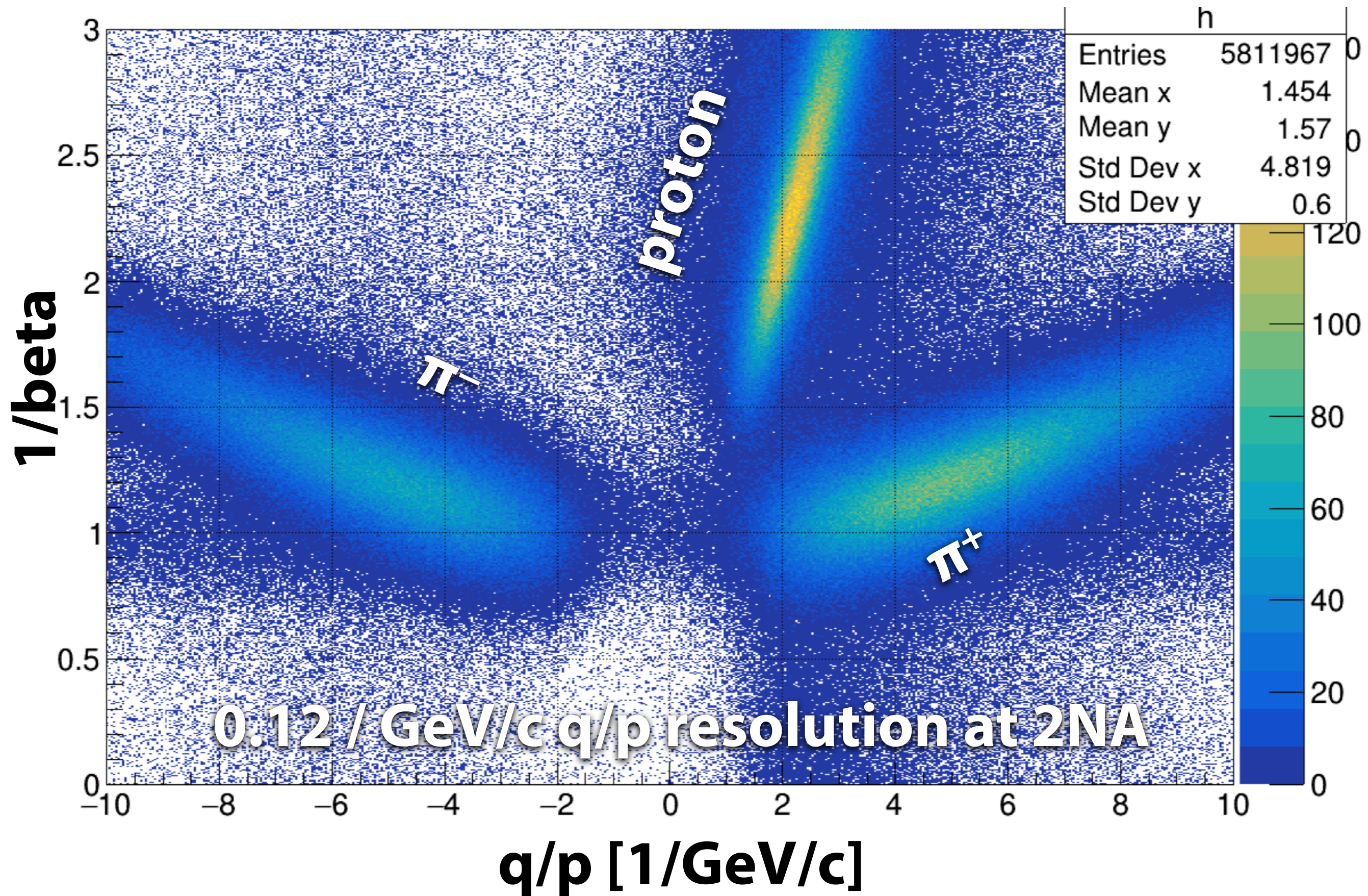


- MDC (Mini Drift Chamber)
Charged particle tracking
- PSB (Plastic Scintillator Barrel)
 ΔE + Timing measurement
- CsI
 γ detection for calibration

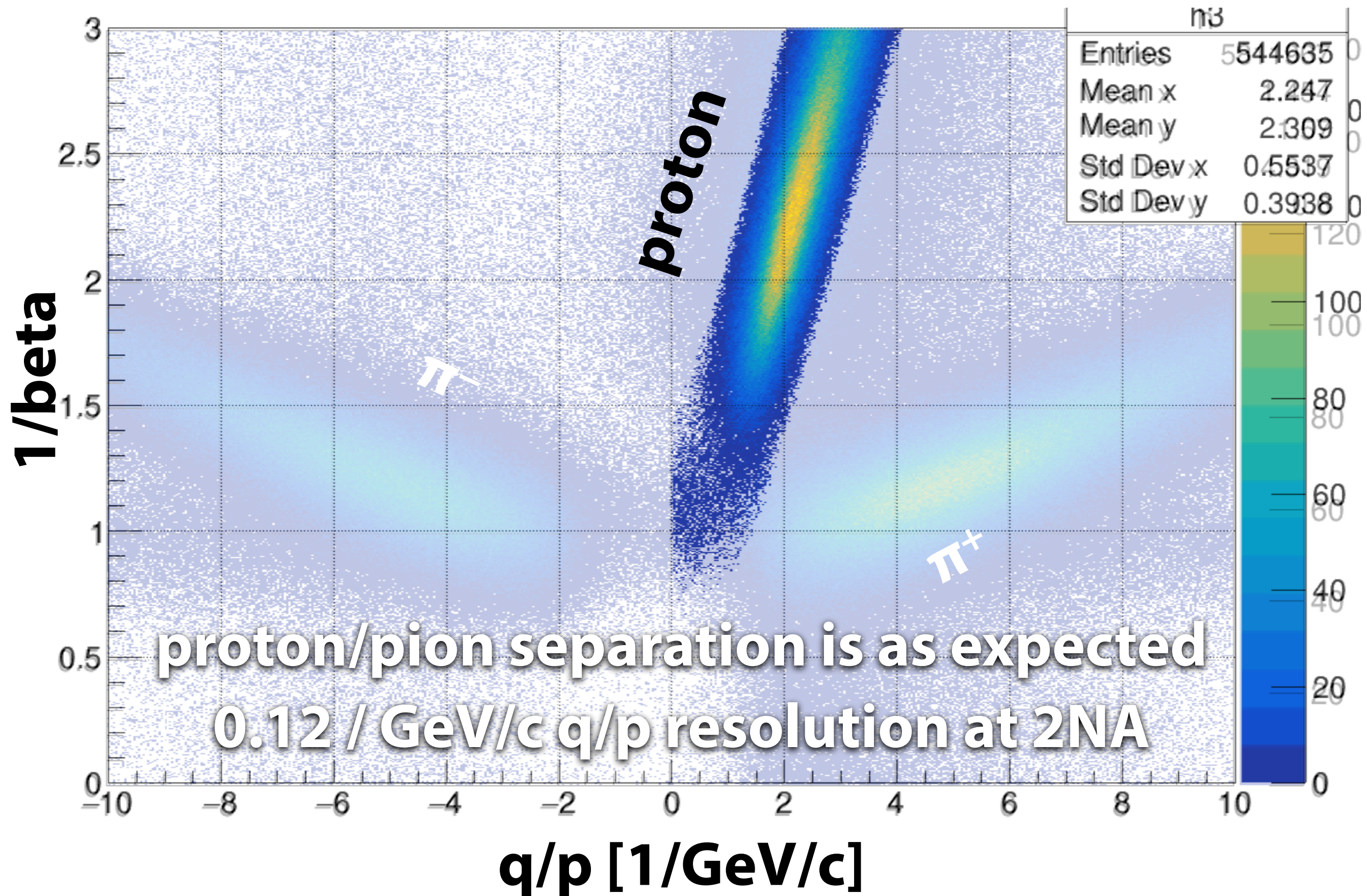
High energy proton tagging
in coincidence with *forward d*



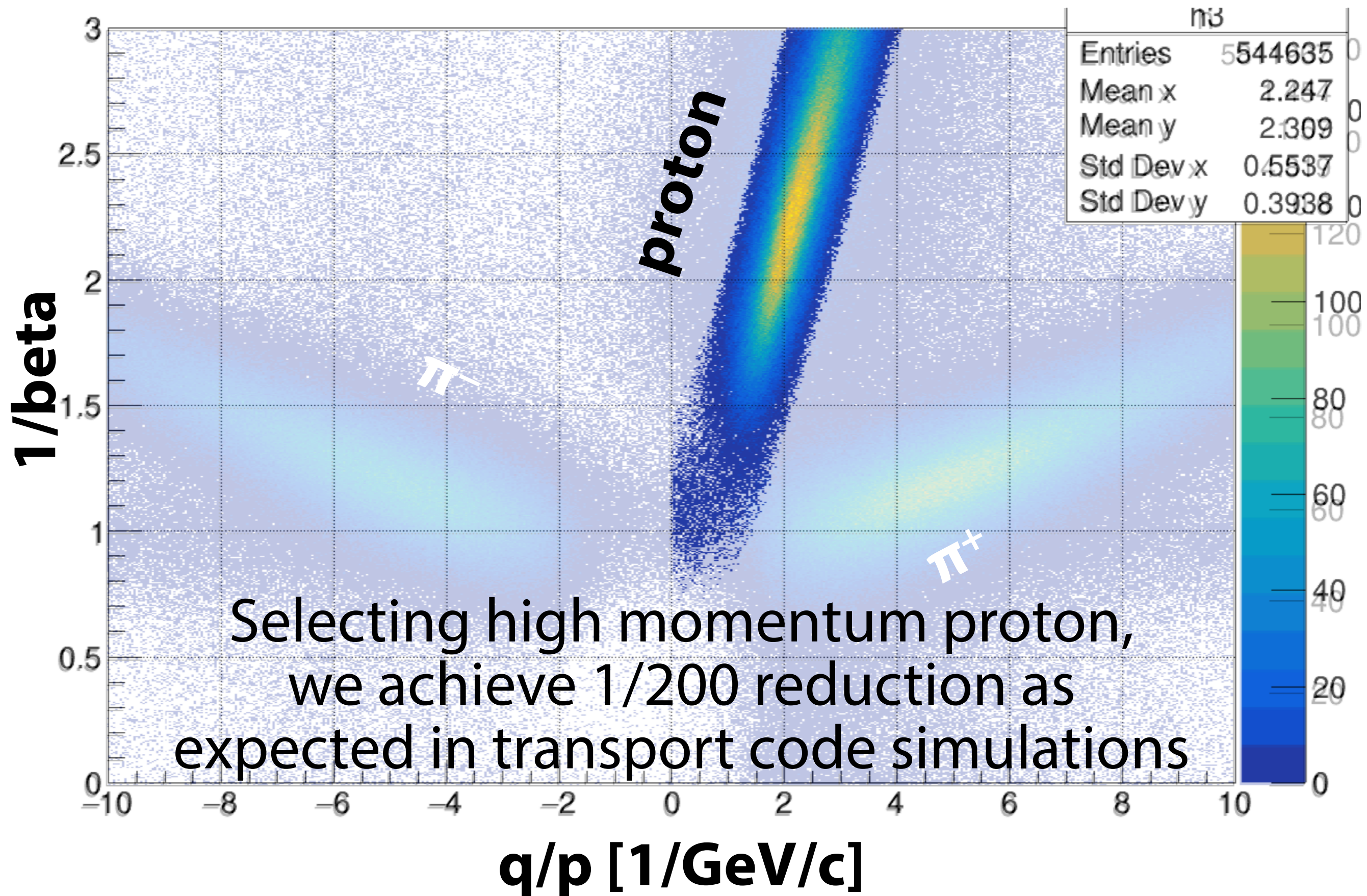
$\eta' NN \rightarrow NN$ tagging in WASA



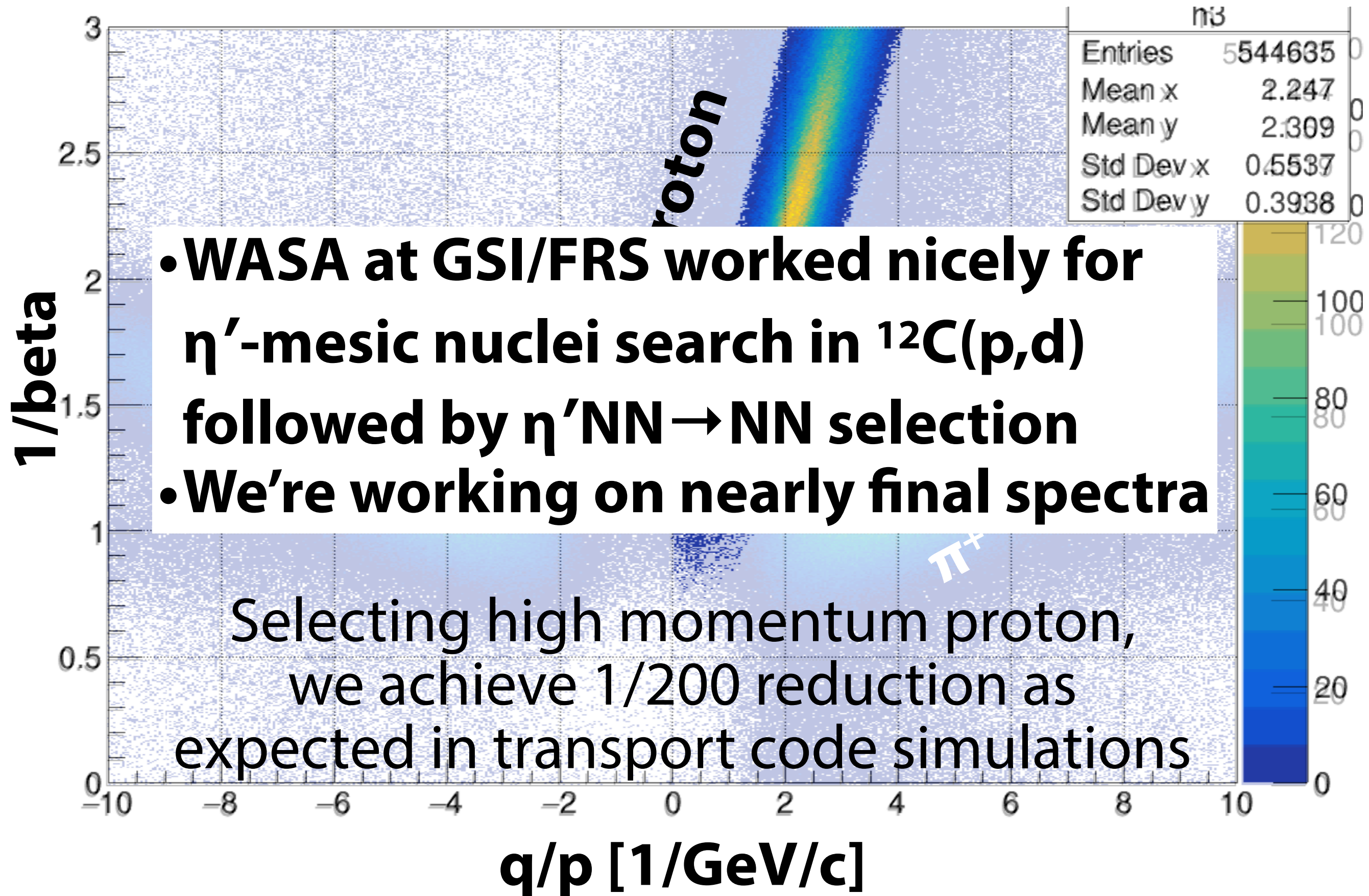
η' NN \rightarrow NN tagging in WASA



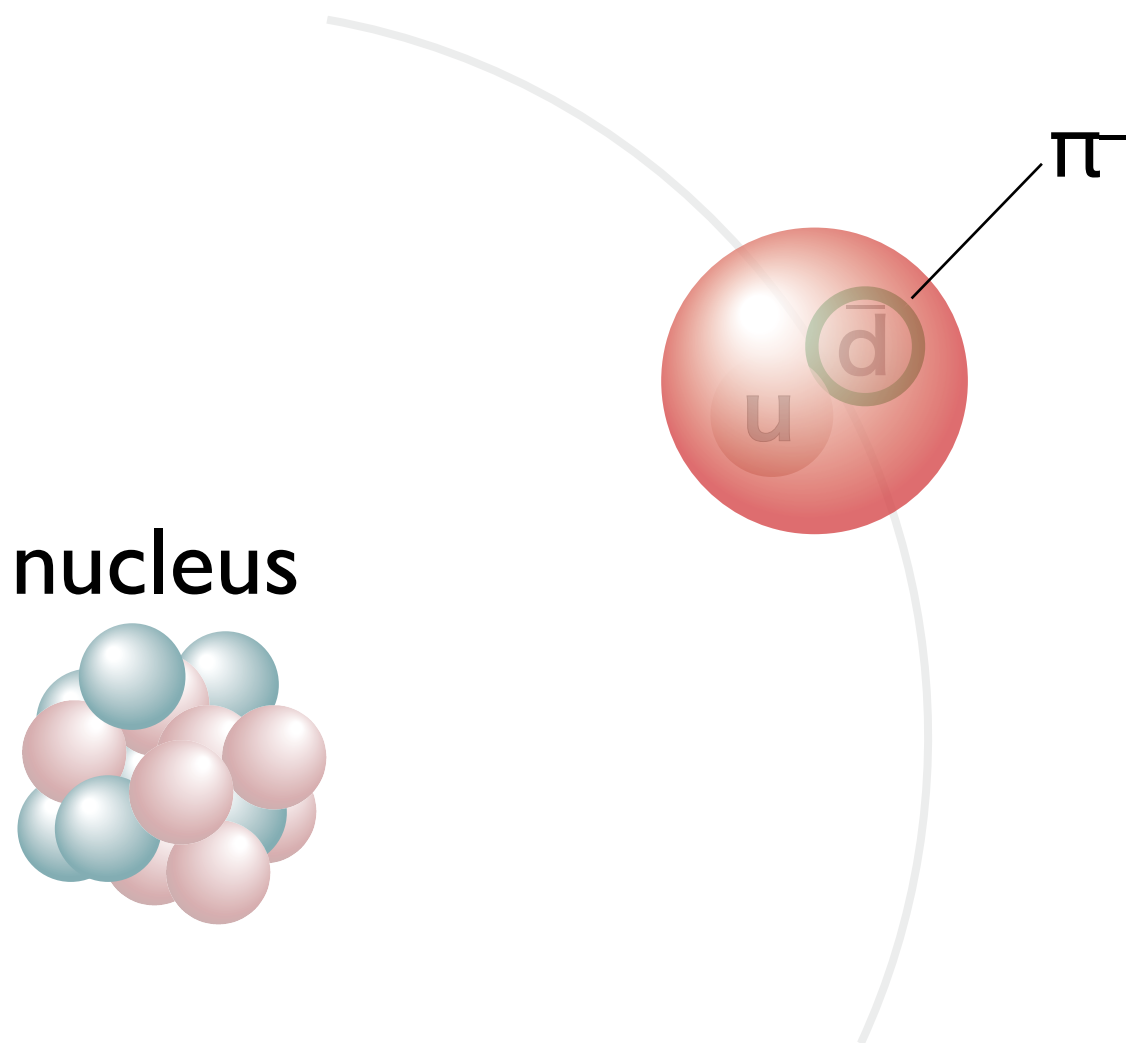
η' NN \rightarrow NN tagging in WASA



η' NN \rightarrow NN tagging in WASA



Piononic atoms

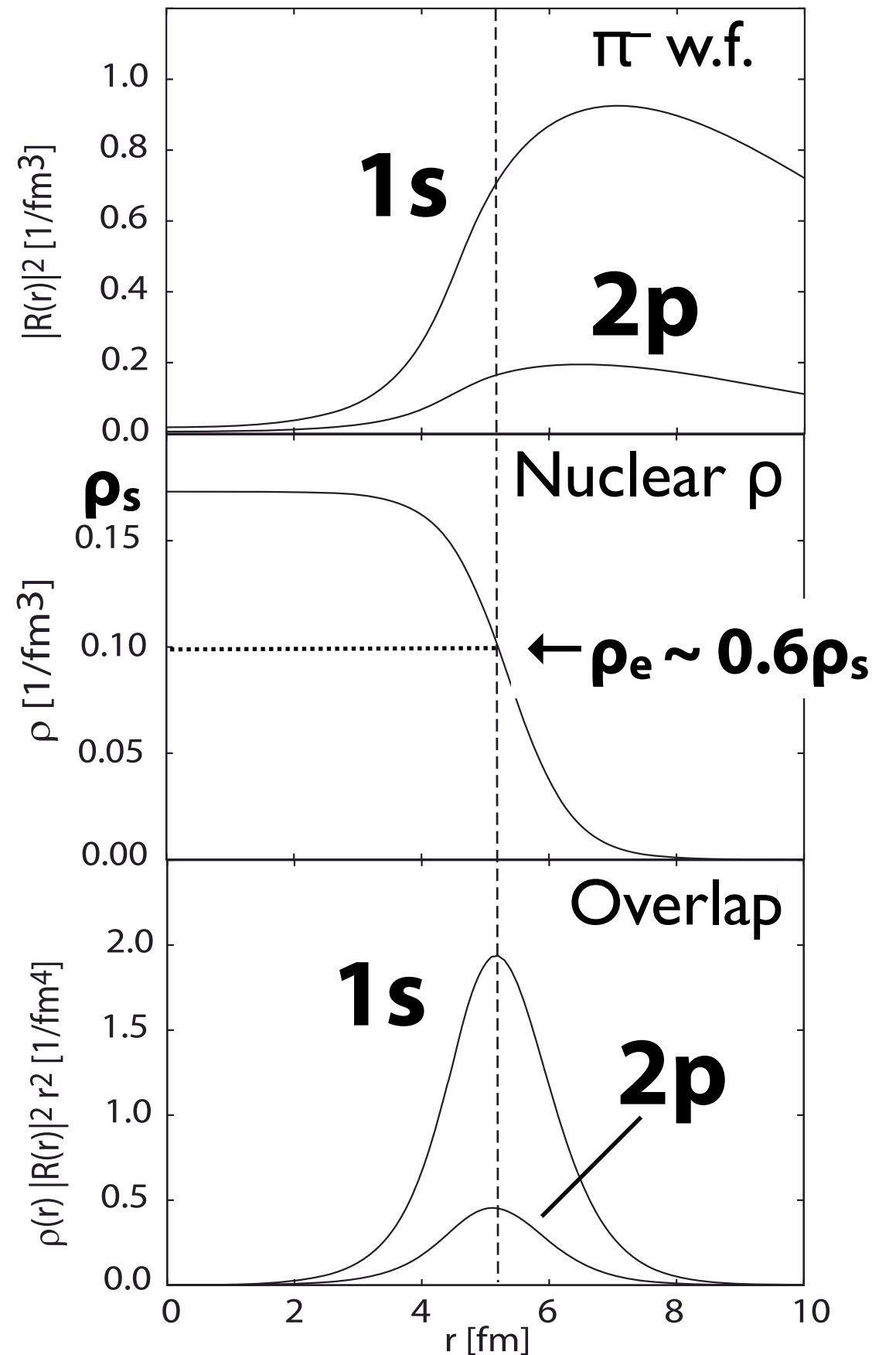


Ericson-Ericson potential

$$U_{\text{opt}}(r) = U_s(r) + U_p(r),$$

$$U_s(r) = b_0 \rho + \mathbf{b}_1 (\rho_n - \rho_p) + B_0 \rho^2$$

$$U_p(r) = \frac{2\pi}{\mu} \vec{\nabla} \cdot [c(r) + \varepsilon_2^{-1} C_0 \rho^2(r)] L(r) \vec{\nabla}$$



Pion-nucleus interaction

Overlap between
pion w.f. and nucleus
→ π works as a probe
at $\rho_e \sim 0.6\rho_0$



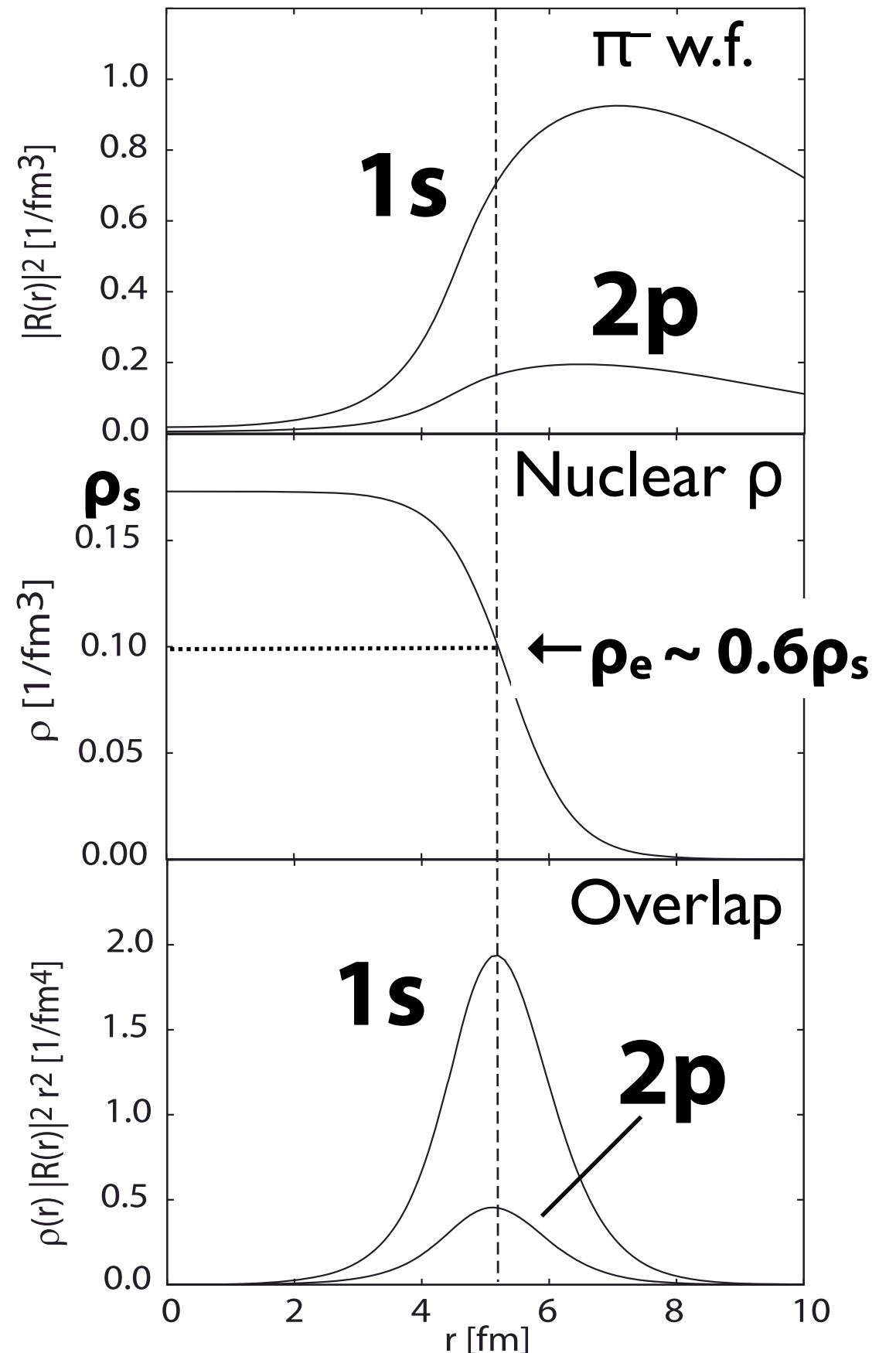
π -nucleus interaction is changed
for wavefunction renormalization
of medium effect

Ericson-Ericson potential

$$U_{\text{opt}}(r) = U_s(r) + U_p(r),$$

$$U_s(r) = b_0 \rho + \mathbf{b}_1 (\rho_n - \rho_p) + B_0 \rho^2$$

$$U_p(r) = \frac{2\pi}{\mu} \vec{\nabla} \cdot [c(r) + \varepsilon_2^{-1} C_0 \rho^2(r)] L(r) \vec{\nabla}$$



Pion-nucleus interaction and chiral condensate

Overlap between
pion w.f. and nucleus
→ π works as a probe
at $\rho_e \sim 0.6\rho_0$



π -nucleus interaction is changed
for wavefunction renormalization
of medium effect

Ericson-Ericson potential

$$U_{\text{opt}}(r) = U_s(r) + U_p(r),$$

$$U_s(r) = b_0 \rho + \mathbf{b}_1 (\rho_n - \rho_p) + B_0 \rho^2$$

$$U_p(r) = \frac{2\pi}{\mu} \vec{\nabla} \cdot [c(r) + \varepsilon_2^{-1} C_0 \rho^2(r)] L(r) \vec{\nabla}$$

In-medium Glashow-Weinberg relation

$$\frac{\langle \bar{q}q \rangle^*}{\langle \bar{q}q \rangle} \simeq \left(\frac{b_1^v}{b_1} \right)^{1/2} \left(1 - \gamma \frac{\rho}{\rho_0} \right)$$

$$\gamma = 0.184 \pm 0.003$$

Jido, Hatsuda, Kunihiro, PLB670, 109 (2008)

Pion-nucleus interaction and chiral condensate

Gell-Mann-Oakes-Renner relation

$$f_{\pi}^2 m_{\pi}^2 = -2m_q \langle \bar{q}q \rangle$$

Tomozawa-Weinberg relation

$$b_1 = -\frac{m_{\pi}}{8\pi f_{\pi}^2}$$

$$\frac{\langle \bar{q}q \rangle_{\rho}}{\langle \bar{q}q \rangle_0} \approx \frac{b_1^{\text{free}}}{b_1(\rho)}$$

M. Gell-Mann *et al.*, PR175(1968)2195.
Y. Tomozawa, NuovoCimA46(1966)707.
S. Weinberg, PRL17(1966)616.

In-medium Glashow-Weinberg relation

$$\frac{\langle \bar{q}q \rangle^*}{\langle \bar{q}q \rangle} \simeq \left(\frac{b_1^{\text{v}}}{b_1} \right)^{1/2} \left(1 - \gamma \frac{\rho}{\rho_0} \right)$$

$$\gamma = 0.184 \pm 0.003$$

Jido, Hatsuda, Kunihiro, PLB670, 109 (2008)

Pion-nucleus interaction and chiral condensate

Gell-Mann-Oakes-Renner relation

$$f_\pi^2 m_\pi^2 = -2m_q \langle \bar{q}q \rangle$$

Tomozawa-Weinberg relation

$$b_1 = -\frac{m_\pi}{8\pi f_\pi^2}$$

$$\frac{\langle \bar{q}q \rangle_\rho}{\langle \bar{q}q \rangle_0} \approx \frac{b_1^{\text{free}}}{b_1(\rho)}$$

In-medium Glashow-Weinberg relation

$$\frac{\langle \bar{q}q \rangle^*}{\langle \bar{q}q \rangle} \simeq \left(\frac{b_1^{\text{v}}}{b_1} \right)^{1/2} \left(1 - \gamma \frac{\rho}{\rho_0} \right)$$

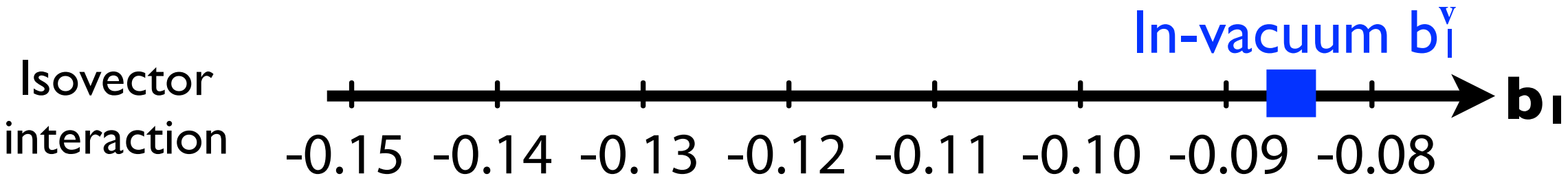
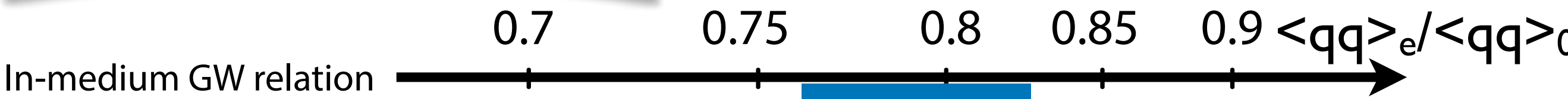
$$\gamma = 0.184 \pm 0.003$$

Jido, Hatsuda, Kunihiro, PLB670, 109 (2008)

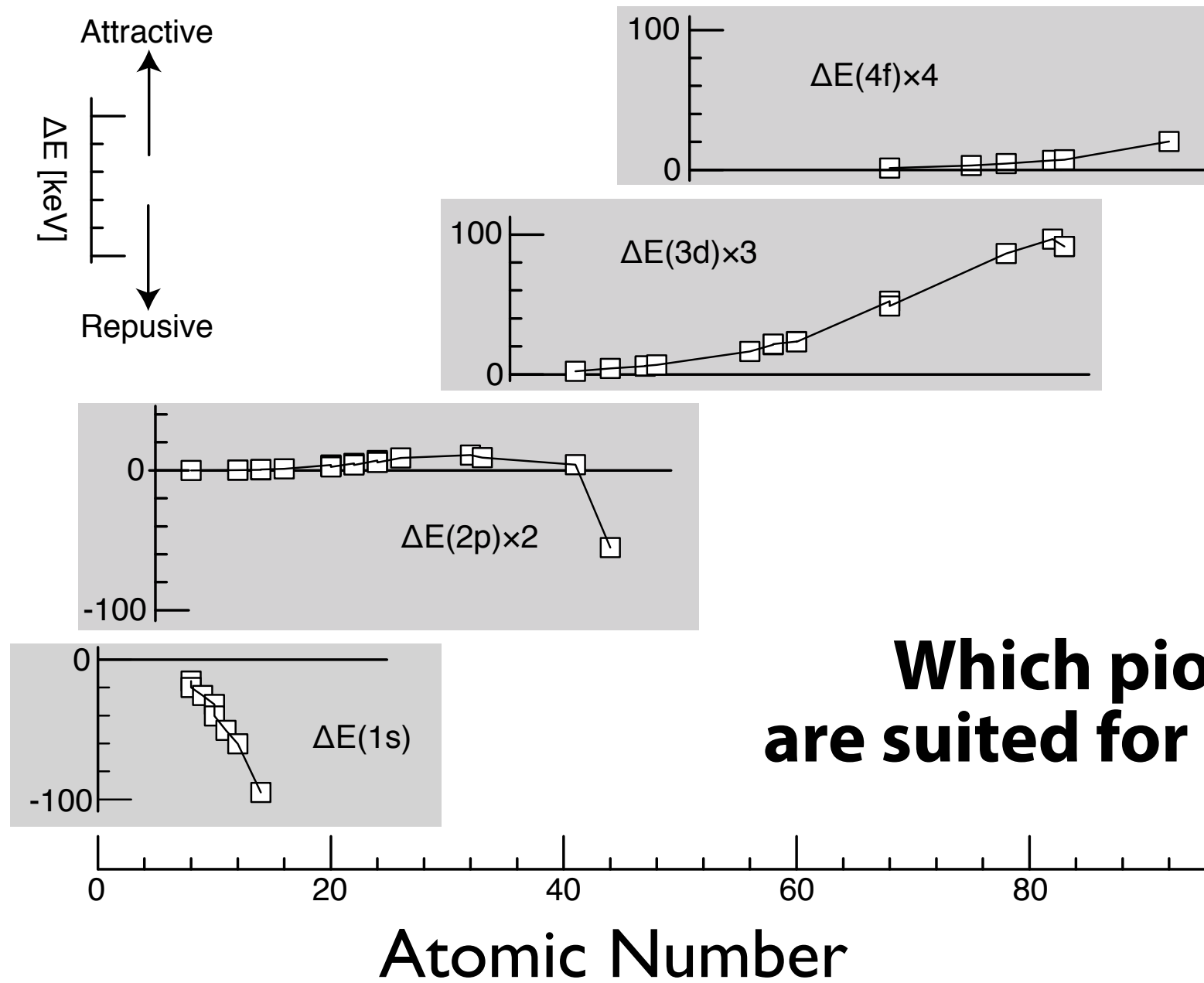
Pionic hydrogen and deuterium

$$b_1^{\text{v}} = 0.0866 \pm 0.0010$$

Hirtl et al., EPJA57, 70 (2021)



Level shifts in pionic X-ray measurements



Which pionic atoms are suited for b_1 deduction?

Ericson-Ericson potential

$$U_{\text{opt}}(r) = U_s(r) + U_p(r),$$

$$U_s(r) = b_0 \rho + b_1 (\rho_n - \rho_p) + B_0 \rho^2$$

$$U_p(r) = \frac{2\pi}{\mu} \vec{\nabla} \cdot [c(r) + \varepsilon_2^{-1} C_0 \rho^2(r)] L(r) \vec{\nabla}$$

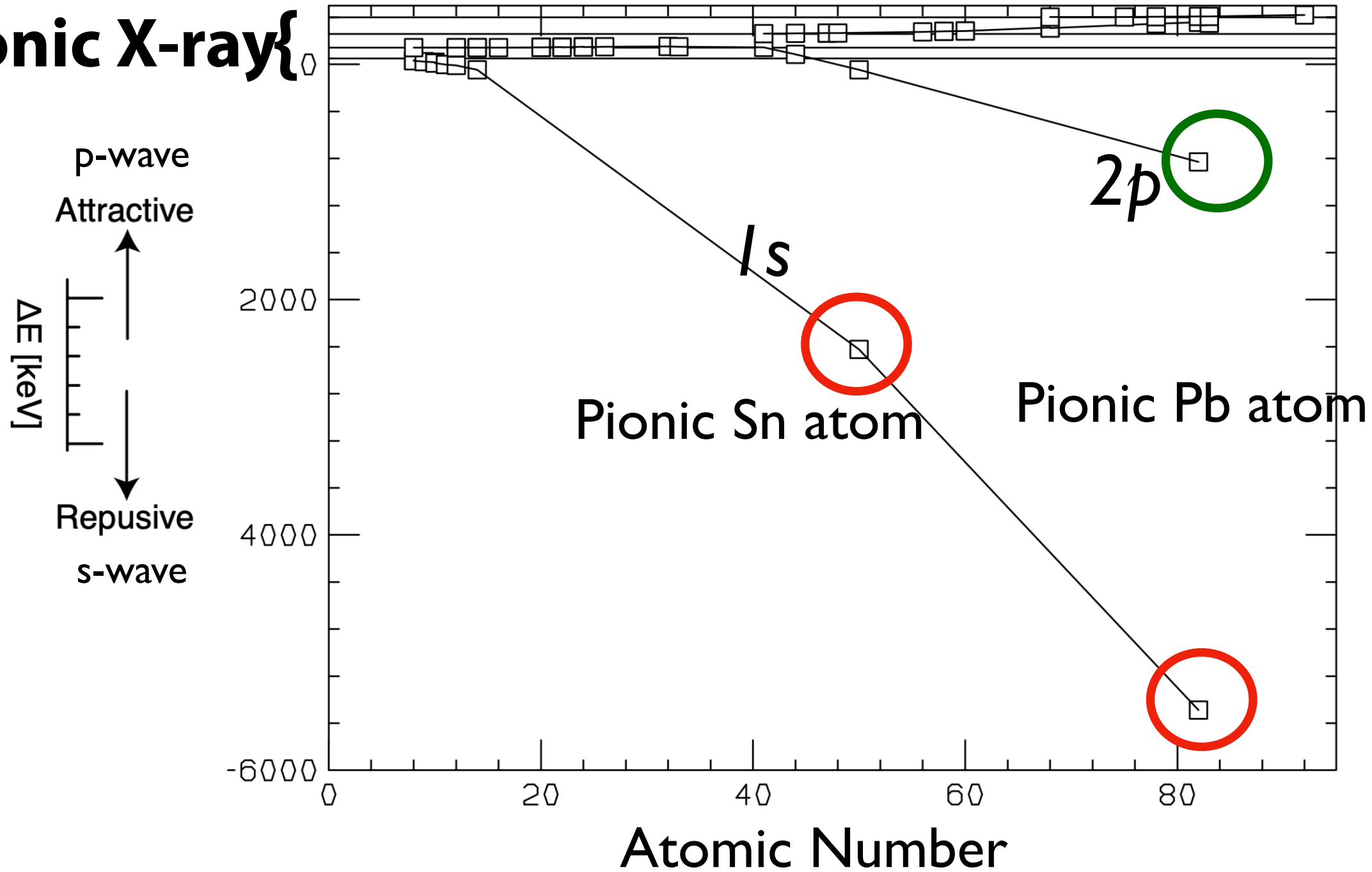
—————→ **s-wave = repulsive = negative shift**

—————→ **p-wave = attractive = positive shift**

Deeply bound pionic atoms

Level shifts

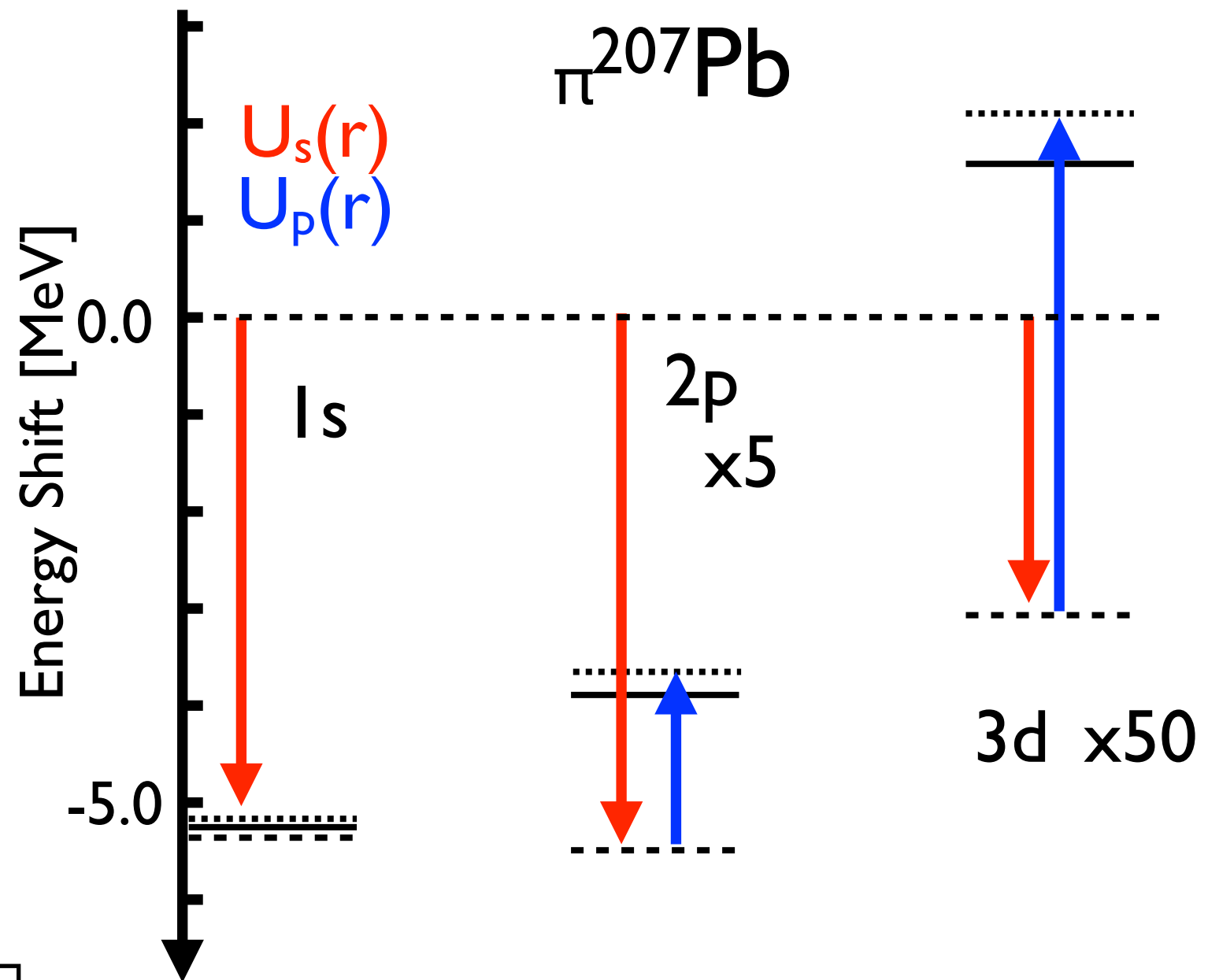
Pionic X-ray



Deeply bound atoms have "super" repulsive shifts and provide s-wave information

πA and π -nucleus interaction

Deeply bound states are sensitive to s-wave cf. Pionic X-rays are to p-wave



Ericson-Ericson potential

$$U_{\text{opt}}(r) = U_s(r) + U_p(r),$$

$$U_s(r) = b_0 \rho + \mathbf{b}_1 (\rho_n - \rho_p) + B_0 \rho^2$$

$$U_p(r) = \frac{2\pi}{\mu} \vec{\nabla} \cdot [c(r) + \varepsilon_2^{-1} C_0 \rho^2(r)] L(r) \vec{\nabla}$$

s-wave interaction is dominant in **1s shift**, whereas p-wave is larger in 3d

PHYSICAL REVIEW C, VOLUME 62, 024606

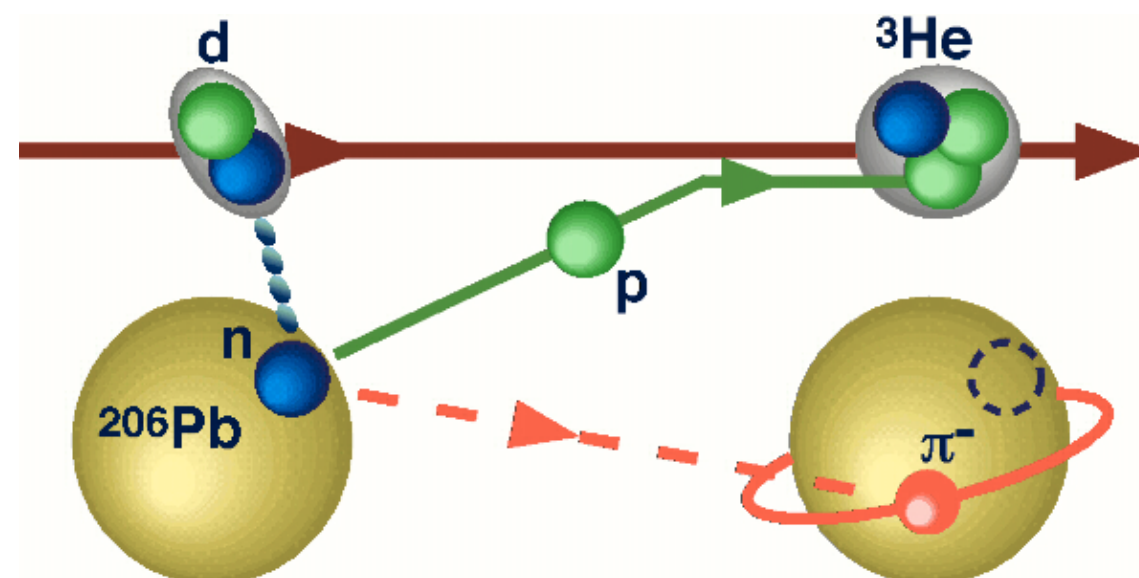
Isotope dependence of deeply bound pionic states in Sn and Pb

Y. Umemoto,¹ S. Hirenzaki,¹ K. Kume,¹ and H. Toki²

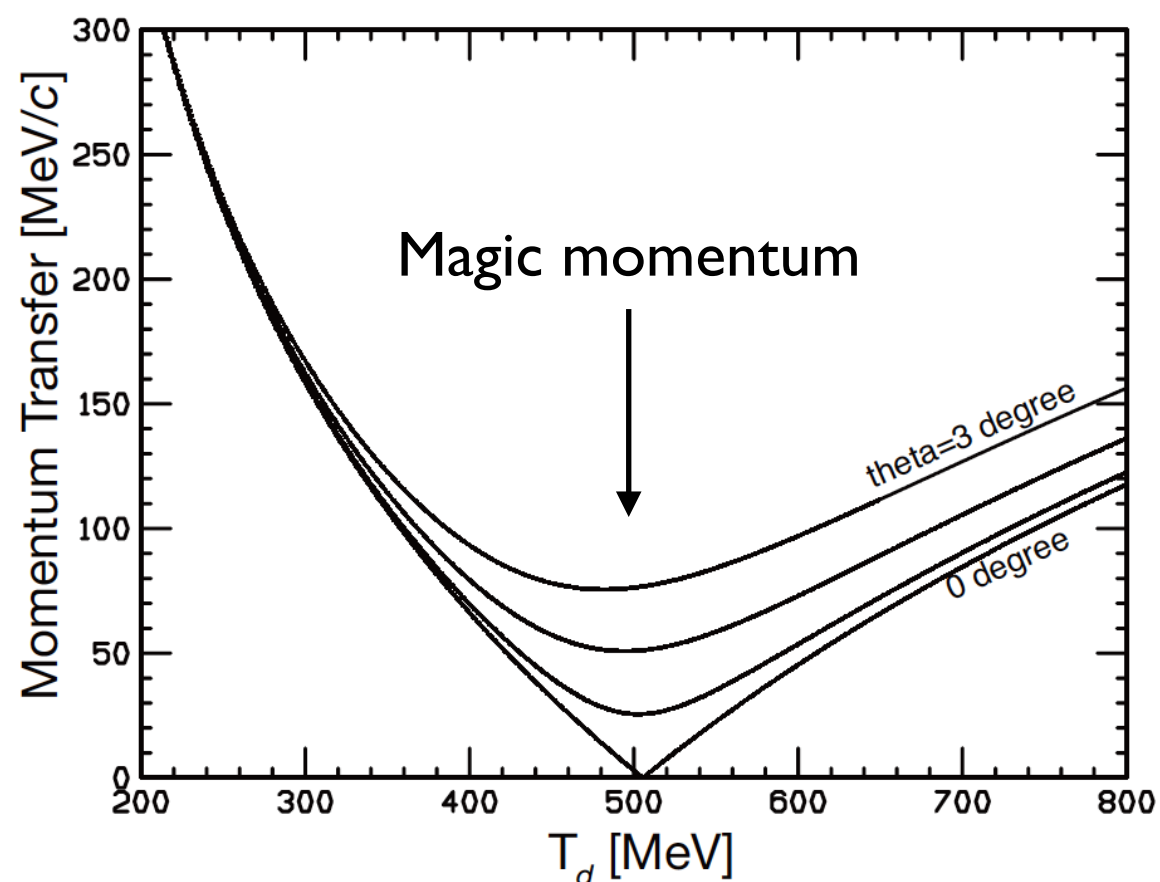
Spectroscopy of pionic atoms in $(d, {}^3\text{He})$ reactions

Missing mass spectroscopy to measure excitation spectrum of pionic atoms

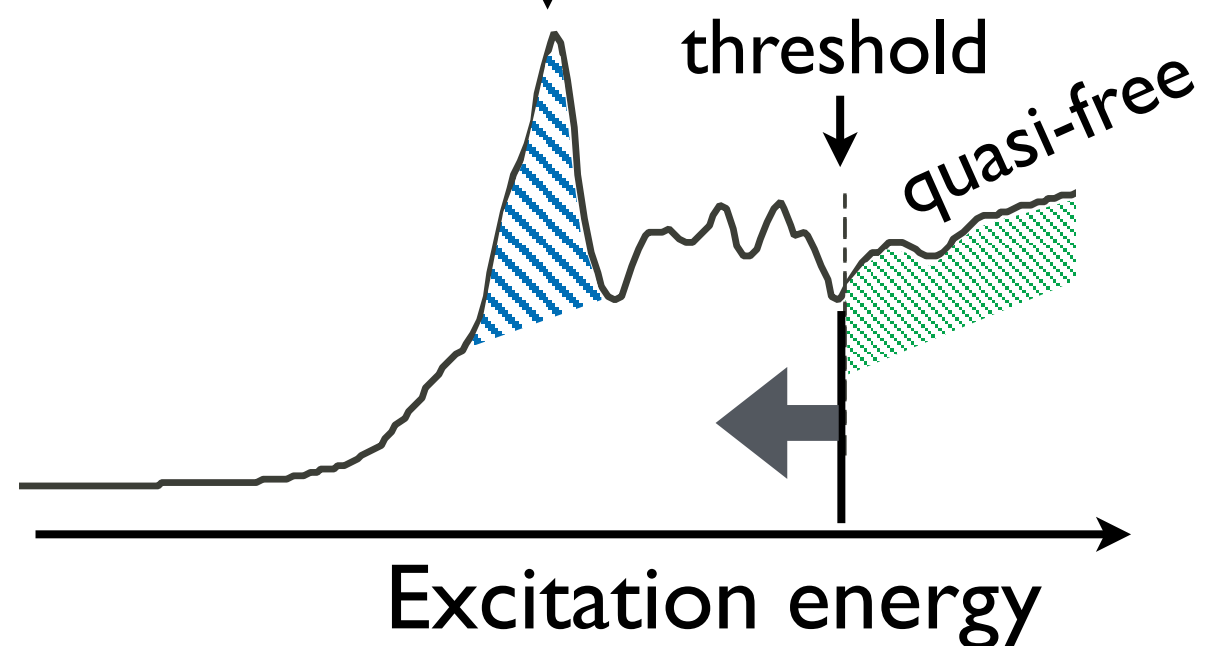
Direct production of pionic atoms



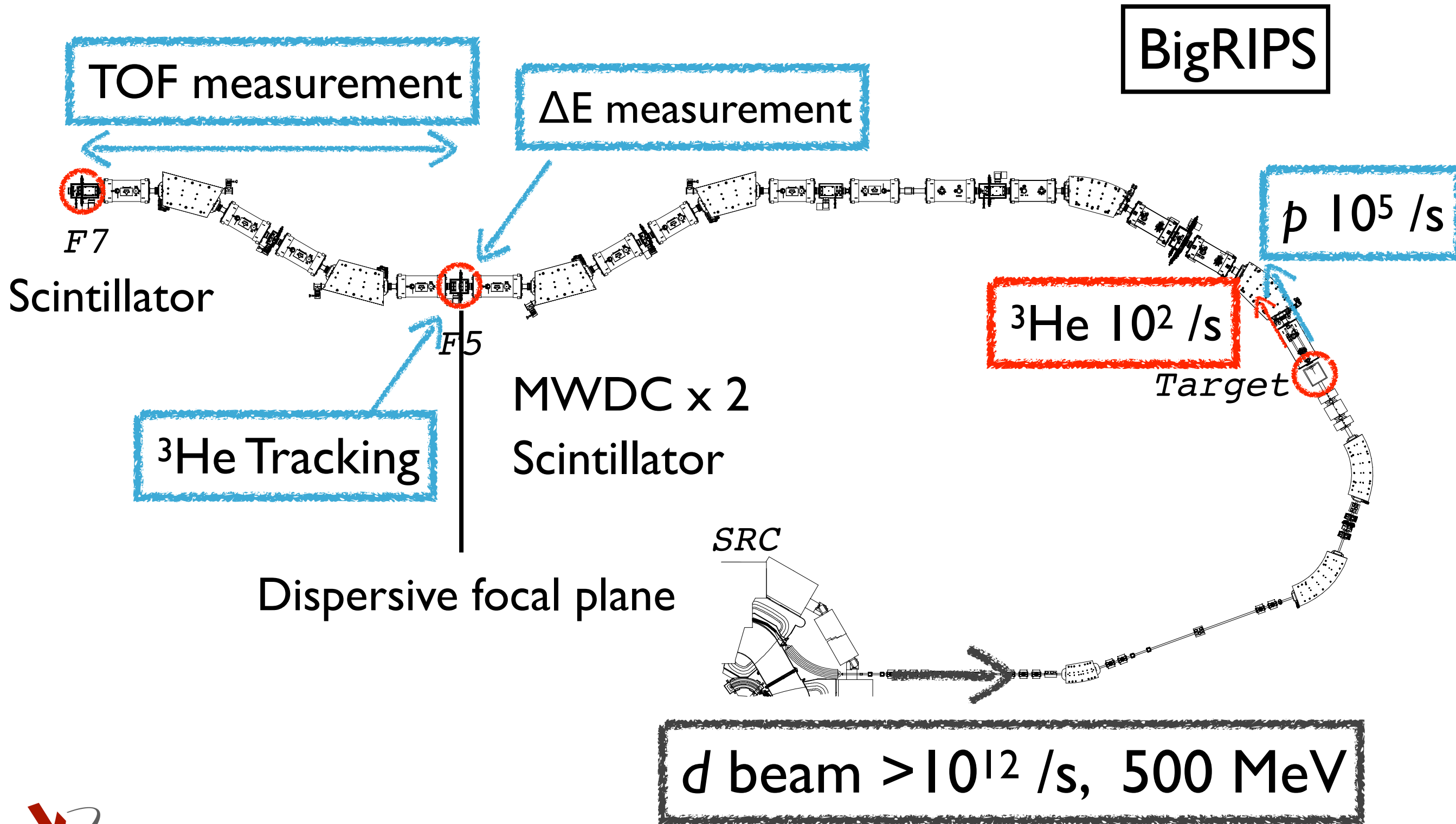
Momentum transfer



Pion bound state (coupled with n hole)

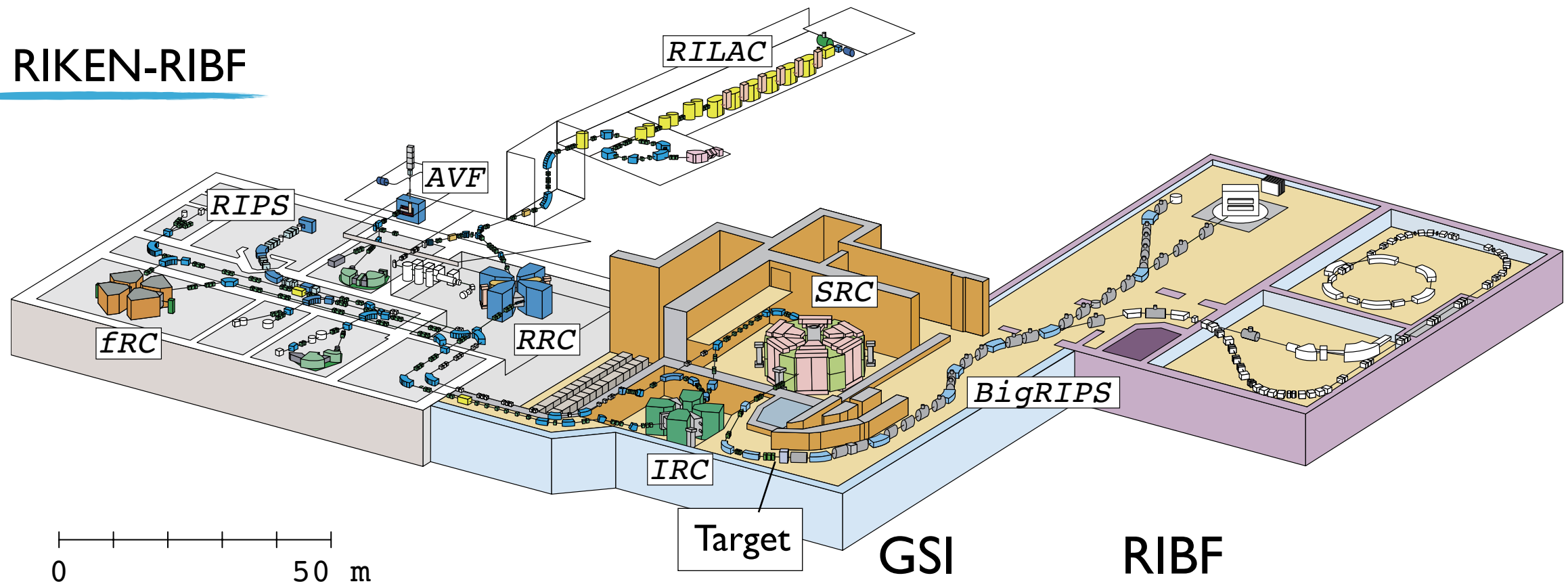


(d,³He) Reaction Spectroscopy in RIBF



RI Beam Factory

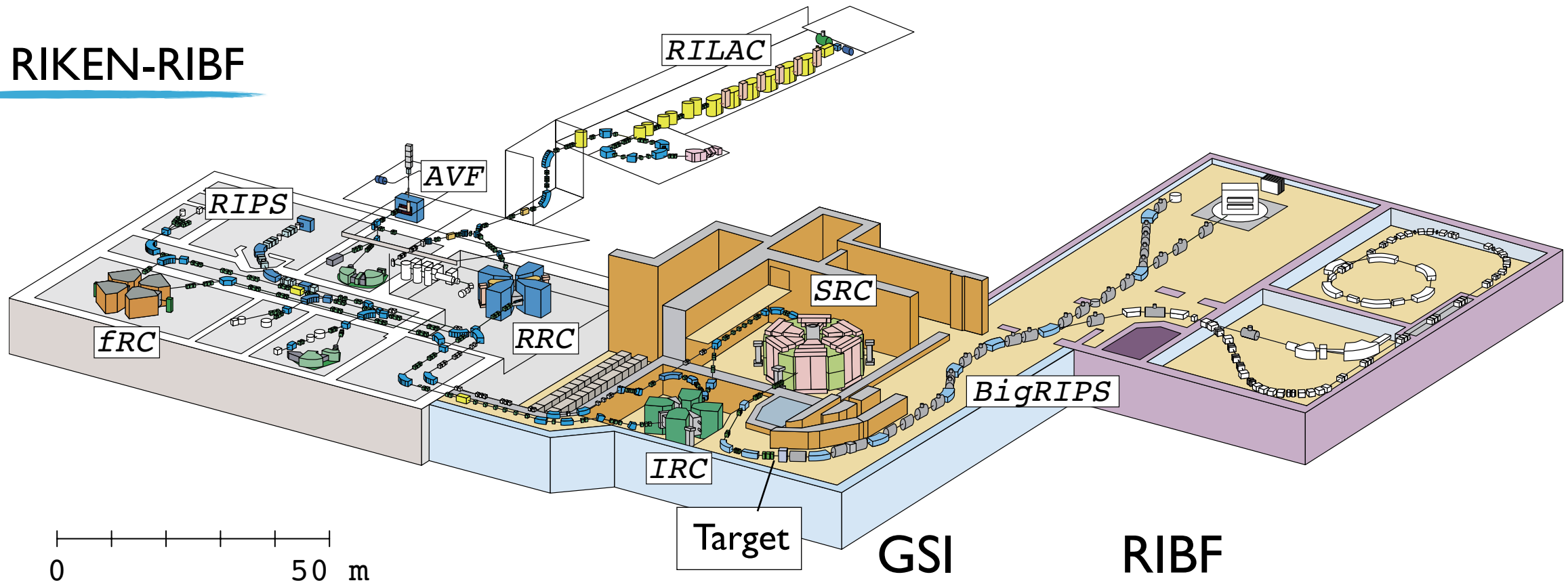
RIKEN-RIBF



	GSI	RIBF
d beam Intensity	$10^{11}/\text{spill}$	$> 10^{12}/\text{s}$
Target	$20 \text{ mg}/\text{cm}^2$	$10 \text{ mg}/\text{cm}^2$
$\Delta p_d/p_d$ (FWHM)	0.02%	0.06%
Resolution (FWHM)	400 keV	$\sim 1000 \text{ keV}$
Acceptance (mrad)	15H, 10V	40H, 60V

RI Beam Factory

RIKEN-RIBF



	GSI	RIBF
d beam Intensity	$10^{11}/\text{spill}$	$> 10^{12}/\text{s}$
Target	$20 \text{ mg}/\text{cm}^2$	$10 \text{ mg}/\text{cm}^2$
$\Delta p_d/p_d$ (FWHM)	0.02%	0.06%
Resolution (FWHM)	400 keV	$\sim 300 \text{ keV}$
Acceptance (mrad)	15H, 10V	40H, 60V

Dispersion matching

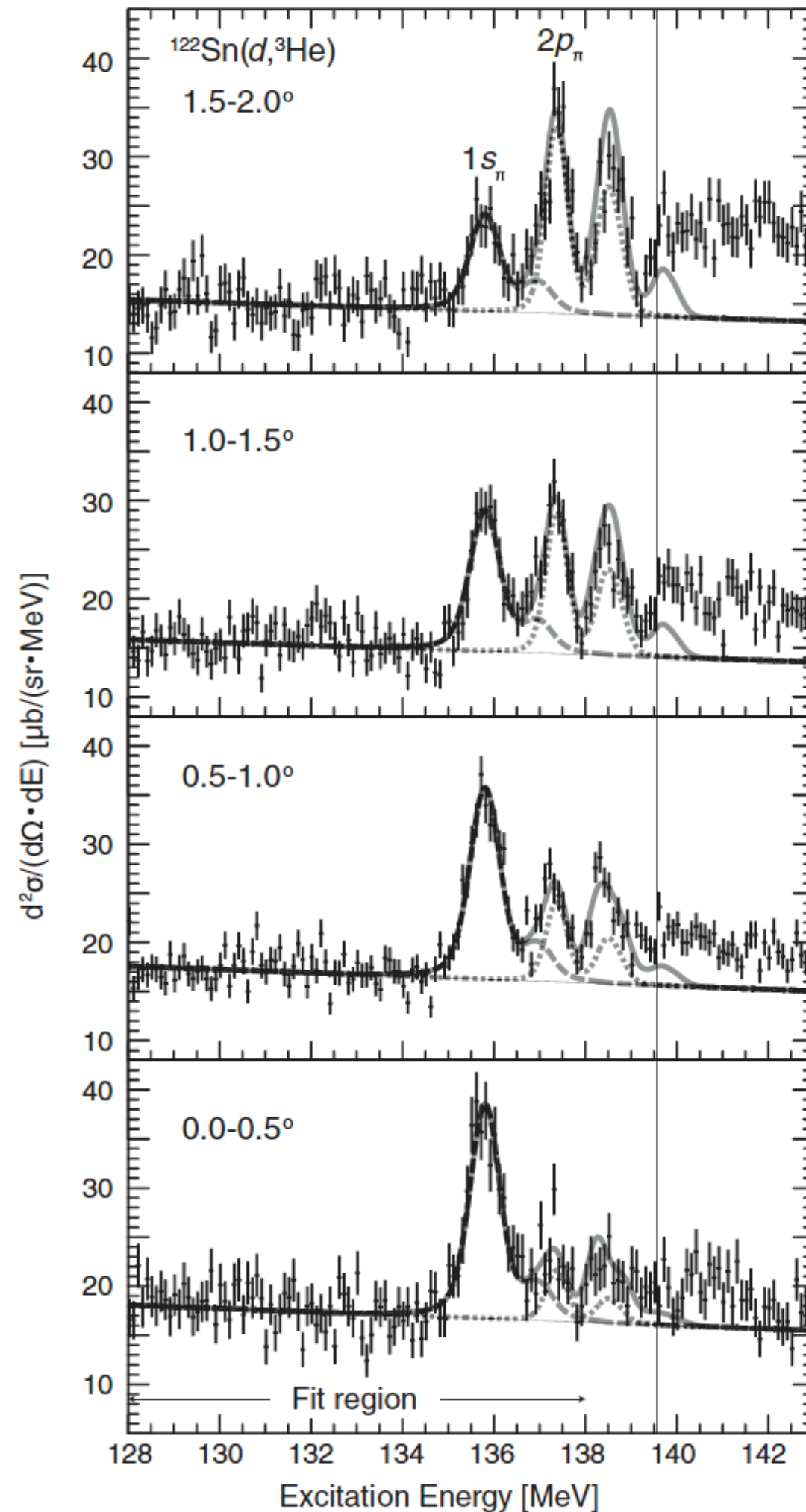
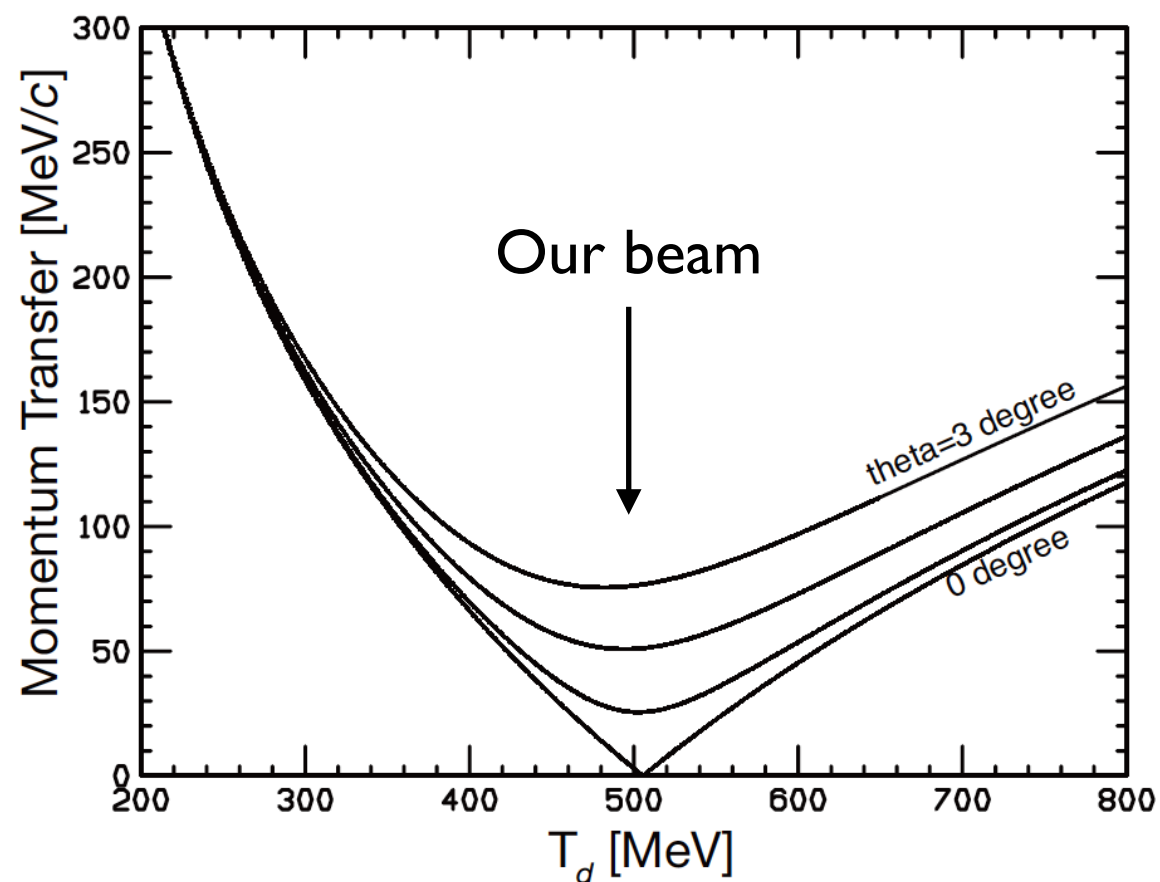
Pionic ^{121}Sn atom

Pilot run

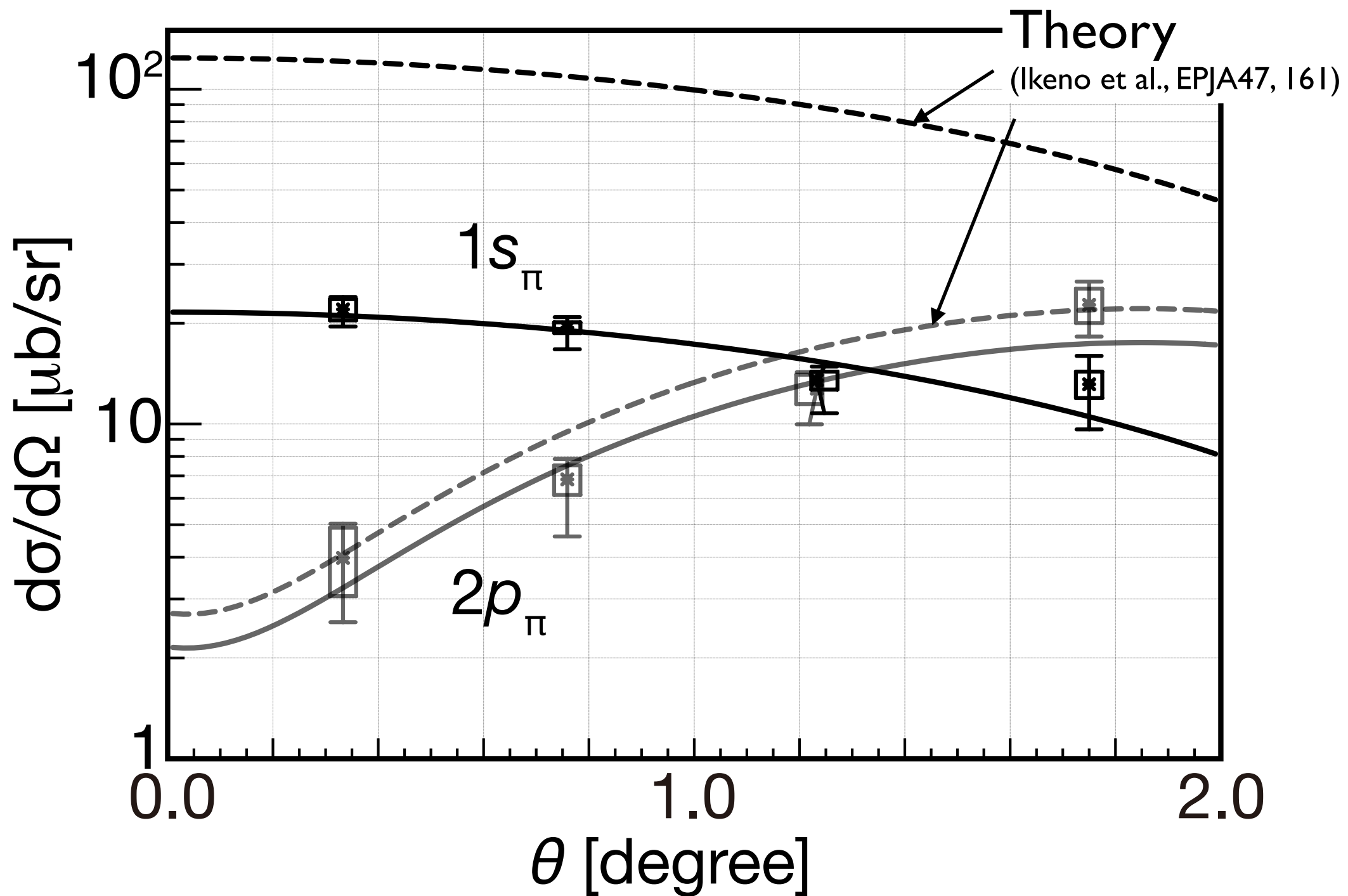
15 hours DAQ in 2010

First observation of
 θ dependence of
 π atom cross section

$$\Delta L \sim R \times q$$



1s and 2p pionic atom cross sections in (d, ³He)



θ dependence is well reproduced.
Theory calculates 5x larger cross section for 1s

Pionic ^{121}Sn atom

Pilot run

15 hours DAQ in 2010

First simultaneous $1s$ and $2p$ observation

$$B_{1s} = 3.828 \pm 0.013(\text{stat})_{-0.033}^{+0.036}(\text{syst}) \text{ MeV}$$

$$\Gamma_{1s} = 0.252 \pm 0.054(\text{stat})_{-0.070}^{+0.053}(\text{syst}) \text{ MeV}$$

$$B_{2p} = 2.238 \pm 0.015(\text{stat})_{-0.043}^{+0.046}(\text{syst}) \text{ MeV}$$

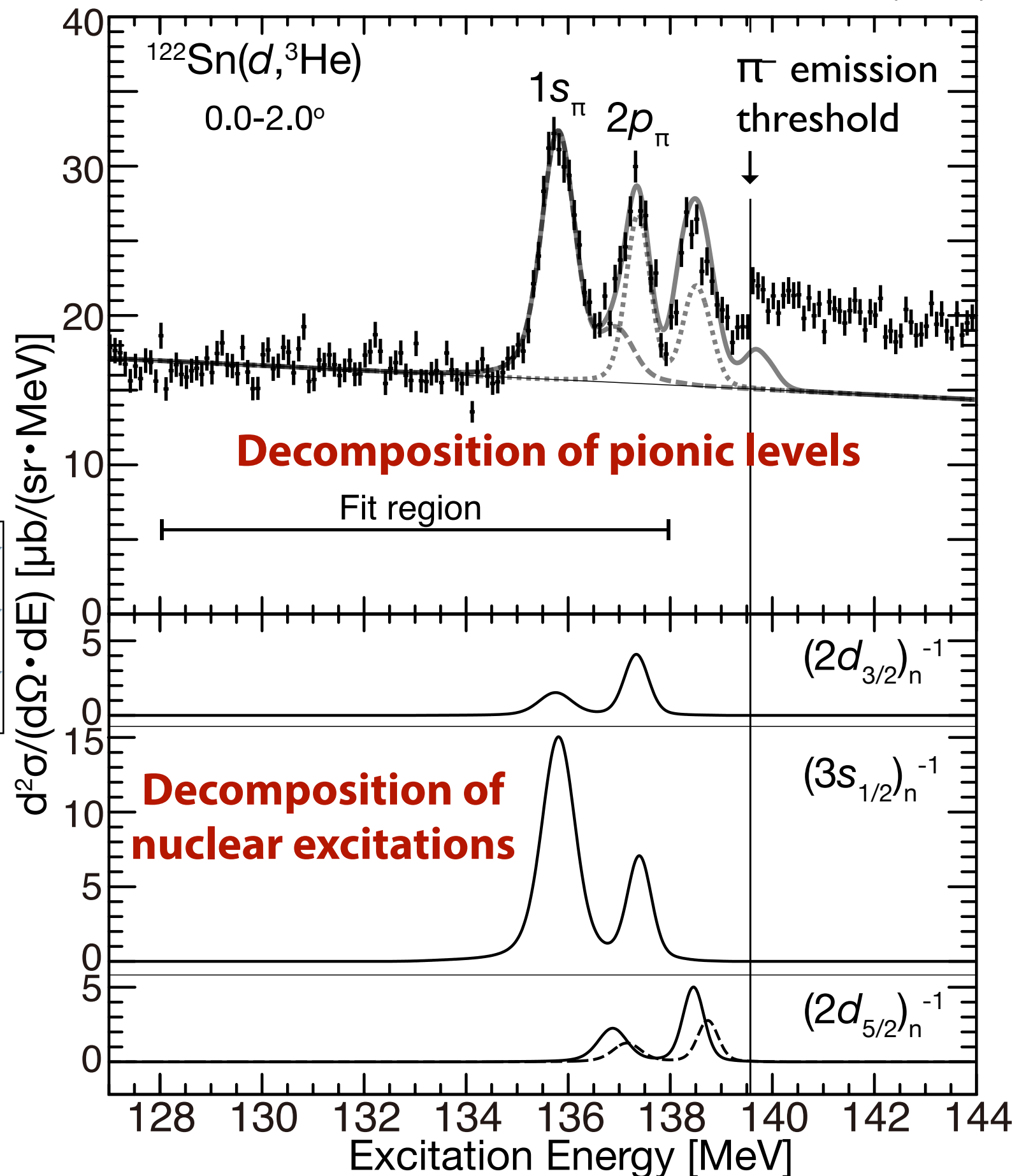
Resolution 394 keV (FWHM)

Theories

$$B_{1s} = 3.787\text{--}3.850 \text{ MeV}$$

$$\Gamma_{1s} = 0.306\text{--}0.324 \text{ MeV}$$

$$B_{2p} = 2.257\text{--}2.276 \text{ MeV}$$

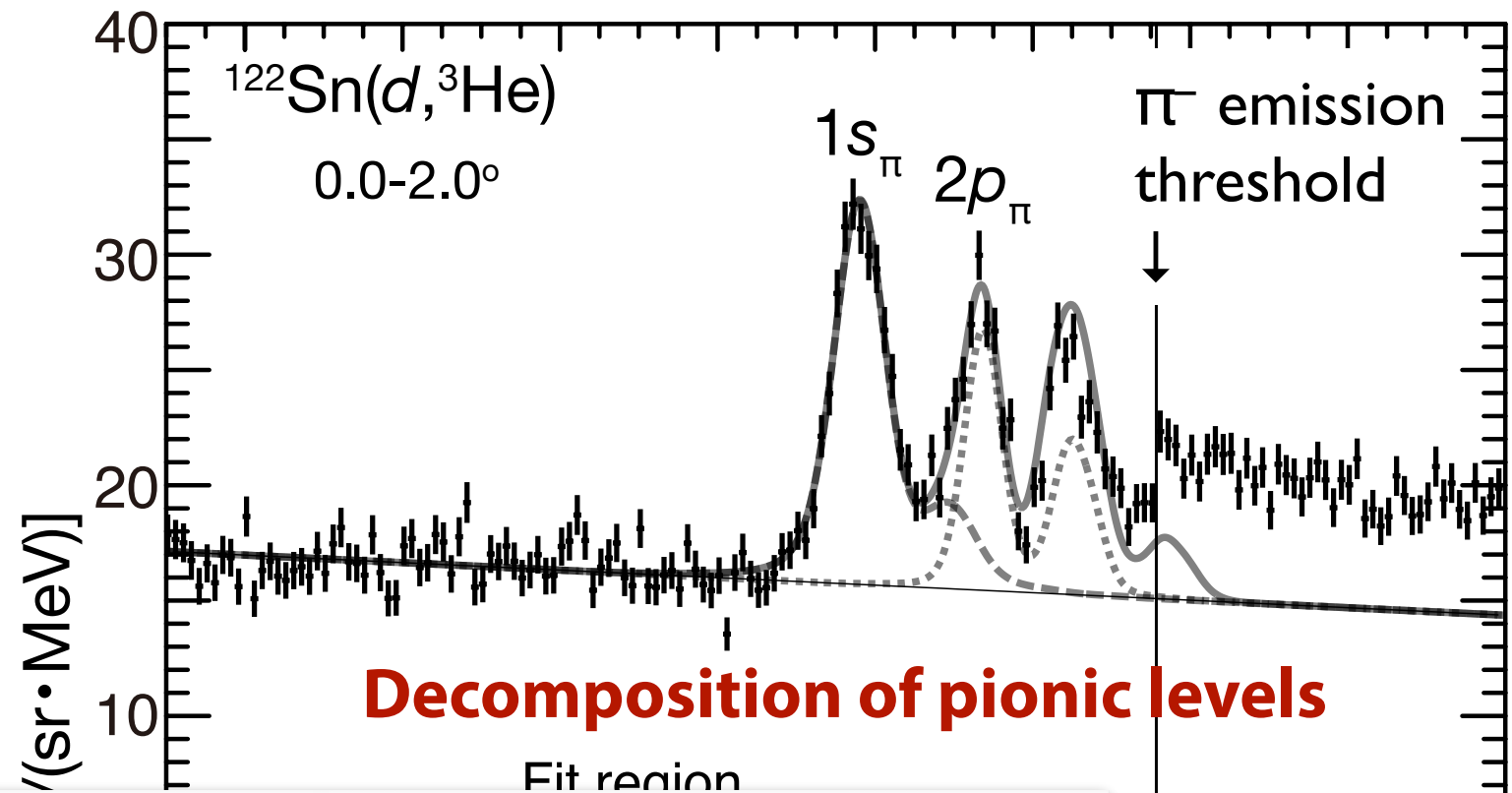


Piononic ^{121}Sn atom

Pilot run

15 hours DAQ in 2010

First simultaneous $1s$ and $2p$ observation



$$B_{1s} = 3.828 \pm 0.015 \text{ (stat)} \pm 0.070 \text{ (syst)} \text{ MeV}$$

$$\Gamma_{1s} = 0.252 \pm 0.015 \text{ (stat)} \pm 0.070 \text{ (syst)} \text{ MeV}$$

$$B_{2p} = 2.238 \pm 0.015 \text{ (stat)}^{+0.046}_{-0.043} \text{ (syst)} \text{ MeV}$$

However, precision was not enough...

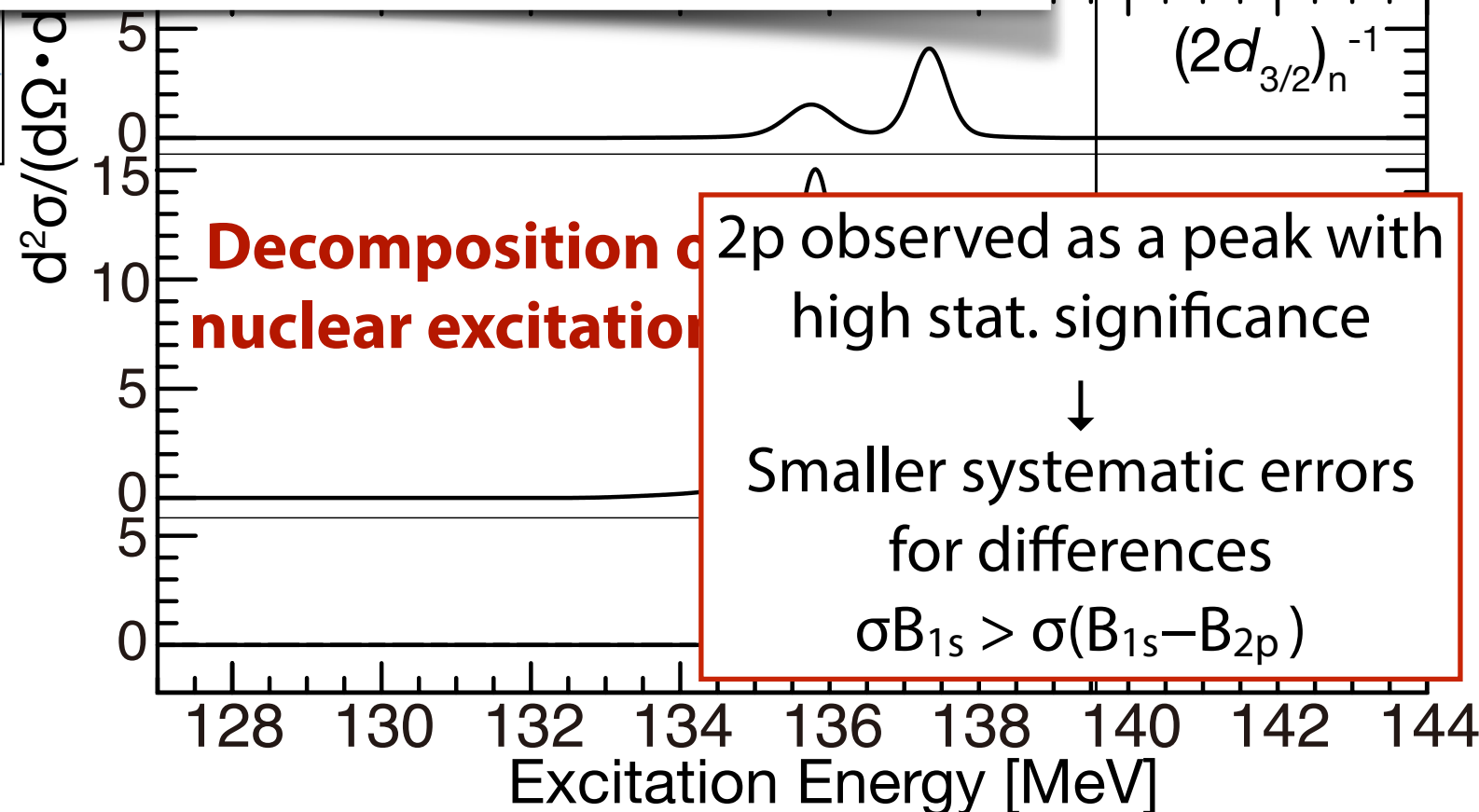
Resolution 394 keV (FWHM)

Theories

$$B_{1s} = 3.787\text{--}3.850 \text{ MeV}$$

$$\Gamma_{1s} = 0.306\text{--}0.324 \text{ MeV}$$

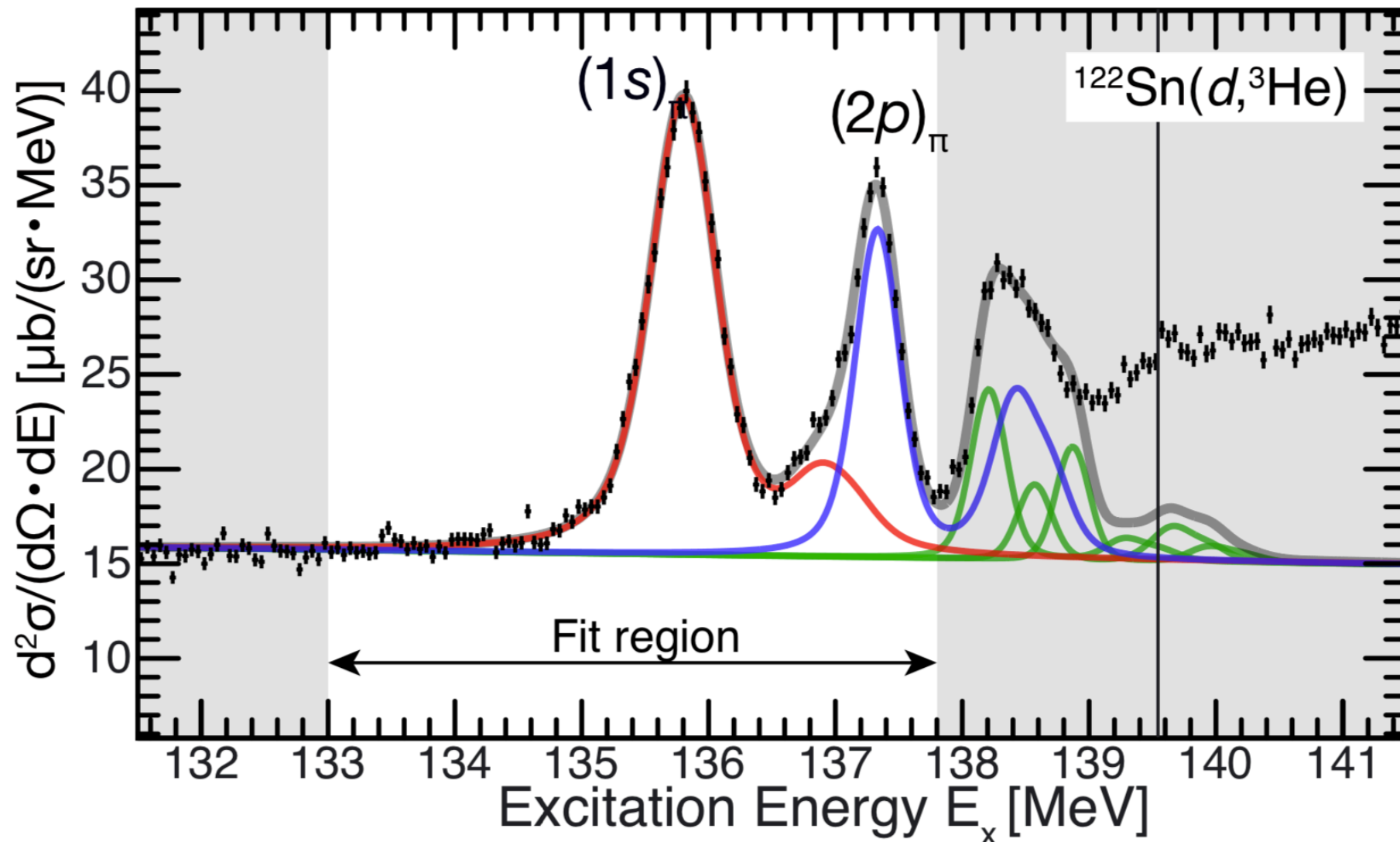
$$B_{2p} = 2.257\text{--}2.276 \text{ MeV}$$



High Precision Spectrum of $^{122}\text{Sn}(d,^3\text{He})$ in 2014 run

Pionic atom unveils hidden structure of QCD vacuum

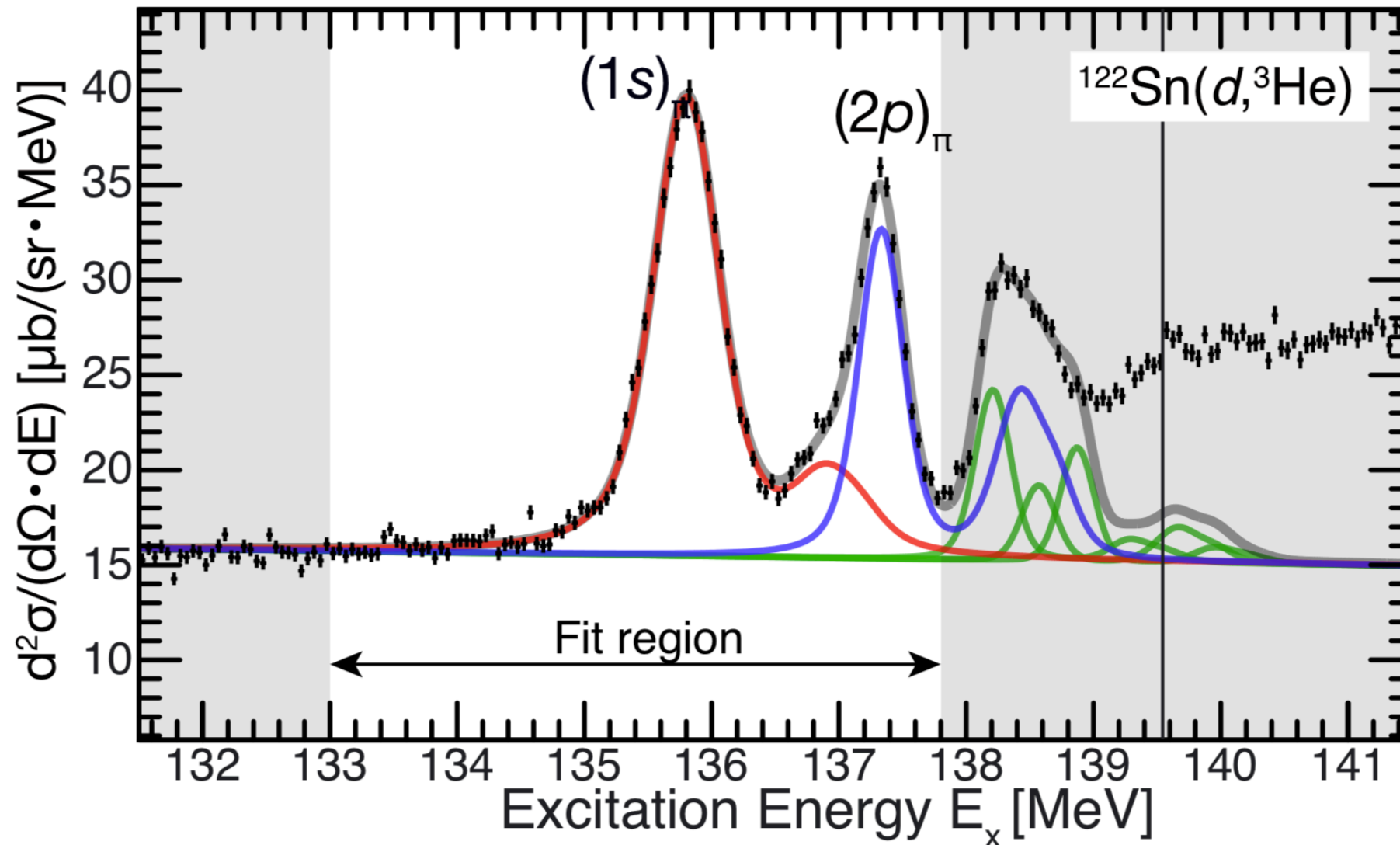
Takahiro Nishi¹, Kenta Itahashi^{1,*}, DeukSoon Ahn^{1,2}, Georg P.A. Berg³, Masanori Dozono¹, Daijiro Etoh⁴, Hiroyuki Fujioka⁵, Naoki Fukuda¹, Nobuhisa Fukunishi¹, Hans Geissel⁶, Emma Haettner⁶, Tadashi Hashimoto¹, Ryugo S. Hayano⁷, Satoru Hirenzaki⁸, Hiroshi Horii⁷, Natsumi Ikeno⁹, Naoto Inabe¹, Masahiko Iwasaki¹, Daisuke Kameda¹, Keichi Kisamori¹⁰, Yu Kiyokawa¹⁰, Toshiyuki Kubo¹, Kensuke Kusaka¹, Masafumi Matsushita¹⁰, Shin'ichiro Michimasa¹⁰, Go Mishima⁷, Hiroyuki Miya¹, Daichi Murai¹, Hideko Nagahiro⁸, Megumi Niikura⁷, Naoko Nose-Togawa¹¹, Shinsuke Ota¹⁰, Naruhiko Sakamoto¹, Kimiko Sekiguchi⁴, Yuta Shiokawa⁴, Hiroshi Suzuki¹, Ken Suzuki¹², Motonobu Takaki¹⁰, Hiroyuki Takeda¹, Yoshiki K. Tanaka¹, Tomohiro Uesaka¹, Yasumori Wada⁴, Atomu Watanabe⁴, Yuni N. Watanabe⁷, Helmut Weick⁶, Hiroki Yamakami⁵, Yoshiyuki Yanagisawa¹, and Koichi Yoshida¹



2p observed as a peak with high stat. significance
↓
Smaller systematic errors for differences
 $\sigma B_{1s} > \sigma(B_{1s} - B_{2p})$

Under review
arXiv: 2204.05568

High Precision Spectrum of $^{122}\text{Sn}(d,^3\text{He})$ in 2014 run

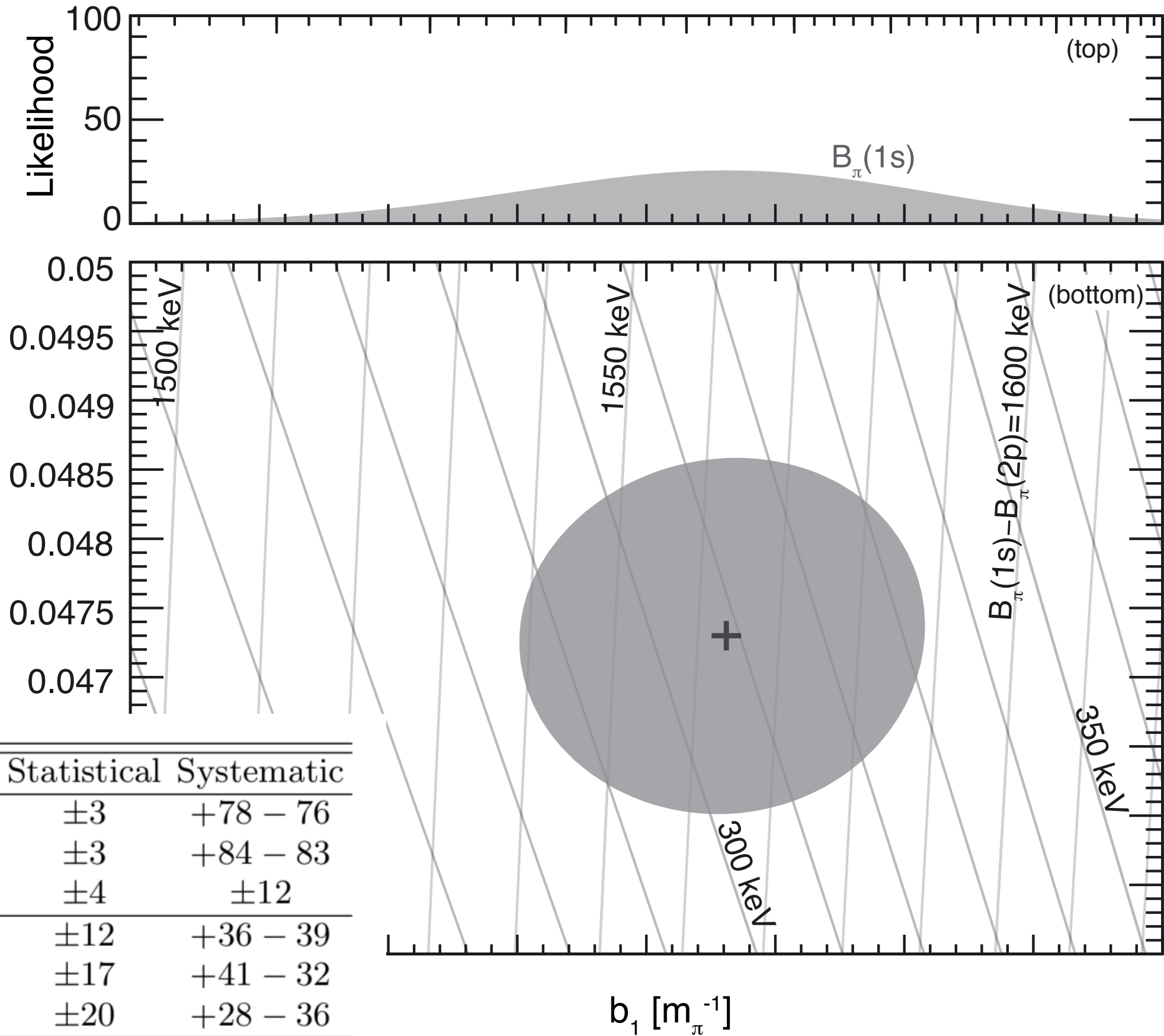


	[keV]	Statistical	Systematic
$B_\pi(1s)$	3831	± 3	+78 – 76
$B_\pi(2p)$	2276	± 3	+84 – 83
$B_\pi(1s) - B_\pi(2p)$	1555	± 4	± 12
$\Gamma_\pi(1s)$	316	± 12	+36 – 39
$\Gamma_\pi(2p)$	164	± 17	+41 – 32
$\Gamma_\pi(1s) - \Gamma_\pi(2p)$	152	± 20	+28 – 36

2p observed as a peak with high stat. significance
 \downarrow
 Smaller systematic errors for differences
 $\sigma B_{1s} > \sigma(B_{1s} - B_{2p})$

b1 parameter Deduction

based on
pionic C, N, O,
and Sn atoms

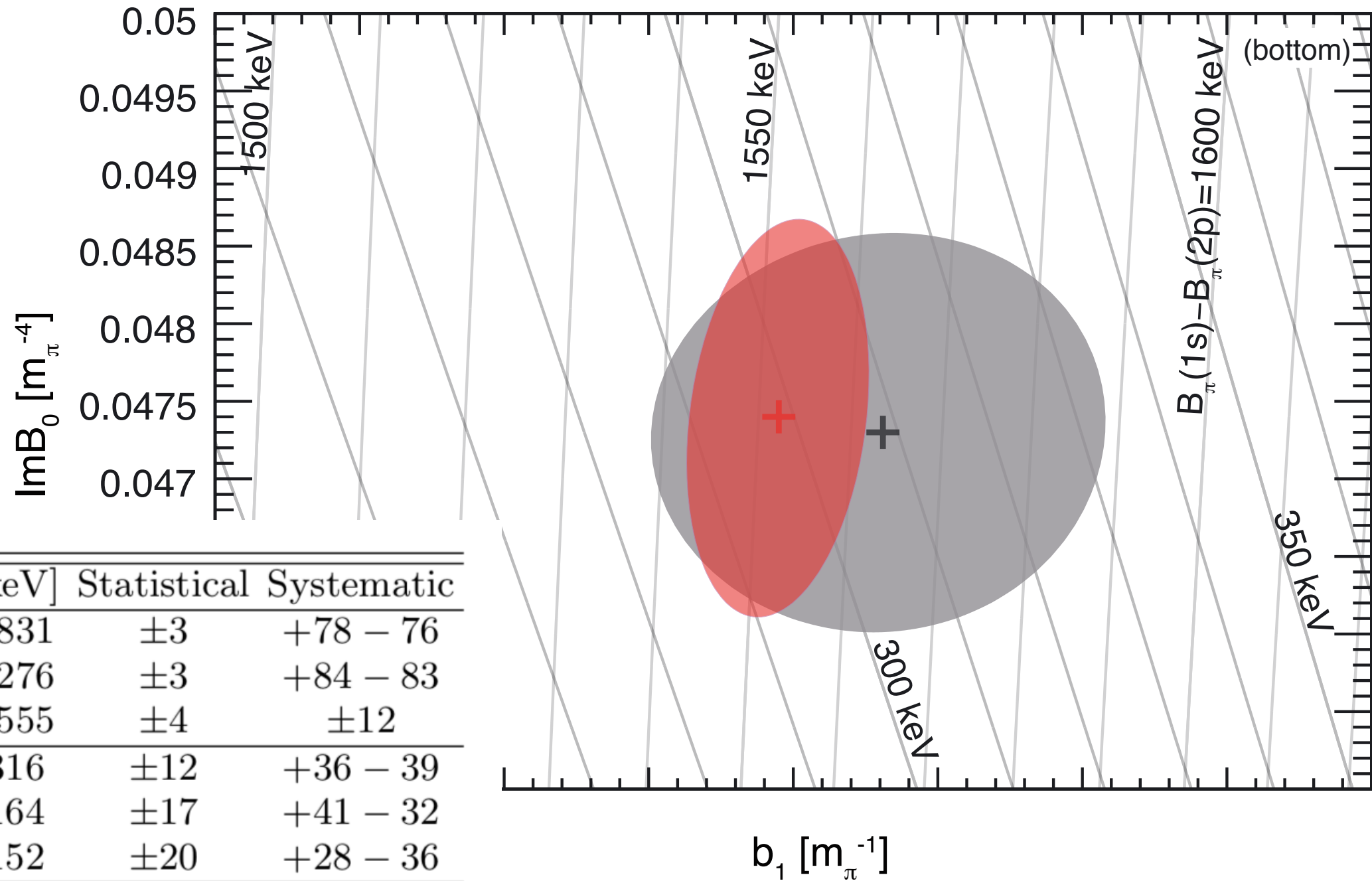
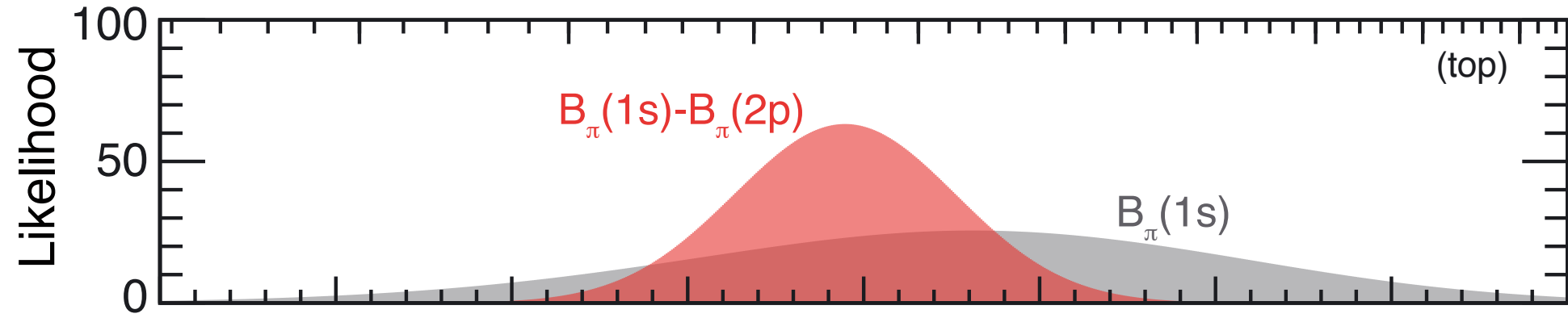


	[keV]	Statistical	Systematic
$B_{\pi}(1s)$	3831	± 3	+78 - 76
$B_{\pi}(2p)$	2276	± 3	+84 - 83
$B_{\pi}(1s) - B_{\pi}(2p)$	1555	± 4	± 12
$\Gamma_{\pi}(1s)$	316	± 12	+36 - 39
$\Gamma_{\pi}(2p)$	164	± 17	+41 - 32
$\Gamma_{\pi}(1s) - \Gamma_{\pi}(2p)$	152	± 20	+28 - 36

b1 parameter Deduction

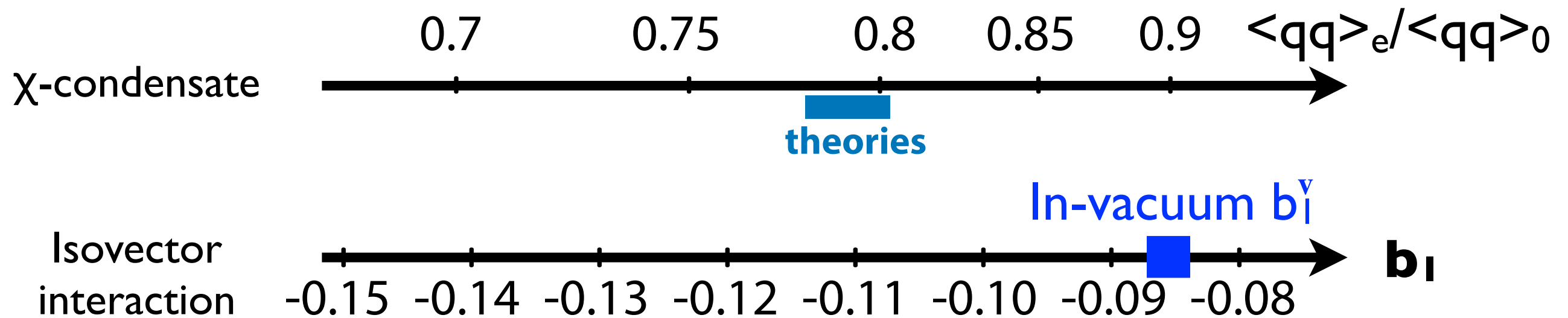
based on
pionic C, N, O,
and Sn atoms

$b_1 = -0.1005$ was deduced



	[keV]	Statistical	Systematic
$B_\pi(1s)$	3831	± 3	+78 - 76
$B_\pi(2p)$	2276	± 3	+84 - 83
$B_\pi(1s) - B_\pi(2p)$	1555	± 4	± 12
$\Gamma_\pi(1s)$	316	± 12	+36 - 39
$\Gamma_\pi(2p)$	164	± 17	+41 - 32
$\Gamma_\pi(1s) - \Gamma_\pi(2p)$	152	± 20	+28 - 36

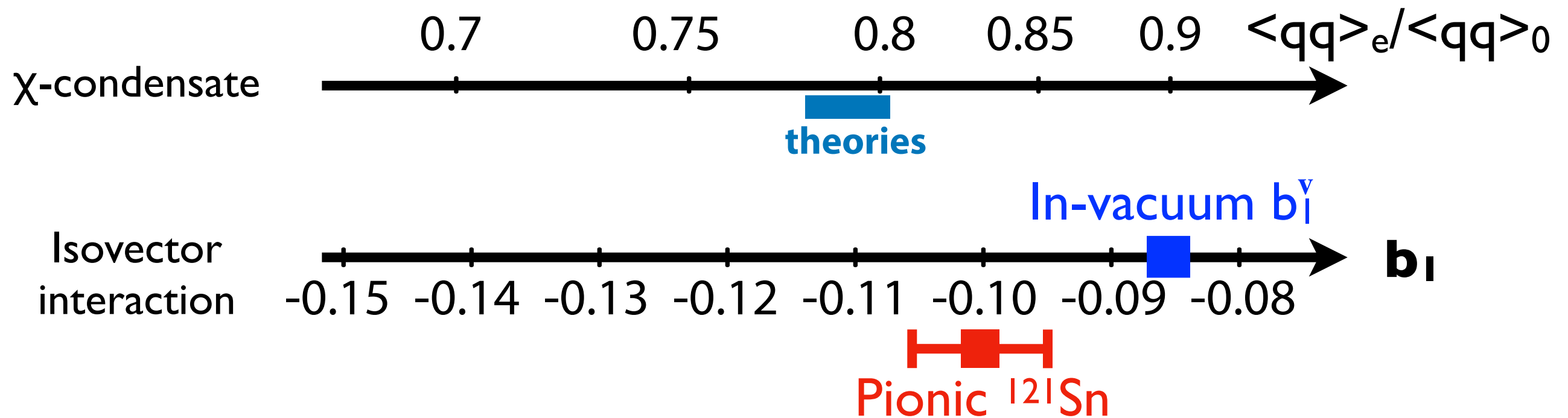
Deduced b_1 and chiral condensate at ρ_e



$b_1 = -0.1005$ was deduced

	[keV]	Statistical	Systematic
$B_\pi(1s)$	3831	± 3	+78 – 76
$B_\pi(2p)$	2276	± 3	+84 – 83
$B_\pi(1s) - B_\pi(2p)$	1555	± 4	± 12
$\Gamma_\pi(1s)$	316	± 12	+36 – 39
$\Gamma_\pi(2p)$	164	± 17	+41 – 32
$\Gamma_\pi(1s) - \Gamma_\pi(2p)$	152	± 20	+28 – 36

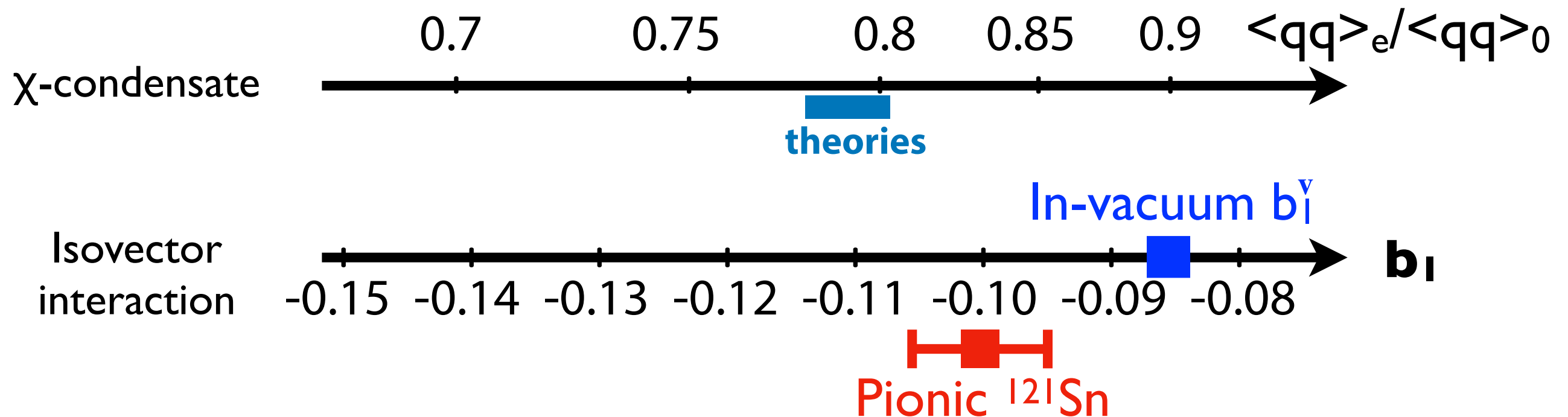
Deduced b_1 and chiral condensate at ρ_e



$b_1 = -0.1005$ was deduced

	[keV]	Statistical	Systematic
$B_\pi(1s)$	3831	± 3	+78 - 76
$B_\pi(2p)$	2276	± 3	+84 - 83
$B_\pi(1s) - B_\pi(2p)$	1555	± 4	± 12
$\Gamma_\pi(1s)$	316	± 12	+36 - 39
$\Gamma_\pi(2p)$	164	± 17	+41 - 32
$\Gamma_\pi(1s) - \Gamma_\pi(2p)$	152	± 20	+28 - 36

Updated / newly introduced

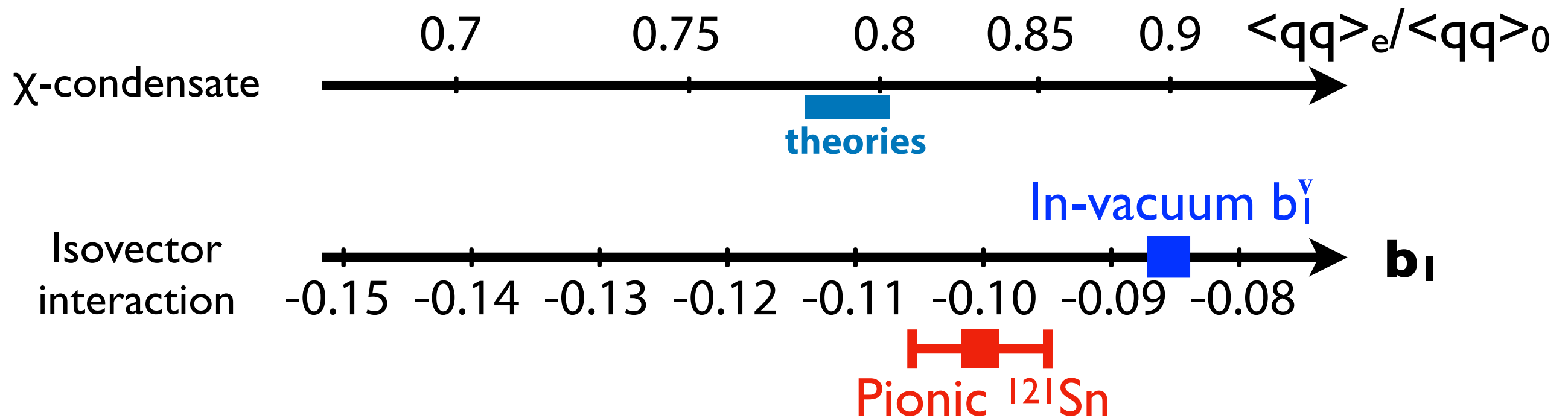


$b_1 = -0.1005$ was deduced

	[keV]	Statistical	Systematic
$B_\pi(1s)$	3831	± 3	+78 – 76
$B_\pi(2p)$	2276	± 3	+84 – 83
$B_\pi(1s) - B_\pi(2p)$	1555	± 4	± 12
$\Gamma_\pi(1s)$	316	± 12	+36 – 39
$\Gamma_\pi(2p)$	164	± 17	+41 – 32
$\Gamma_\pi(1s) - \Gamma_\pi(2p)$	152	± 20	+28 – 36

LLE : short-range correction
 Sn ρ : neutron density distribution
 Abs. : representation of absorption term
 Green : cross section calculation method
 Res. : Residual interaction
 Spec. : neutron spectroscopic factors

Updated / newly introduced

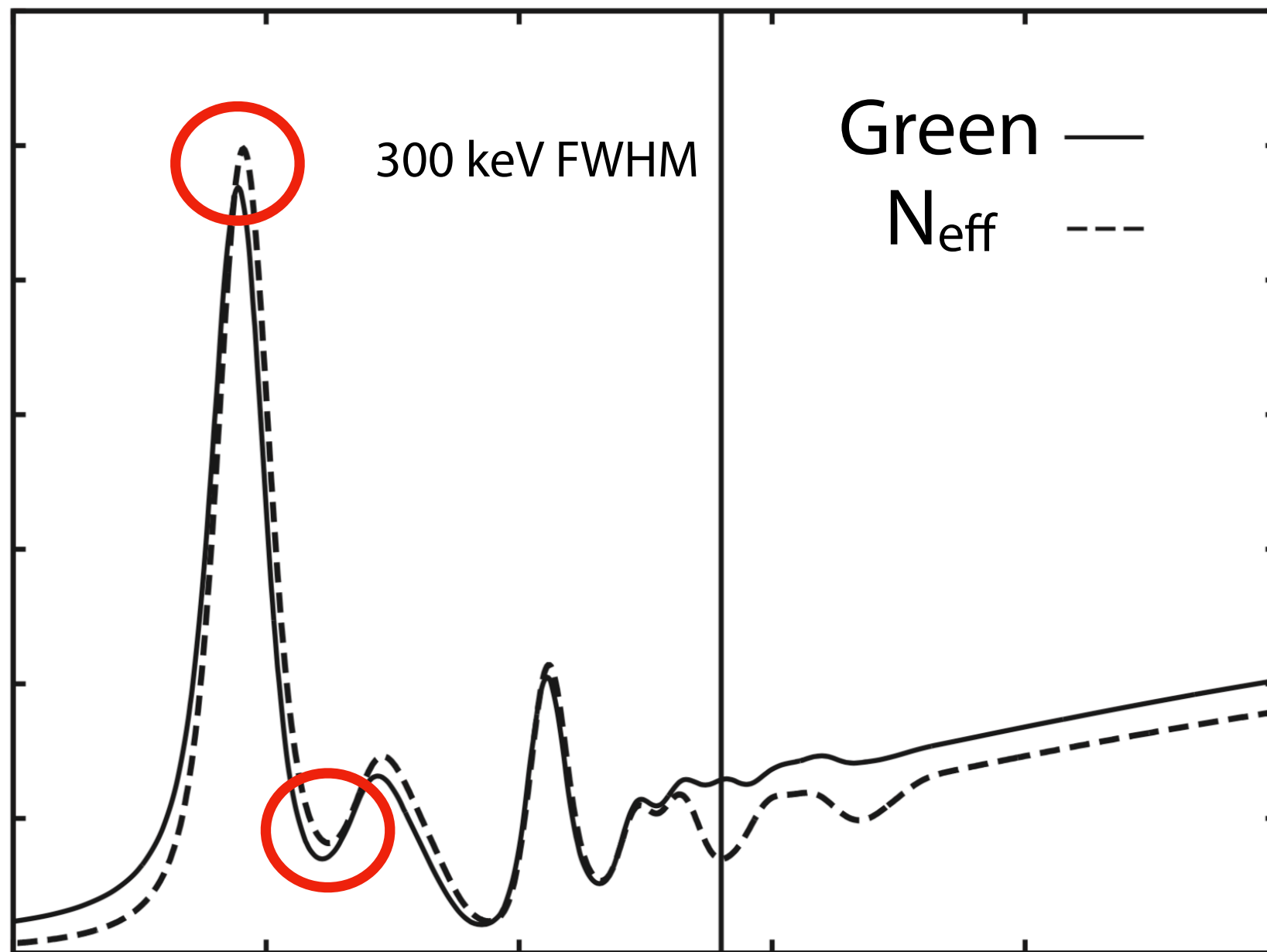


$b_1 = -0.1005$ was deduced

	[keV]	Statistical	Systematic
$B_\pi(1s)$	3831	± 3	+78 – 76
$B_\pi(2p)$	2276	± 3	+84 – 83
$B_\pi(1s) - B_\pi(2p)$	1555	± 4	± 12
$\Gamma_\pi(1s)$	316	± 12	+36 – 39
$\Gamma_\pi(2p)$	164	± 17	+41 – 32
$\Gamma_\pi(1s) - \Gamma_\pi(2p)$	152	± 20	+28 – 36

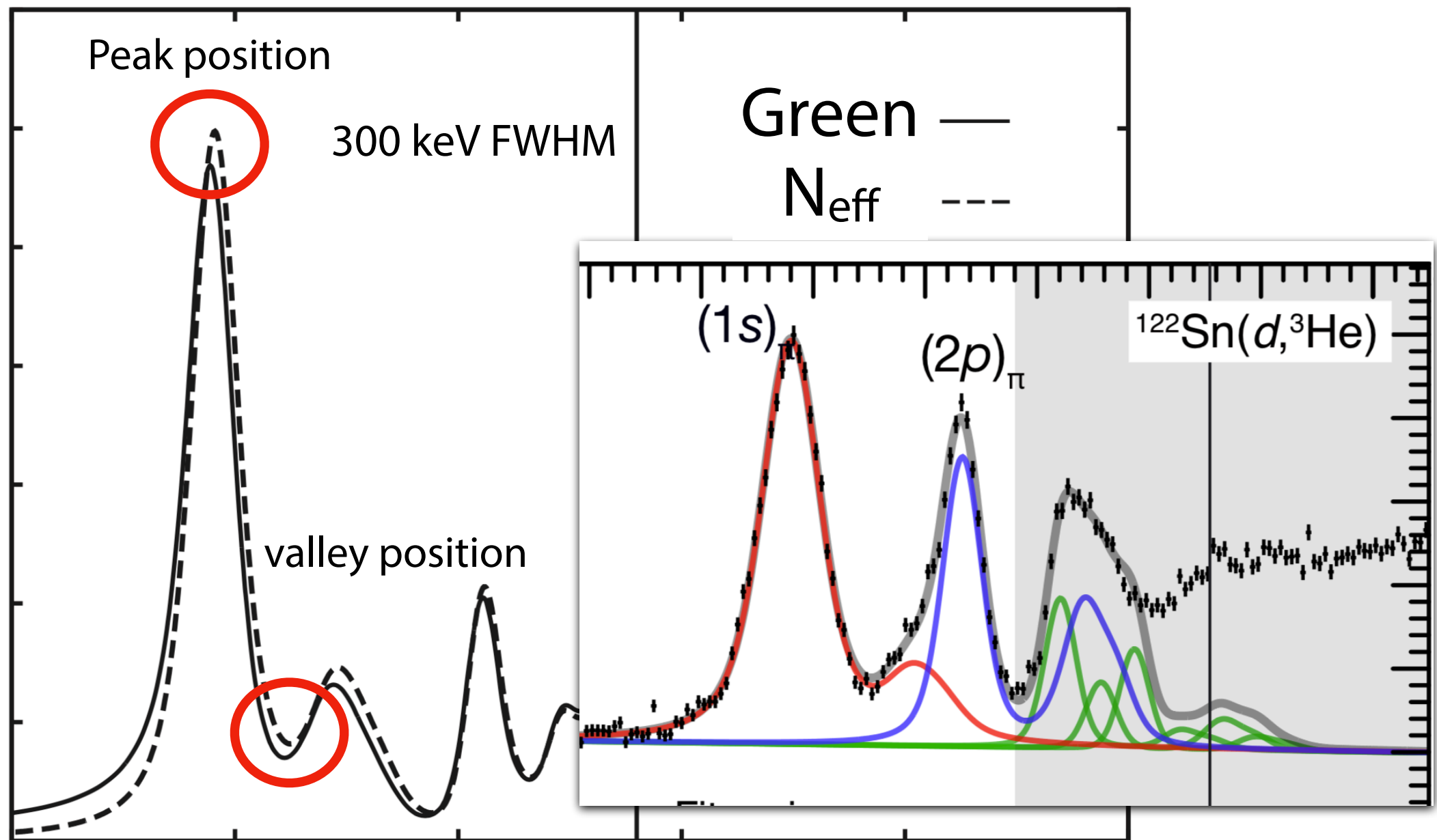
LLE : short-range correction
 Sn ρ : neutron density distribution
 Abs. : representation of absorption term
Green : cross section calculation method
 Res. : Residual interaction
 Spec. : neutron spectroscopic factors

$^{122}\text{Sn}(d,^3\text{He})$ spectra calculated with N_{eff} and Green's function methods



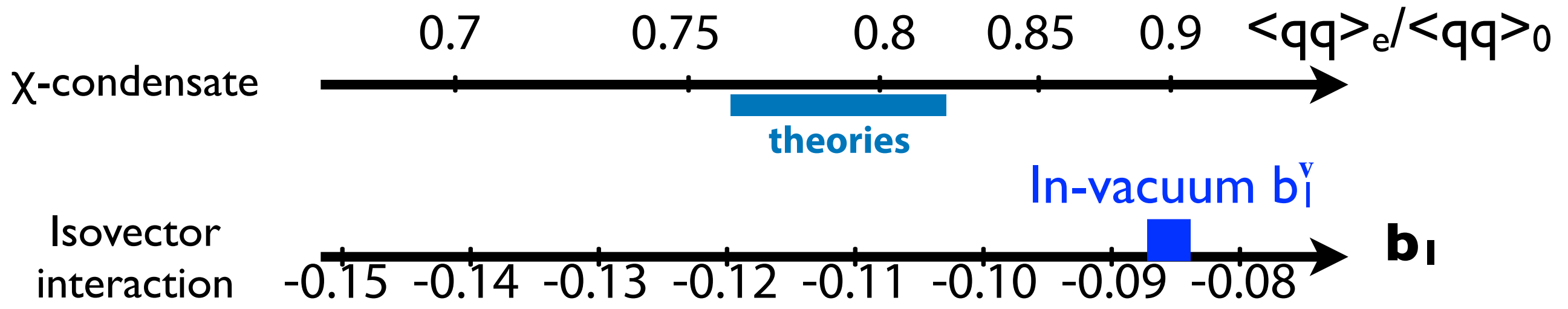
Green's function method calculates slightly different spectral shapes from N_{eff} approach

$^{122}\text{Sn}(d,^3\text{He})$ spectra calculated with Neff and Green's function methods

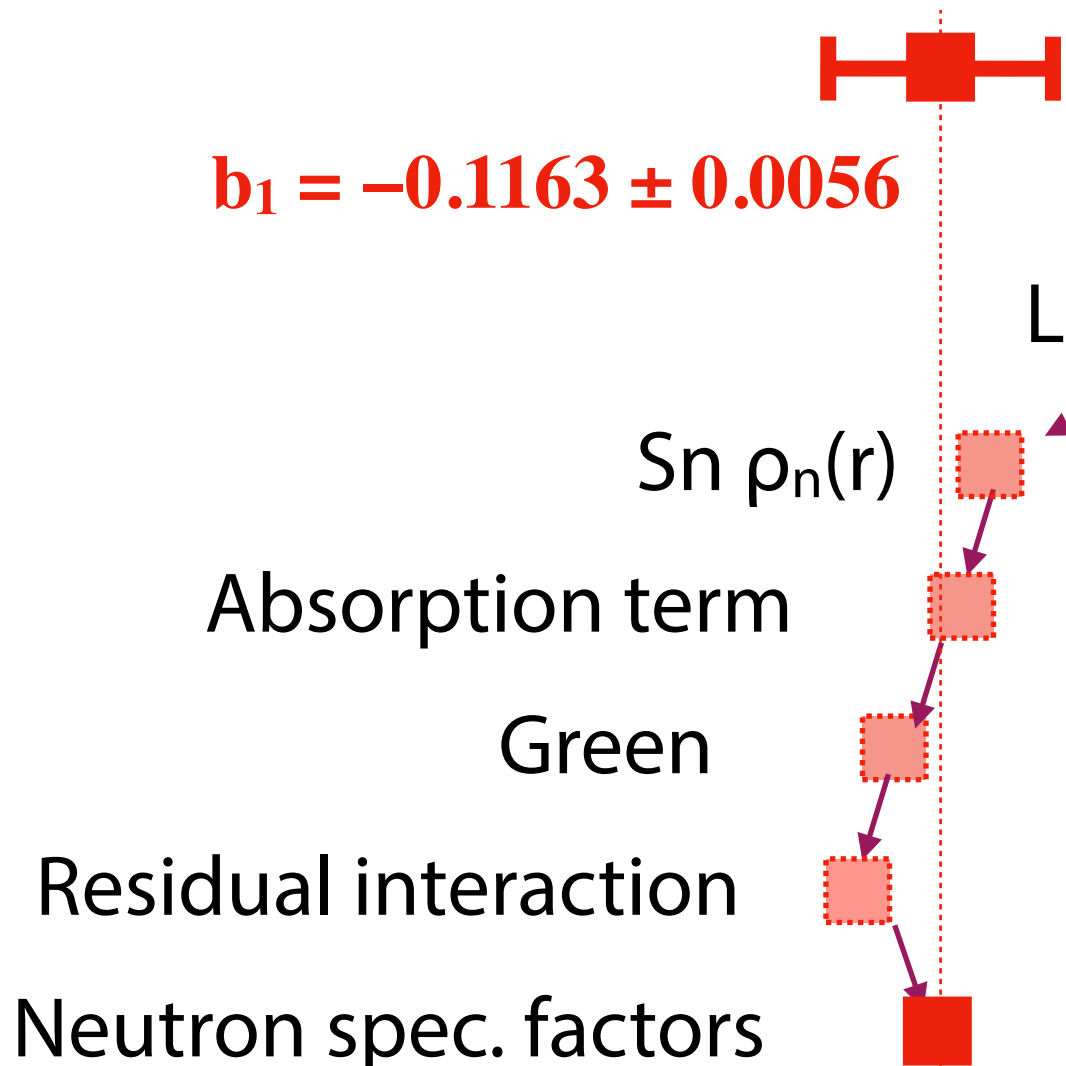


Green's function method calculates slightly different spectral shapes from N_{eff} approach

Deduced b_1 after all



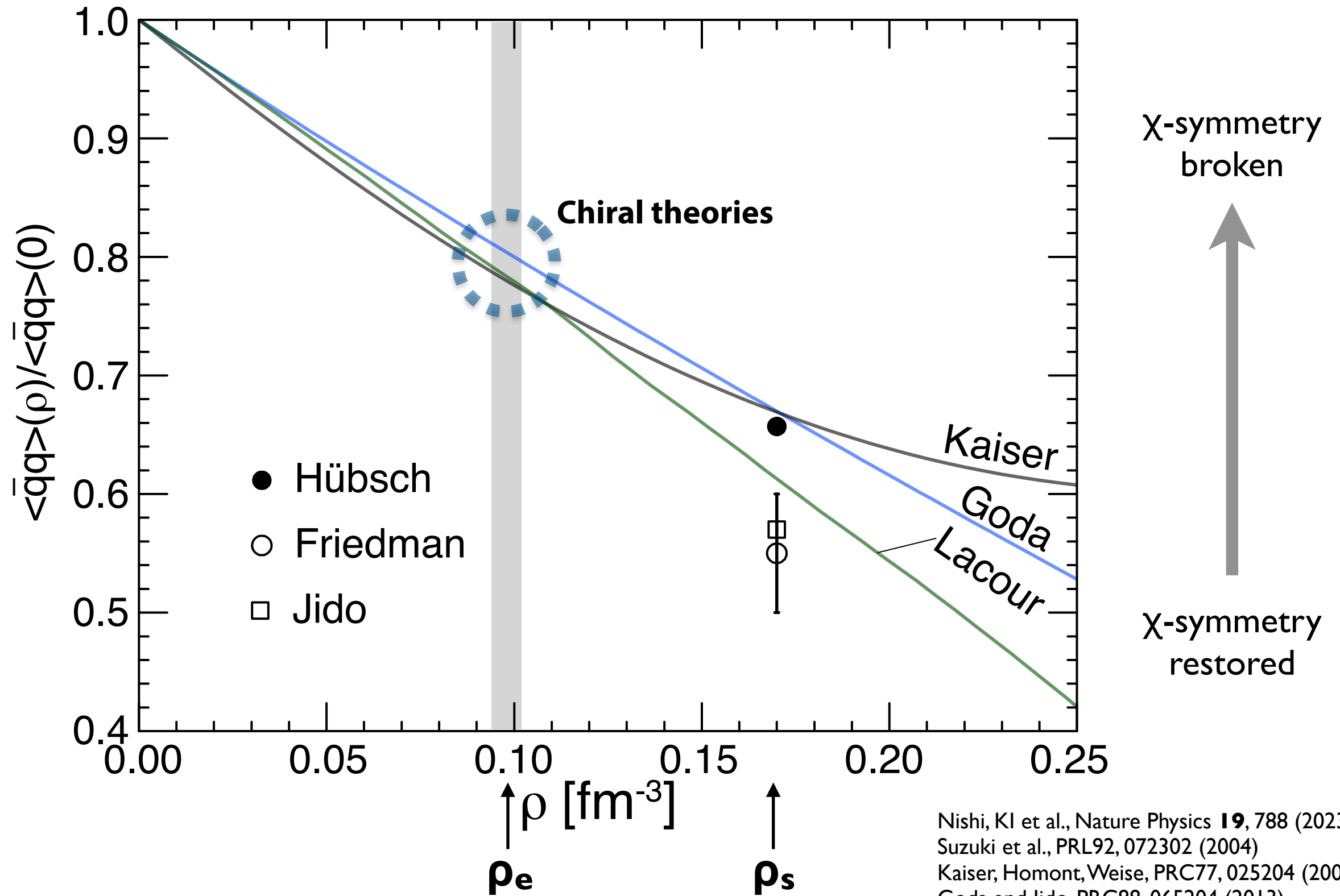
$$b_1 = -0.1163 \pm 0.0056$$



LLE : short-range correction
Sn ρ : neutron density distribution
Abs. : representation of absorption term
Green : cross section calculation method
Res. : Residual interaction
Spec. : neutron spectroscopic factors

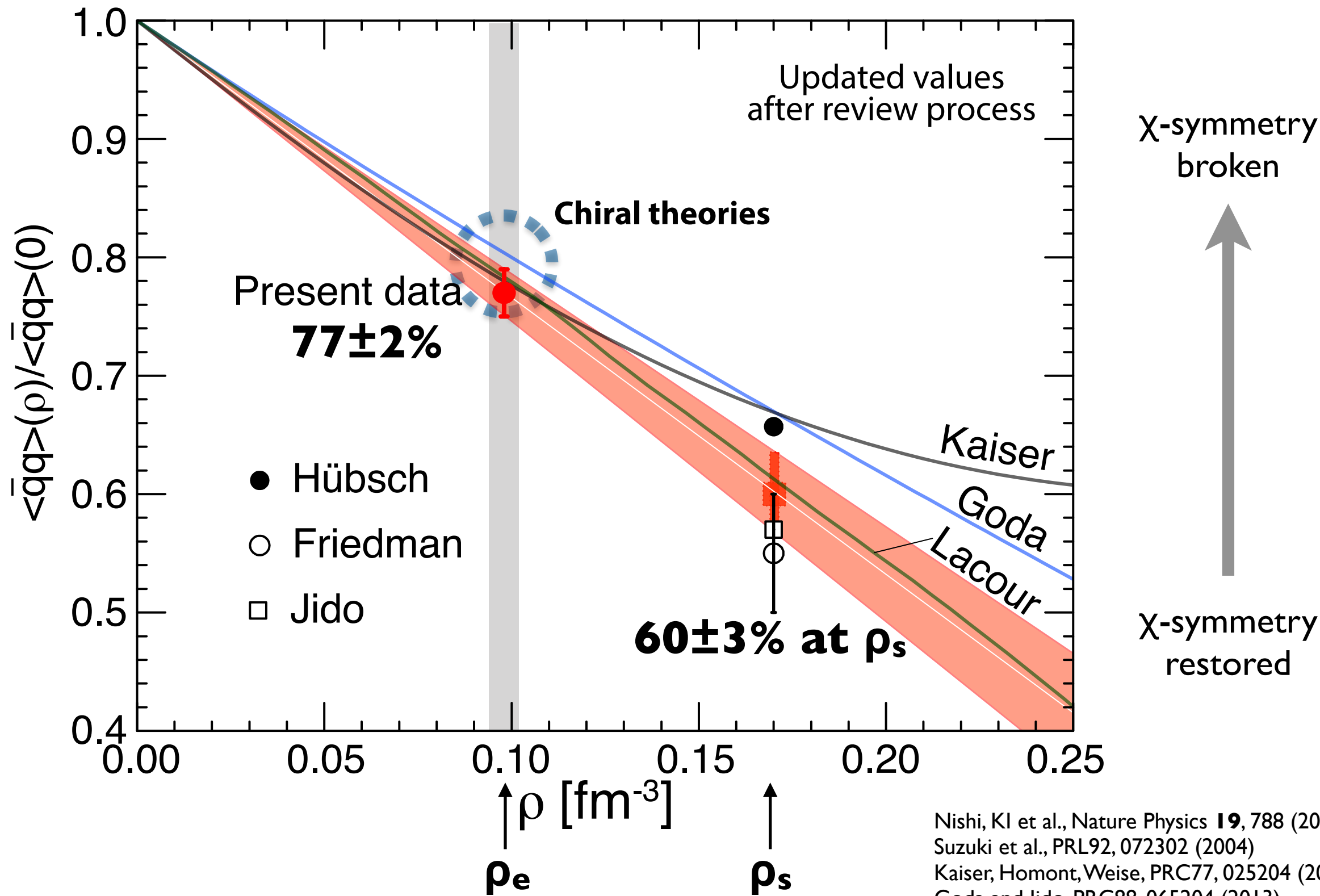
N. Ikeno et al., PTEP 2015, 033D01 (2015)
 Terashima et al., PHYSICAL REVIEW C 77, 024317 (2008)
 Nose-Togawa et al., PRC71, 061601(R) (2005)
 Szwec et al., PRC104,054308

Result: deduced chiral condensate



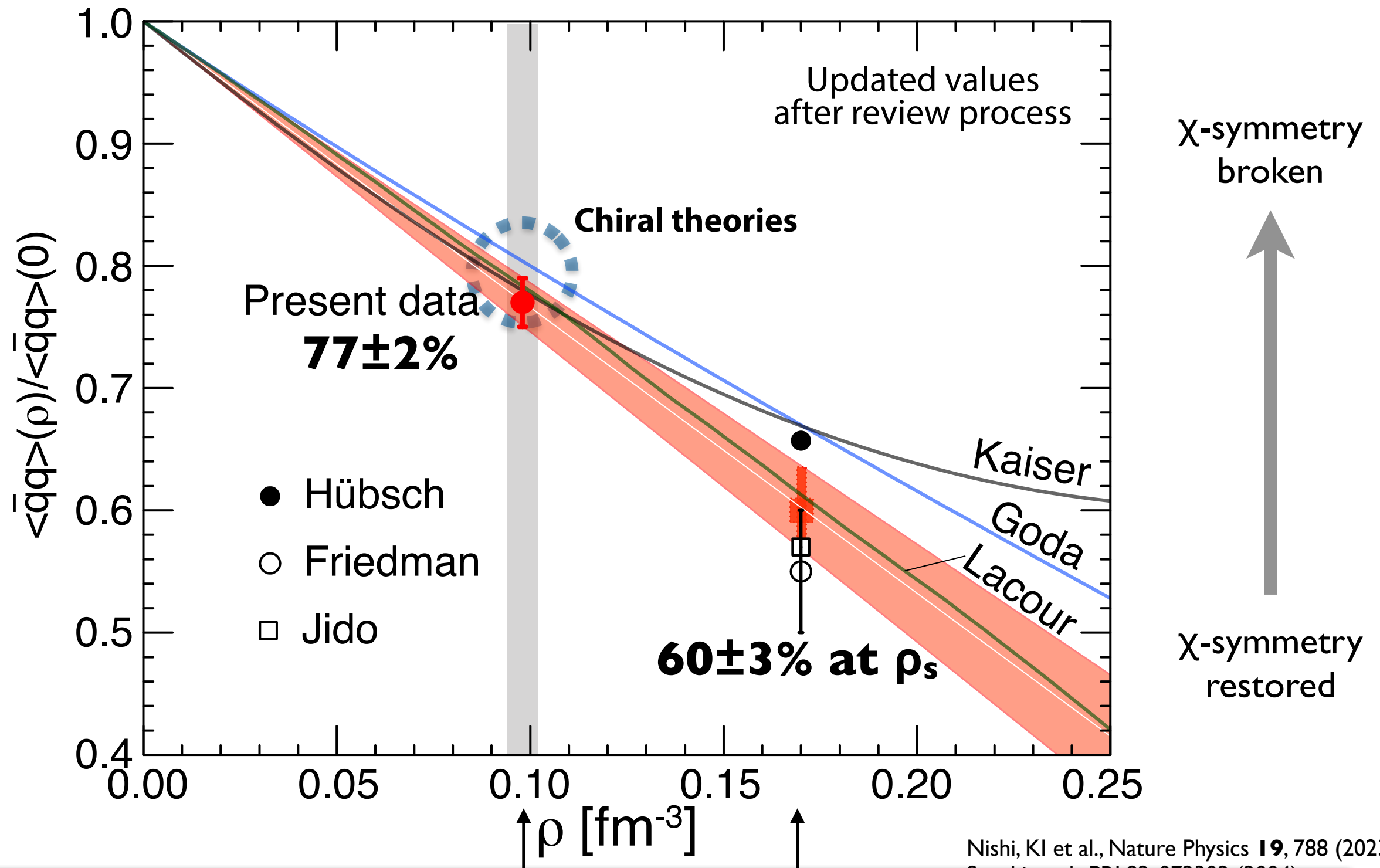
Nishi, KI et al., Nature Physics **19**, 788 (2023)
 Suzuki et al., PRL92, 072302 (2004)
 Kaiser, Homont, Weise, PRC77, 025204 (2008)
 Goda and Jido, PRC88, 065204 (2013)
 Huebsch, Jido, PRC104, 015202 (2021)
 Friedman, Gal, PLB792, 340 (2019)
 Jido, Hatsuda, Kunihiro, PLB670, 109 (2008)
 Lacour, Oller, Meissner, J. Phys. G. 37, 125002 (2010)

Result: deduced chiral condensate



Nishi, KI et al., Nature Physics **19**, 788 (2023)
 Suzuki et al., PRL92, 072302 (2004)
 Kaiser, Homont, Weise, PRC77, 025204 (2008)
 Goda and Jido, PRC88, 065204 (2013)
 Huebsch, Jido, PRC104, 015202 (2021)
 Friedman, Gal, PLB792, 340 (2019)
 Jido, Hatsuda, Kunihiro, PLB670, 109 (2008)
 Lacour, Oller, Meissner, J. Phys. G. 37, 125002 (2010)

Result: deduced chiral condensate

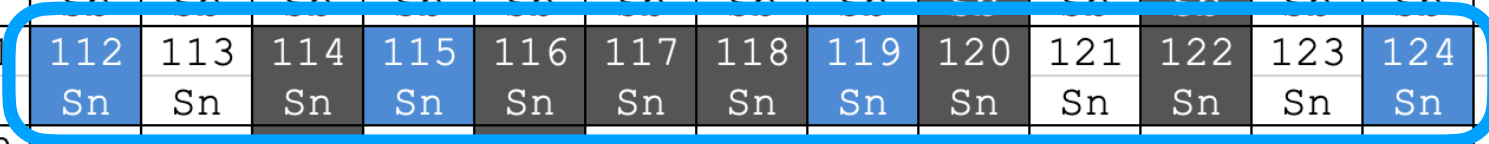


The experimental result shows good agreement with chiral perturbation theories

Next plans

- **Systematic spectroscopy of pionic Sn atoms (RIBF-135)**
- **Inverse kinematics for ^{136}Xe (RIBF-214)**
- **Pionic unstable nuclei**

																	140	141	142	143	144	145	146	
																		Eu	Eu	Eu	Eu	Eu	Eu	Eu
																		139	140	141	142	143	144	145
																		Sm	Sm	Sm	Sm	Sm	Sm	Sm
																		138	139	140	141	142	143	144
																		Pm	Pm	Pm	Pm	Pm	Pm	Pm
																		137	138	139	140	141	142	143
																		Nd	Nd	Nd	Nd	Nd	Nd	Nd
																		136	137	138	139	140	141	142
																		Pr	Pr	Pr	Pr	Pr	Pr	Pr
																		135	136	137	138	139	140	141
Ce	Ce	Ce	Ce	Ce	Ce	Ce	Ce	Ce	Ce	Ce	Ce	Ce	Ce	Ce	Ce	Ce	Ce	Ce	Ce	Ce	Ce	Ce	Ce	
117	118	119	120	121	122	123	124	125	126	127	128	129	130	131	132	133	134	135	136	137	138	139	140	
La	La	La	La	La	La	La	La	La	La	La	La	La	La	La	La	La	La	La	La	La	La	La	La	
116	117	118	119	120	121	122	123	124	125	126	127	128	129	130	131	132	133	134	135	136	137	138	139	
Ba	Ba	Ba	Ba	Ba	Ba	Ba	Ba	Ba	Ba	Ba	Ba	Ba	Ba	Ba	Ba	Ba	Ba	Ba	Ba	Ba	Ba	Ba	Ba	
115	116	117	118	119	120	121	122	123	124	125	126	127	128	129	130	131	132	133	134	135	136	137	138	
Cs	Cs	Cs	Cs	Cs	Cs	Cs	Cs	Cs	Cs	Cs	Cs	Cs	Cs	Cs	Cs	Cs	Cs	Cs	Cs	Cs	Cs	Cs	Cs	
114	115	116	117	118	119	120	121	122	123	124	125	126	127	128	129	130	131	132	133	134	135	136	137	
Xe	Xe	Xe	Xe	Xe	Xe	Xe	Xe	Xe	Xe	Xe	Xe	Xe	Xe	Xe	Xe	Xe	Xe	Xe	Xe	Xe	Xe	Xe	Xe	
113	114	115	116	117	118	119	120	121	122	123	124	125	126	127	128	129	130	131	132	133	134	135	136	
I	I	I	I	I	I	I	I	I	I	I	I	I	I	I	I	I	I	I	I	I	I	I	I	
112	113	114	115	116	117	118	119	120	121	122	123	124	125	126	127	128	129	130	131	132	133	134	135	
Te	Te	Te	Te	Te	Te	Te	Te	Te	Te	Te	Te	Te	Te	Te	Te	Te	Te	Te	Te	Te	Te	Te	Te	
111	112	113	114	115	116	117	118	119	120	121	122	123	124	125	126	127	128	129	130	131	132	133	134	
Sb	Sb	Sb	Sb	Sb	Sb	Sb	Sb	Sb	Sb	Sb	Sb	Sb	Sb	Sb	Sb	Sb	Sb	Sb	Sb	Sb	Sb	Sb	Sb	
110	111	112	113	114	115	116	117	118	119	120	121	122	123	124	125	126	127	128	129	130	131	132	133	
Sn	Sn	Sn	Sn	Sn	Sn	Sn	Sn	Sn	Sn	Sn	Sn	Sn	Sn	Sn	Sn	Sn	Sn	Sn	Sn	Sn	Sn	Sn	Sn	
109	110	111	112	113	114	115	116	117	118	119	120	121	122	123	124	125	126	127	128	129	130	131	132	
In	In	In	In	In	In	In	In	In	In	In	In	In	In	In	In	In	In	In	In	In	In	In	In	
108	109	110	111	112	113	114	115	116	117	118	119	120	121	122	123	124	125	126	127	128	129	130	131	
Cd	Cd	Cd	Cd	Cd	Cd	Cd	Cd	Cd	Cd	Cd	Cd	Cd	Cd	Cd	Cd	Cd	Cd	Cd	Cd	Cd	Cd	Cd	Cd	

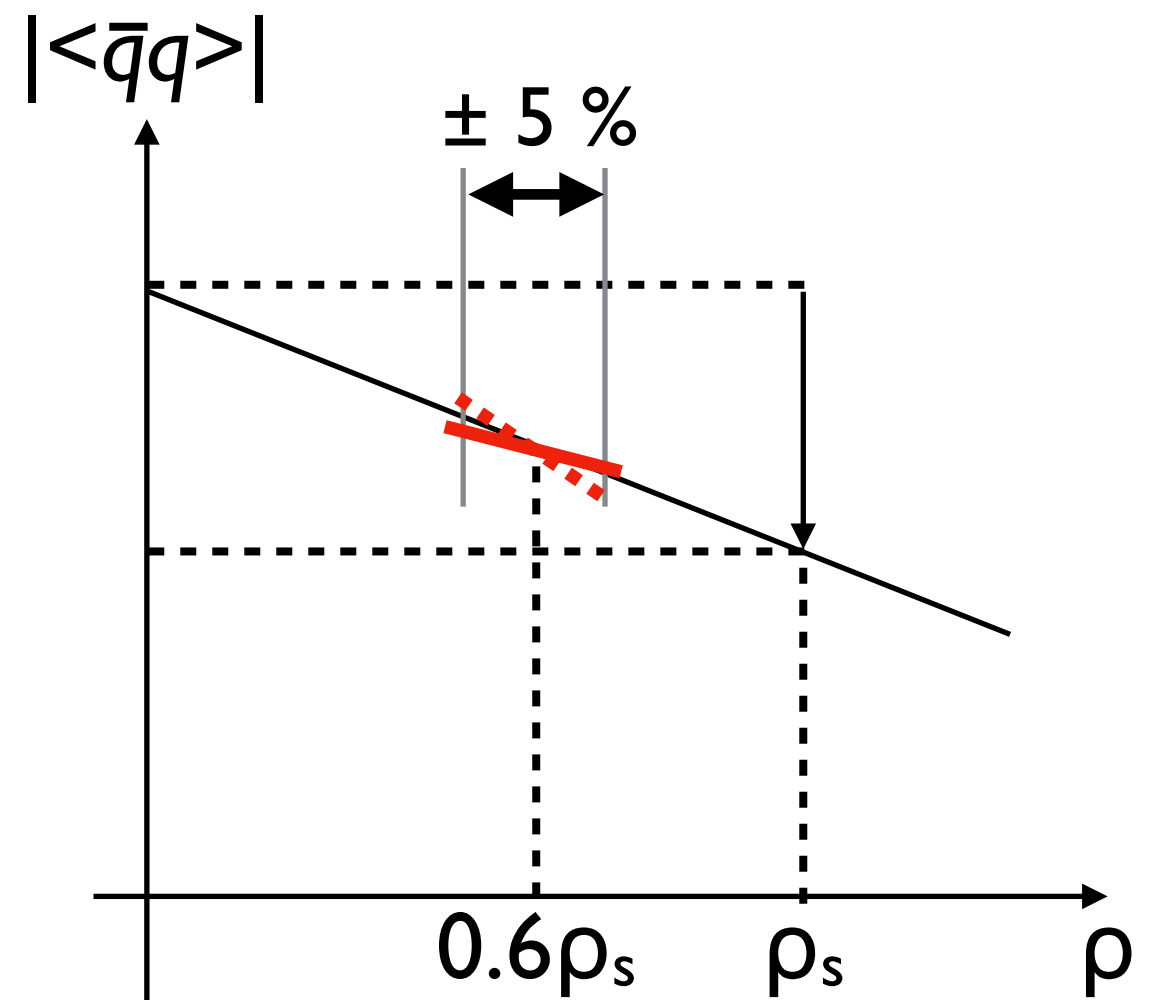


Density Dependence of Chiral Condensate

ρ derivative of $\langle \bar{q}q \rangle = d\langle \bar{q}q \rangle / d\rho$ can be studied by systematic spectroscopy of pionic Sn isotopes

Densities probed by pionic Sn with wide range of A

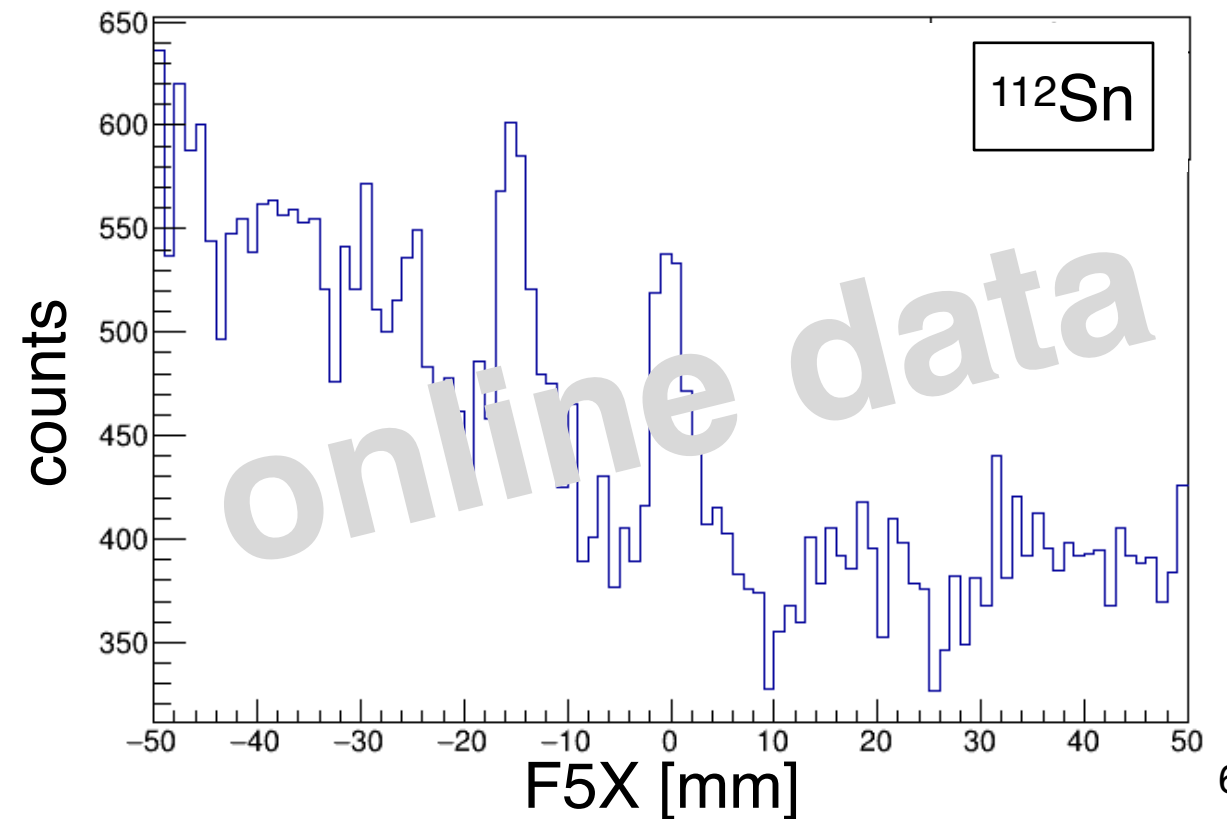
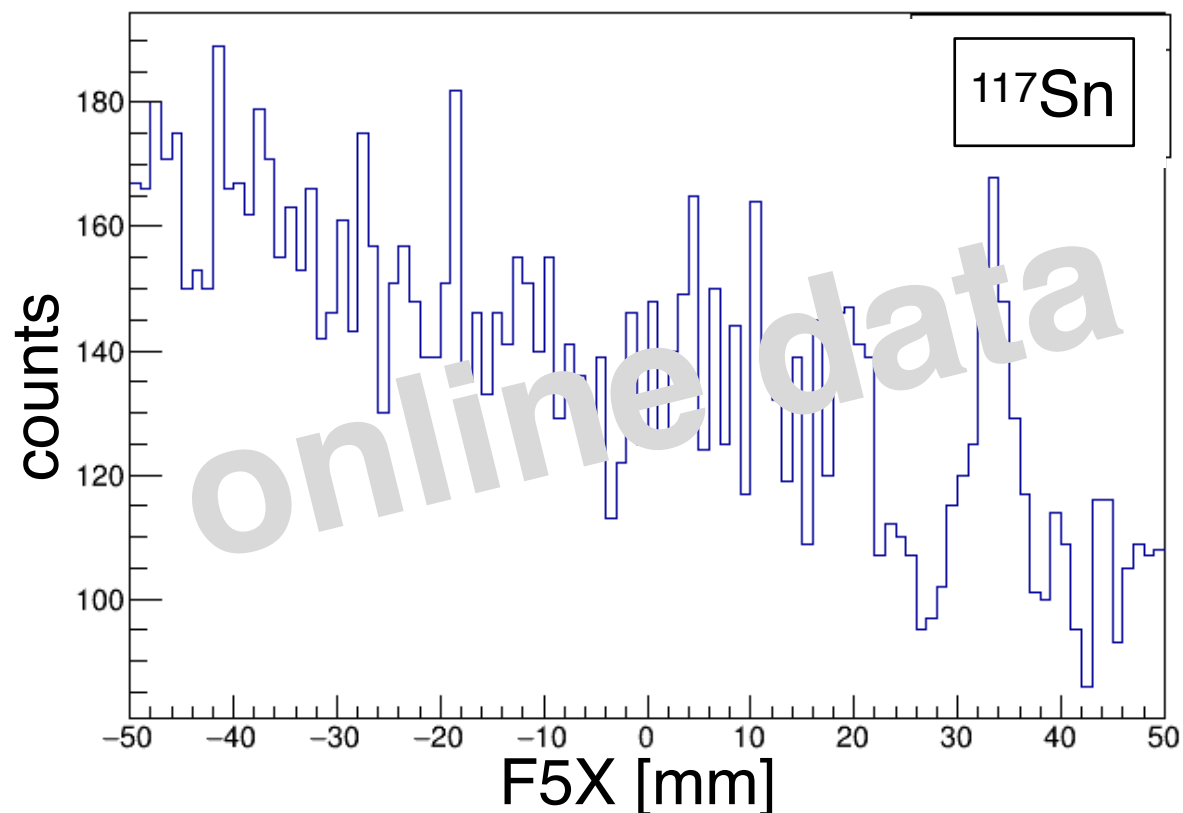
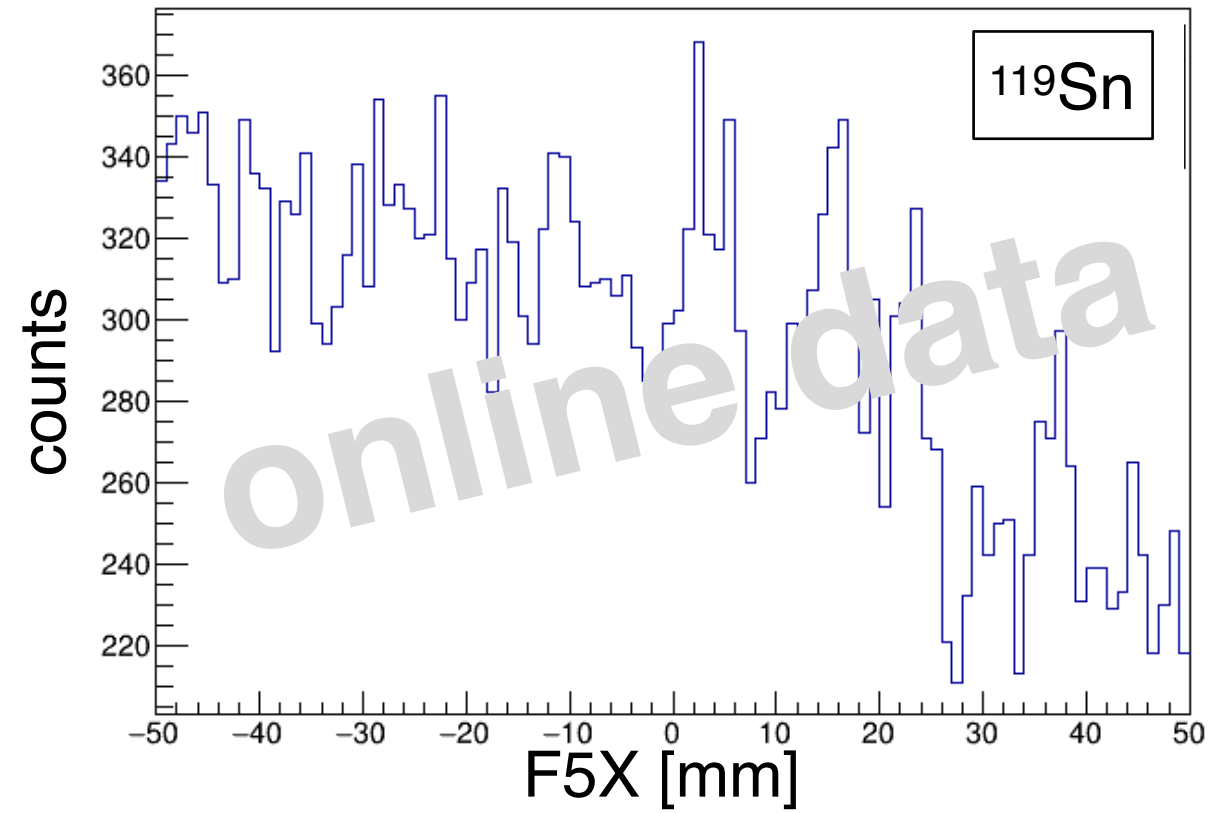
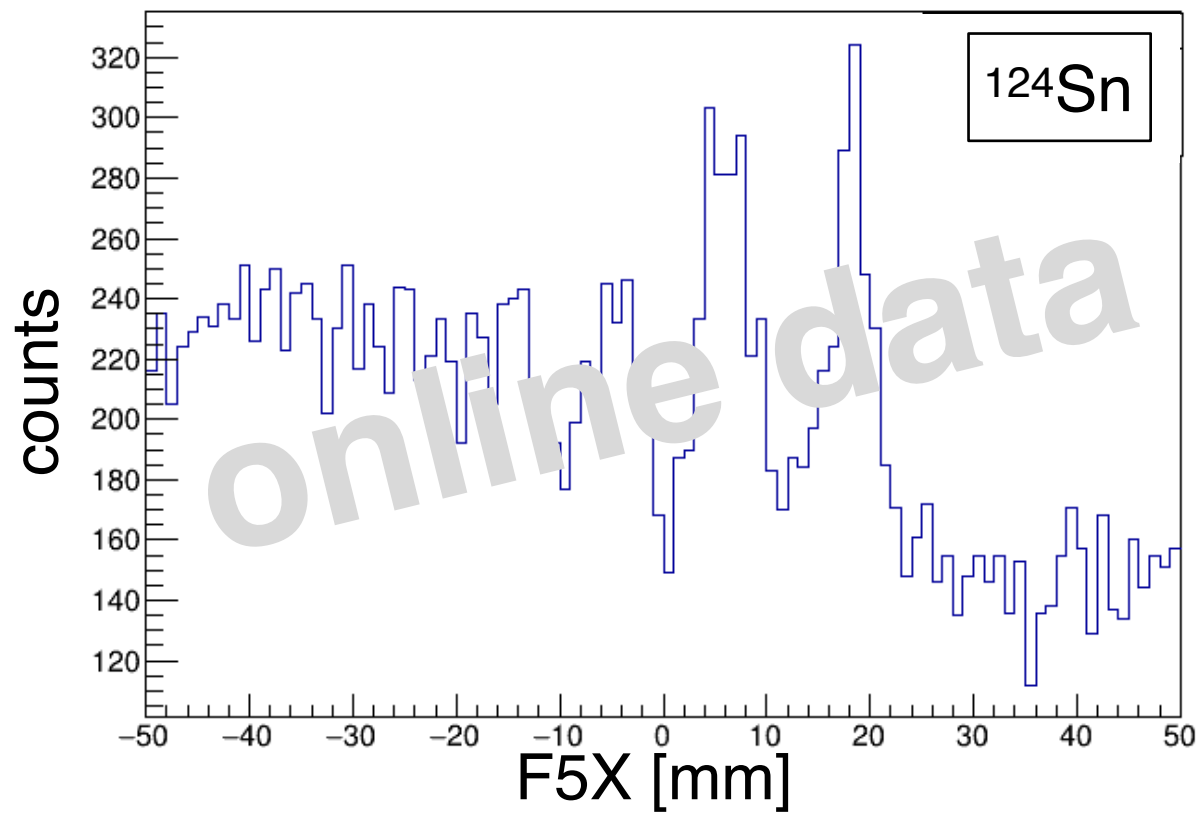
Important for $\sigma_{\pi N}$ for investigation of origin of matter mass



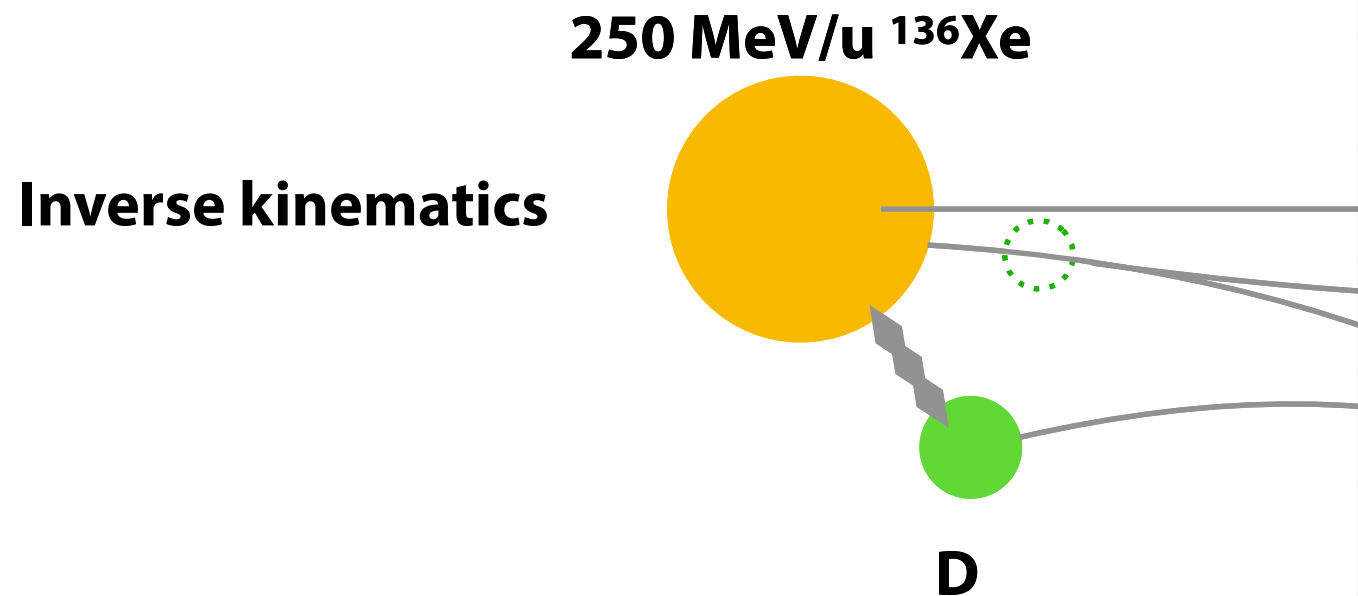
Pionic atoms are known to probe $\sim 0.6\rho_s$

Systematic spectroscopy of pionic Sn isotopes

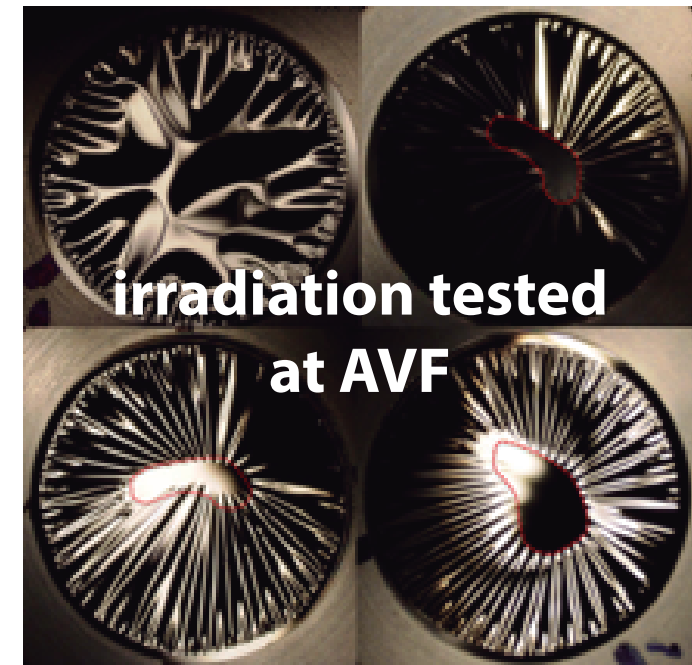
Successful measurement in RIBF-135 (2021)



First application of inverse



1-atm deuterium gas target with
1 μm **graphenic carbon** windows

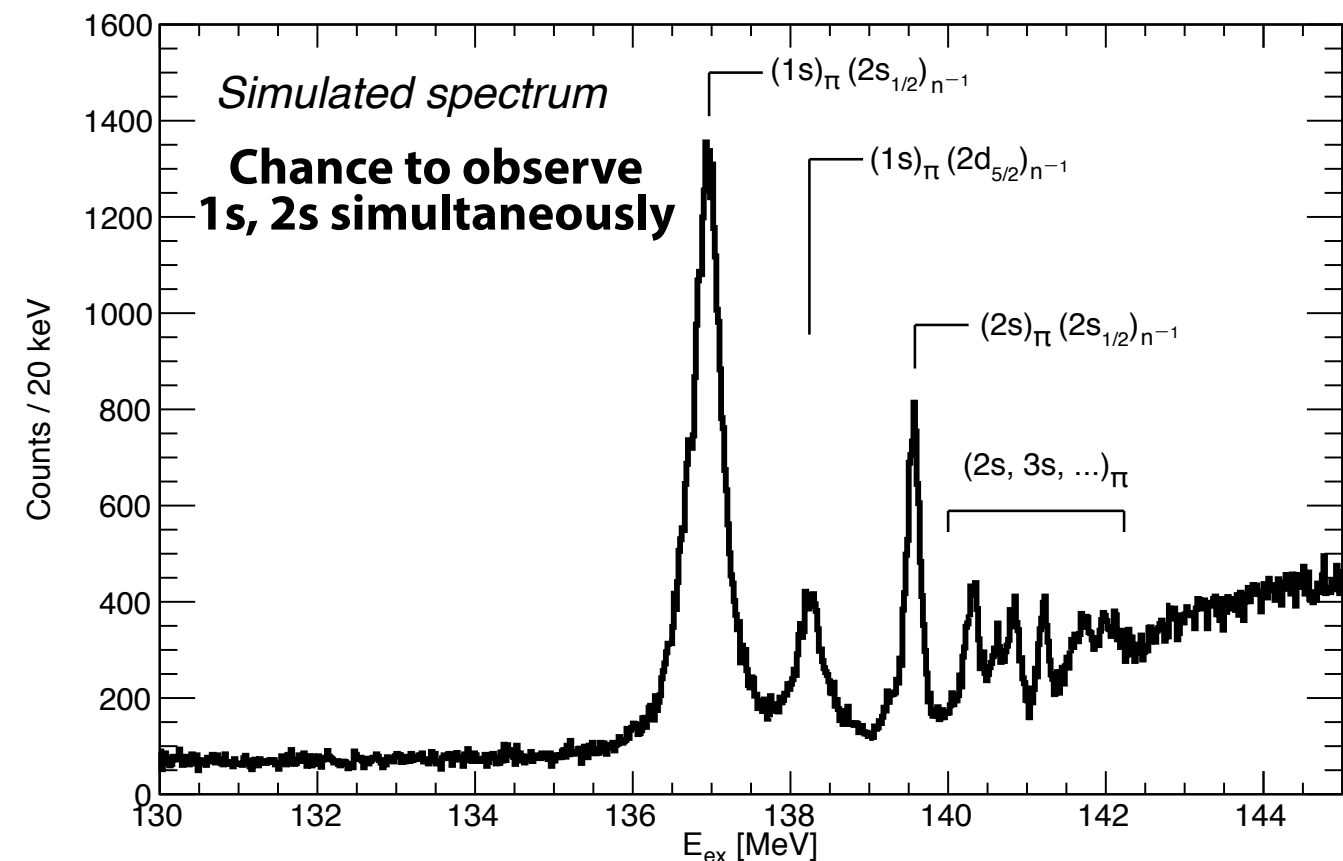


S. Purushothaman et al., APR **53**, 134 (2019)

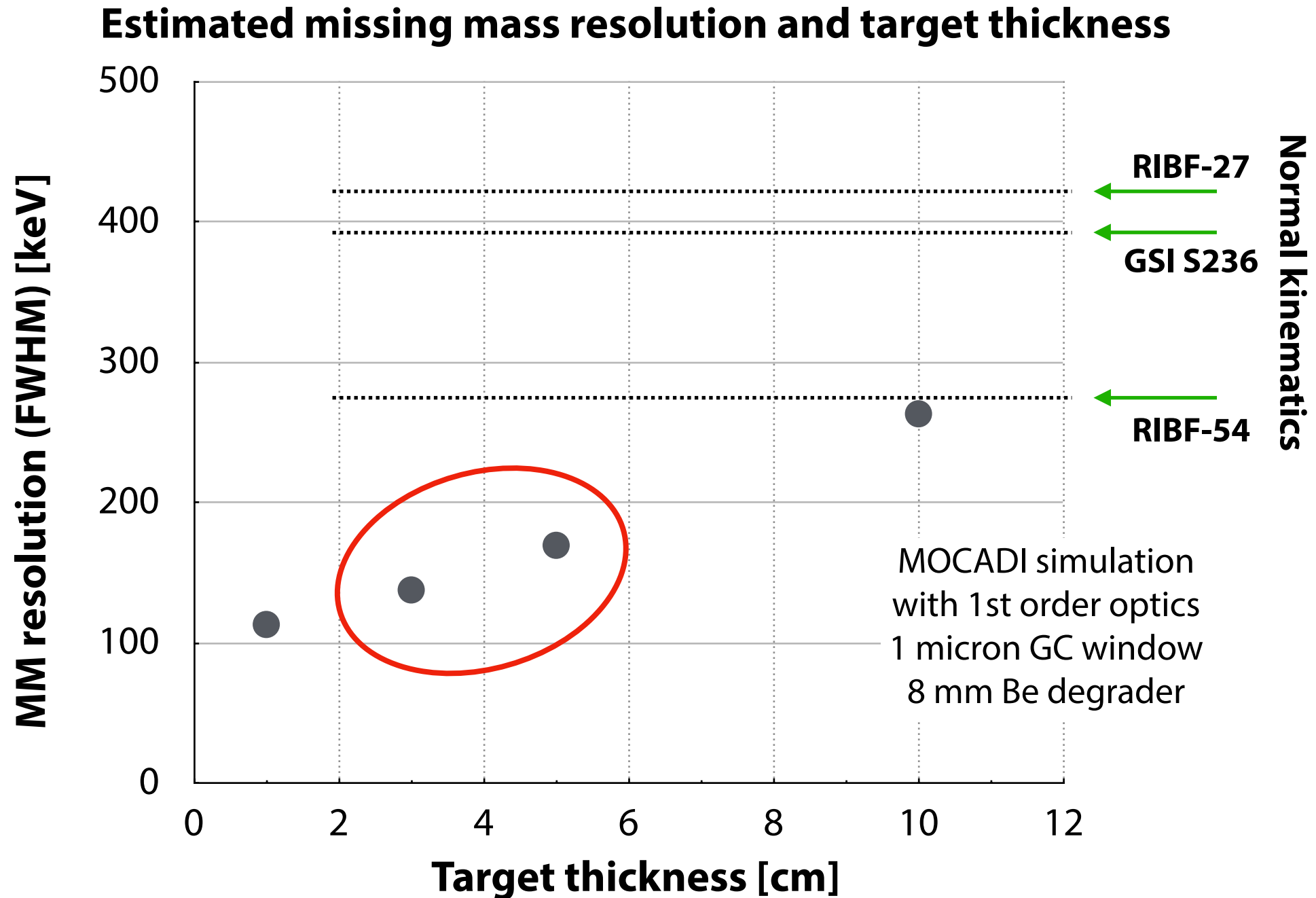
36 hours with $10^{10}/\text{s}$ ^{136}Xe beam

Advantages of inverse kinematics

- Unprecedented resolution**
MM resolution does not depend on incident beam energy spread.
- Extension of piA across nuclear chart**
Use of materials not suited for targets including **radio active nuclei**.



Unprecedented MM resolution can be improved!



Unprecedented resolution can be achieved
 → Important for resolving higher orbitals and
 determine the widths

cf. For normal kinematics,
 resolution has been limited
 by beam properties.

Summary

In-medium meson spectroscopy in missing-mass measurement of meson production reactions is a strong tool to investigate the **structure/symmetry of the vacuum at finite ρ** .

For η' -mesic nuclei search

- η' -mesic nuclei may give some hints of **$U_A(1)$ quantum anomaly**.
- We make use of $^{12}\text{C}(p,d)$ missing-mass measurement + $\eta'NN \rightarrow NN$ tagging.
- WASA at GSI/FRS worked as designed. Background is reduced by 1/200 as simulated.
- We are finalizing the analysis and working on the exclusive spectra.

For pionic atom spectroscopy

- We make use of $\text{Sn}(d,^3\text{He})$ missing-mass measurement for the pionic atoms.
- The binding energies and widths of the $1s$ and $2p$ states in ^{121}Sn were determined. Difference between the $1s$ and $2p$ values reduces the systematic errors drastically.
- We deduced pion-nucleus interaction after including recent updates. The interaction is modified for the w.f. renormalization of the medium effect.
- **Chiral condensate at $\rho_e \sim 0.6\rho_0$ is evaluated to be reduced by a factor of $77 \pm 2\%$.**
- We continue study for **ρ dependence of $\langle \bar{q}q \rangle$** . We plan measurement with “inverse kinematics” with better resolution, leading to future experiments of pionic unstable nuclei.